Fall 2022

The Role of Gut Microbiome and SCFA Butyrate in the Development of Obesity Associated Pre-HFpEF

Jomana Hatahet

LOYOLA UNIVERSITY CHICAGO

THE ROLE OF GUT MICROBIOME AND SCFA BUTYRATE IN THE DEVELOPMENT OF OBESITY ASSOCIATED PRE-HFPEF

A DISSERTATION SUBMITTED TO

THE FACULTY OF THE GRADUATE SCHOOL

IN CANDIDACY FOR THE DEGREE OF

DOCTOR OF PHILOSOPHY

PROGRAM IN CELL AND MOLECULAR PHYSIOLOGY

BY

JOMANA HATAHET

CHICAGO, ILLINOIS

DECEMBER 2022

ACKNOWLEDGEMENTS

Completion of this work would not have been possible without the tremendous support I received from the amazing people in my life. A great thanks to my mentor Dr. Gregory Aubert for his guidance and mentorship that helped me grow as an independent scientist over the last four years. I would like to thank my dissertation committee members: Drs. Seth Robia, Jordan Beach, Dave Barefield, and Sophia Zang. Their guidance and feedback have been a critical part for the development of this project. I would like to thank the department of Cell and Molecular Physiology for having a supportive and challenging research environment that provided me with the tools to grow scientifically and personally and helped prepare me for a career as a research scientist. A special thank you to Dr. Virgnie Mansuy-Aubert who provided constant feedback and helpful suggestions during our joint lab meetings. I am truly lucky that I was part of Dr. Aubert's lab where I met and worked with amazing colleagues and friends who made this journey truly fun and enjoyable.

I am extremely grateful to my parents and siblings for their continuous love, support, and understanding. Thank you for always believing in me and encouraging me throughout my entire PhD journey. I could not have done this without you.

For Mom and Dad.

TABLE OF CONTENTS

LIST OF FIGURES

LIST OF TABLES

LIST OF ABBREVIATIONS

HFpEF	Heart Failure with Preserved Ejection Fraction
HFrEF	Heart Failure with Reduced Ejection Fraction
T2D	Type 2 Diabetes
CVDs	Cardiovascular Diseases
COPD	Chronic Obstructive Pulmonary Disease
CKD	Chronic Kidney Disease
LVEF	Left Ventricle Ejection Fraction
GLS	Global Longitudinal Strain
LSRr	Longitudinal Strain Rate Reverse
LVPWd	Left Ventricle Posterior Wall Thickness in Diastole
CO	Cardiac Output
HR	Heart Rate
SCFAs	Short Chain Fatty Acids
FMT	Fecal Microbiome Transplantation
SGLT2	Sodium-Glucose Cotransporter 2
HFD	High Fat Diet
DIO	Diet-Induced Obesity
MCTs	Monocarboxylate Transporters
SMCTs	Sodium-dependent Monocarboxylate Transporters
GPCRs	G Protein-coupled Receptors

FFARs	Free Fatty Acid Receptors
HCAR2	Hydrocarboxylic Acid Receptor
β1-AR	Beta 1 Adrenergic Receptor
β2-AR	Beta 2 Adrenergic Receptor
α-AR	Alpha Adrenergic Receptor
mAChRs	Muscarinic Acetylcholine Receptors
nAChRs	Nicotinic Acetylcholine Receptors
ACh	Acetylcholine
ANS	Autonomic Nervous System
SNS	Sympathetic Nervous System
PNS	Parasympathetic Nervous System
ENS	Enteric Nervous System
NE	Norepinephrine
BDNF	Brain-Derived Neurotrophic Factor
BAT	Brown Adipose Tissue
PYY	Peptide Tyrosine Tyrosine
HRV	Heart Rate Variability
HRR	Heart Rate Recovery
ART	Autonomic Regulation Therapy
GRKs	G-Protein–Coupled Receptor Kinases
HDAC	Histone Deacetylation
HAT	Histone Acetyltransferase
cAMP	Cyclic Adenosine Monophosphate

NO	Nitric Oxide
NOS	Nitric Oxide Synthase
RAAS	Renin-Angiotensin-Aldosterone System
TNF- α	Tumor Necrosis Factor-α
IL-6	Interleukin-6
IL-1β	Interleukin-1β
UPR	Unfolded Protein Response
ER	Endoplasmic Reticulum
ROS	Reactive Oxygen Species
cGMP	Cyclic Guanosine Monophosphate
PKG	Protein Kinase G
TGF-β	Transforming Growth Factor β
VCAM	Vascular Cell Adhesion Molecule
ECM	Extracellular Matrix
IRE1α	Inositol-Requiring Enzyme 1α
XBP1	X-box Binding Protein 1
AngII	Angiotensin II
DOCP	Desoxycorticosterone Pivalate
L-NAME	N^{ω}-nitro-l-arginine Methyl Ester
PPARγ	Peroxisome Proliferator-activated Receptor Gamma
IBS	Irritable Bowel Syndrome
IBD	Inflammatory Bowel Disease
MS	Multiple Sclerosis

WAT	White Adipose Tissue
Olfr78	Olfactory Receptor 78
MetS	Metabolic Syndrome
TGs	Triglycerides
HDL	High-Density Lipoprotein
LDL	Low-Density Lipoprotein
LPS	Lipopolysaccharides
TLR4	Toll-like Receptor 4
NGT	Normal Glucose Tolerance
LPL	Lipoprotein Lipase
GLUT4	Glucose Transporter Type 4
GLP-1	Glucagon-Like Peptide-1
GIP	Glucose-Dependent Insulinotropic Polypeptide
CMD	Cardiometabolic Disease
DOCA	Deoxycorticosterone Acetate
Rasal1	Renin-Angiotensin System Protein Activator-Like 1
Cyp4a14	Cytochrome P450 Family 4 Subfamily α Polypeptide 14
CCK	Cholecystokinin
Egr1	Early Growth Response-1
AC3	Adenylate Cyclase Type 3
ApoE	Apolipoprotein E
NF-κB	Nuclear Factor Kappa B
CCL2	Chemokine (C-C motif) Ligand 2

CMT	Cecal Microbial Transplantation
MI	Myocardial Infarction
LAD	Left Anterior Descending Coronary Artery
CHF	Chronic Heart Failure
ICM	Ischemic Cardiomyopathy
DCM	Dilated Cardiomyopathy
4-HNE	4-Hydroxynonenal
LCFAs	Long Chain Fatty Acids
CPT-1	Carnitine Palmitoyltransferase-1
FAO	Fatty Acid Oxidation
BHB	β-Hydroxybutyrate
TAC	Transverse Aortic Constriction
PAAC	Partial Abdominal Aorta Constriction
TCA	Tricarboxylic Acid
WD	Western Diet
NC	Normal Chow
HFHS	High Fat High Sucrose
BMI	Body Mass Index
rRNA	Ribosomal Ribonucleic Acid
ATP	Adenosine Triphosphate
STZ	Streptozotocin
OCR	Oxygen Consumption Rate
iPSCs	Induced Pluripotent Stem Cells

HSkMC	Human Skeletal Muscle Cells
LAT1	L-Type Amino Acid Transporter 1
LAT2	L-Type Amino Acid Transporter 2
BCAAs	Branched Chain Amino Acids
BCAT	Branched-Chain Amino Acid Transferase
BCKA	Branched-Chain α-keto Acid
KIV	α-Ketoisovaleric Acid
KIC	α-Ketoisocaproic Acid
KMV	3-Methyl-2-Oxovaleric Acid
BCKDH	BCKA Dehydrogenase Complex
PP2Cm	Protein Phosphatase 2Cm
BDK	BCKD Kinase
P.copri	Prevotella Copri
PBS	Phosphate Buffer Saline
KLF15	Krüppel-like factor 15
MAPK	Mitogen-Activated Protein Kinase
PBMCs	Peripheral Blood Mononuclear Cells
ECs	Endothelial Cells
FDR	False Discovery Rate
SR	Sarcoplasmic Reticulum
SERCA	Sarco-/Endoplasmic Reticulum Ca^{2+} ATPase
TSA	Trichostatin A
NG	Nodose Ganglia

UA	Uric Acid
MDA	Malondialdehyde
LDH	Lactate Dehydrogenase

CHAPTER ONE

STATEMENT OF THE PROBLEM

Heart Failure (HF) continues to be one of the main causes of mortality worldwide. It occurs due to an impairment in ventricular filling and/or contraction to pump sufficient blood to the body. HF is a complex disorder that involves many signs and symptoms such as shortness of breath, inability to exercise, fatigue, pulmonary edema, and many others. HF is classified by left ventricle ejection fraction (LVEF) as either heart failure with reduced ejection fraction (HFrEF), where LVEF ≤ 40%, or heart failure with preserved ejection fraction (HFpEF), where LVEF ≥ 50%.

HFpEF is one of the most prevalent medical conditions in the United States, where it accounts for more than half of heart failure patients. HFpEF is a heterogenous disease in which multiple systems such as cardiac, pulmonary, and renal disorders contribute to its clinical pathophysiology. It evolves from different comorbidities such as hypertension, aging, obesity, and type 2 diabetes (T2D) which requires phenotype-specific treatment strategy. The presence of a new pathological identity named “pre-HFpEF” has been recently identified where patients have no signs and symptoms of heart failure, they have normal ejection fraction of >50%, however they show structural abnormalities to their hearts that are similar to those found in clinical HFpEF, such as cardiac hypertrophy. The need to understand and act on the early cardiac changes

observed in pre-HFpEF prior to transition to clinical HFpEF is very critical, therefore this dissertation focuses on investigating the pre-HFpEF stage.

The epidemic of obesity continues to be one of the major health issues in the United States with over 40% of adults being obese. It is one of the key risk factors that contribute to the development of pre-HFpEF and is one of the main comorbidities seen in HFpEF patients with more than 80% of HFpEF patients being obese. Giving rise to a specific pathological entity of obesity associated HFpEF. The physio pathological processes of obesity associated HFpEF involve obesity induced systemic inflammation, cardiomyocyte hypertrophy, oxidative and nitrosative stress, and mitochondrial and metabolic dysfunction all of which contribute to HFpEF's complex clinical pathophysiology. Therefore, the work in this dissertation focuses on obesity associated pre-HFpEF.

An emerging area of research on the link between obesity and cardiovascular diseases (CVDs) is the modulation of gut microbiome and its metabolites. Obesity is known to cause gut microbiome imbalance in which beneficial bacteria is decreased and harmful bacteria is increased. Gut microbiome imbalance has been linked to the development of many CVDs such as hypertension and heart failure with reduced ejection fraction (HFrEF), which has been attributed to the changes in the production of short chain fatty acids (SCFAs). Gut microbiome produces SCFAs mainly butyrate, propionate, and acetate through fermentation of dietary fibers. The supplementation of SCFAs was found to be beneficial in several CVDs through reducing inflammation and oxidative stress, improving metabolic regulation, glucose homeostasis, and lipid metabolism.

The association between gut microbiome and HFpEF development has only recently been explored where gut microbiome composition was found to be significantly altered in HFpEF patients compared to control groups. In addition, there was a significant decrease in the SCFAs producing bacteria in HFpEF patients. However, the molecular mechanisms on the link between gut microbiome modulation, short chain fatty acids reduction and the development of obesity associated HFpEF has yet to be investigated. A recent study by our collaborators showed obese mice (WD-fed mice) to have a significant decrease in their gut bacterial diversity, and that to be improved with fecal microbiome transplantation (FMT) from lean mice, which is used to reconstruct the normal composition and function of gut microbiome. In addition to significant reduction in microbial diversity, they found a significant reduction in butyrate producing bacteria, *Lactobacillus*, in obese mice. As well as a significant increase in butyrate serum levels in obese mice after FMT treatment. Taken together, these data indicate gut microbiome and its metabolite butyrate to be associated with obesity progression and that in turn might play a role in the development of obesity associated HFpEF. Since our main goal is to test whether obesity associated HFpEF progression can be prevented by looking at early changes to the heart in the pre-HFpEF stage and target those for treatment, the central hypothesis for this dissertation is that gut microbiome imbalance plays a significant role in the development and progression of obesity associated pre-HFpEF through changes in the short chain fatty acid butyrate. The goals of this dissertation were to: 1. Determine the effect of gut microbiome modulation by FMT on early cardiac dysfunction in obese pre-HFpEF mice, 2. Determine the effect of the SCFA Butyrate supplementation on early cardiac dysfunction in obesity associated pre-HFpEF,

3. Identify the molecular mechanism(s) by which gut microbiome modulation and butyrate affect cardiac function.

We have developed a diet-induced obesity pre-HFpEF mouse model where mice had normal systolic and diastolic function. However, they developed early cardiac dysfunction and LV hypertrophy that is consistent with pre-HFpEF phenotype. Using this model, we modulated gut microbiome composition with FMT treatment from lean mice and found that to improve gut microbiome diversity, and to significantly improve early cardiac dysfunction and LV hypertrophy. In addition, FMT treatment increased the production of butyrate-producing bacteria of the *Lactobacillus* genera. Therefore, we treated mice with butyrate supplementation and found it to replicate FMT's effects on cardiac function and hypertrophy. We used a combination of molecular biology, cell culture, and transcriptomic approaches and identified the branched chain amino acids (BCAAs) catabolic pathway as a potential molecular mechanism involved in butyrate's improvement of early cardiac dysfunction in obesity associated pre-HFpEF. Defects in BCAAs degradation has been identified as a metabolic contributor to cardiac dysfunction, and that was attributed to increases in reactive oxygen species (ROS) and inflammation.

Our studies reveal a novel molecular mechanism on the connection between gut microbiome modulation, the SCFA butyrate, and defects in BCAAs catabolism. As well as their role in the development of obesity associated pre-HFpEF. We believe our studies will uncover new preventative therapeutics to halt the evolvement and transition of obesity associated pre-HFpEF to clinical HFpEF.

CHAPTER TWO

LITERATURE REVIEW

Heart Failure with Preserved Ejection Fraction

Cardiovascular diseases (CVDs) are the main cause of death worldwide with heart failure (HF) being one of the main disorders associated with CVDs related mortality (WHO, 2021). The ACC/AHA identified four stages of HF that are used for diagnosis, prevention of HF progression, and the development of therapeutics strategies (Table 1).

Table 1. The ACC/AHA Stages of HF

Stages of HF	Definition
Stage A: At risk for HF	Patients have hypertension, obesity, diabetes without structural changes to their heart of HF symptoms
Stage B: Pre-HF	Structural changes to the heart. No signs and symptoms of HF
Stage C: Symptomatic HF	Structural changes to the heart with symptoms of HF
Stage D: Advanced HF	HF symptoms that hinder everyday life with repeated hospitalization even with medical therapy

Heart failure with reduced ejection fraction (HFrEF)/systolic HF, where left ventricle ejection fraction (LVEF) is ≤40% due to its inability to properly contract and supply the body with blood, was the main type of heart failure until the 1970s where a

group of patients with symptoms of HF and normal LVEF of ≥50% were identified(1-4). This condition was initially termed diastolic HF; however, it was found to involve both systolic and diastolic dysfunction which led to a change in its name to heart failure with preserved ejection fraction (HFpEF) (5-7). HFpEF currently accounts for more than 50% of HF patients, and its prevalence continues to rise due to insufficient understanding of its complex pathophysiology that hinders the ability to find and develop effective therapies(8-10). It is characterized by impaired left ventricle (LV) relaxation during diastole due to stiffness of the LV and reduced compliance that requires higher filling pressure during diastole, LV hypertrophy, inflammation, endothelial dysfunction, and elevated natriuretic peptides (11-17). Furthermore, HFpEF is a heterogenous disease where dysfunctions in multiple different organs, in addition to cardiac abnormalities, contribute to its clinical pathophysiology and give rise to different symptoms and outcomes. This includes pulmonary and renal failure, skeletal muscle abnormalities, vascular insufficiency, and immune and metabolic dysfunctions(13, 18-23).

The Paradigm and Mechanisms of HFpEF Pathophysiology

The paradigm of HFpEF pathophysiology starts with the presence of different comorbidities such as obesity, type 2 diabetes (T2D), hypertension, chronic obstructive pulmonary disease (COPD), and chronic kidney disease (CKD) that induce systemic inflammation(4, 9, 11-13, 19, 24, 25). The intracardiac mechanisms involve chronic inflammation that leads to myocardial remodeling and cardiac fibrosis by interfering in the endothelium-cardiomyocyte signaling process. This is manifested by the increase in the endothelial expression of adhesion molecules such as vascular cell adhesion molecule (VCAM) and E-Selectin. These molecules allow the infiltration of leukocytes

into the interstitial space between the endothelium and cardiomyocytes. Leukocytes then secrete transforming growth factor β (TGF-β), which converts fibroblasts into myofibroblasts that increase the production of extracellular matrix (ECM) components such as collagen(26-30). In addition to myocardial remodeling and fibrosis, cardiac inflammation leads to cardiac hypertrophy by interfering with the NO–cGMP–PKG pathway. This occurs through increase in the production of reactive oxygen species (ROS) that in turn decrease the production of nitric oxide (NO), cyclic guanosine monophosphate (cGMP) content, and protein kinase G (PKG) activity in cardiomyocytes. This causes hypo-phosphorylation and stiffening of titin, the sarcomere protein responsible for muscle elasticity, which in turn contributes to the reduction of LV compliance in diastole(14, 31, 32). The increase in oxidative and nitrosative stress is also seen in HFpEF hearts due to systemic inflammation and mitochondrial dysfunction(21, 28, 33-36). Increase in nitrosative stress is linked to dysfunction in the IRE1α–XBP1 signaling pathway which in turn decreases the unfolded protein response (UPR), increases the accumulation of unfolded proteins and endoplasmic reticulum (ER) stress(33, 37-41).

Extracardiac comorbidities play a significant role in HFpEF development(1, 19, 20). This includes:

- Obesity and T2D causing mitochondrial metabolic defects, inflammation, oxidative stress, lipotoxicity, and exercise intolerance(42-47)
- Skeletal muscle metabolic dysfunction due to reduction in skeletal muscle oxidative capacity reduces ATP production needed for muscle contraction, which causes exercise intolerance(48-52)

- Hypertension, which contributes to increase inflammation, oxidative stress, cardiac hypertrophy, and fibrosis(53-56).
- Pulmonary hypertension and renal failure(57-62).

HFpEF Animal Models and Therapies

This clinical paradigm of HFpEF is significantly different from that of HFrEF which explains the inability of conventional heart failure therapeutics in treating HFpEF(11, 20, 42, 63). The management of associated chronic diseases using a combination of exercise, caloric restriction, diuretics, and beta blockers have been proposed as a strategy to attenuate HFpEF progression(13, 19, 64-66). However, this approach has shown no significant success in reducing HFpEF progression and mortality rates(13, 67). In addition to its complex clinical pathophysiology, a major challenge in the development of successful treatments for HFpEF was the absence of animal models that recapitulates its complexity(19, 68). More recently, three mice models were shown to resemble human clinical HFpEF (Table 2).

The HFD+L-NAME model induced metabolic (obesity) stress with a diet that consisted of >60% fat, and mechanical (hypertension) stress using the inhibition of nitric oxide synthase (NOS)(41).

The HFD+aging+AngII model added the aging element, where mice were 18-22 months of age, to the metabolic stress (obesity induced by high fat diet >60% fat) and mechanical stress (hypertension induced by AngII infusion for chronic stimulation of AngII receptor)(69).

The HFD+aging+DOCP model used 16 months aging mice in addition to high fat diet >60% fat, and desoxycorticosterone pivalate to induce hypertension(70).

Table 2. HFpEF Mouse Models. Current mouse models that recapitulate signs and symptoms of clinical human HFpEF. HFD, high fat diet; L-NAME, Nω-nitro- l-arginine methyl ester; AngII, Angiotensin II; DOCP, desoxycorticosterone pivalate, T2D; type 2 diabetes

Model	EF	Comorbidities	Exercise Intolerance	Diastolic Dysfunction	Lung Congestion	Renal Failure
HFD+L-NAME	Normal	Hypertension, Obesity, T2D	Yes	Yes	Yes	N/A
HFD+Aging+AngII	Normal	Hypertension, Obesity, T2D	Yes	Yes	Yes	N/A
HFD+Aging+DOCP	Normal	Hypertension, Obesity, T2D	Yes	Yes	Yes	N/A

The presence of HFpEF mice models provides a great avenue for understanding the molecular mechanisms as well as testing potential therapeutics of HFpEF. However, many aspects must be taken into consideration when using these models such as the differences in the physiology between the mouse and human heart, and the disease's heterogeneity with other comorbidities that give rise to distinct clinical symptoms which requires the development of phenotype-specific treatments(13, 65). Recently, the use of sodium-glucose cotransporter 2 (SGLT2) inhibitors has shown promising results in alleviating HFpEF symptoms using randomized clinical trials(71). SGLT2 inhibitors are used for the treatment of T2D(72-75), they lower blood sugar levels by blocking the kidney's reuptake of glucose and increasing its excretion in the proximal renal tubule(76). The EMPEROR-Preserved trial provided a positive outcome in reducing the risk of mortality and hospitalization of HFpEF patients after treatment with the sodium-glucose cotransporter 2 (SGLT2) inhibitor empagliflozin(77). These results were confirmed by the PRESERVED-HF trial. HFpEF patients were given the SGLT2 inhibitor dapagliflozin and had significant improvement in heart failure symptoms as well as exercise capacity(78). The molecular mechanisms involved in SGLT2 inhibitors

beneficial effects on HFpEF are still under investigations. Some of the proposed mechanisms of SGLT2i are increasing in myocardial energy production, reducing systemic inflammation and oxidative stress, improving insulin resistance, and activating fatty acid oxidation(79-84). However, more studies need to be performed to further confirm these suggested mechanisms.

Despite these positive findings, another possible approach to better understand and halt the pathogenesis of clinical HFpEF is focusing on the asymptomatic pre-HFpEF stage were patients have no sign and symptoms of HF but have structural abnormalities to their heart that are similar to those in clinical HFpEF patients, as well as an increase in cardiac dysfunction biomarkers(19, 85-87). Some of the proposed main abnormalities involved in the transition from pre-HFpEF to clinical HFpEF are pulmonary hypertension, atrial failure, kidney dysfunction, and systemic inflammation(88). Addressing and targeting these abnormalities in the pre-HFpEF stage might provide a better therapeutic approach that prevents further HFpEF progression.

Obesity Associated HFpEF

Obesity and T2D are two of the main drivers of HFpEF development where more than 80% of HFpEF are obese/overweight giving rise to a distinct phenotype called “obesity associated HFpEF”(89-94). The pathophysiology of obesity associated HFpEF include hemodynamic effects, neurohormonal effects and inflammatory effects. The hemodynamic effects include increase in plasma volume, LV mass, LV hypertrophy, and LV filling pressure(46, 91, 95-98). The neurohormonal effects include the increase in sympathetic nervous system activity, renin-angiotensin-aldosterone system (RAAS) activation, sodium retention, and hypertension(89, 93, 99).

The inflammatory effects occur due to visceral adiposity's increase in proinflammatory cytokines like tumor necrosis factor- α (TNF- α) and interleukin-6 (IL-6) which leads to chronic systemic inflammation. In addition, epicardial adiposity increases proinflammatory cytokines such as IL-1 β, IL-6, and TNF-α leading to cardiac inflammation(89, 100-106). As discussed previously, chronic inflammation leads to endothelial dysfunction, cardiac fibrosis, and decrees in NO availability in HFpEF patients. There are many promising potential therapeutics for obesity associated HFpEF including weight loss via caloric restrictions and exercise, as well as SGLT2 inhibitors and anti-inflammatory medications. However, due to HFpEF's heterogeneity more studies are required to investigate whether targeting obesity alone is enough to alleviate the many dysfunctions seen in obese HFpEF patients.

Gut Microbiome and Short Chain Fatty Acids

One of the main effects of obesity and T2D is gut dysbiosis, an imbalance in the gut microbiome composition and diversity which occur either due to loss of good bacteria, having too much growth of harmful bacteria in the stomach, or loss of overall gut microbiome diversity (both good and bad bacteria are lost)(107-110). The gut microbiome consists of trillions of micro-organisms present in the gastrointestinal (GI) tract that play an important role in metabolism and immune function(111-113). It includes five phyla (Bacteroidetes, Firmicutes, Actinobacteria, Proteobacteria and Cerrucomicrobia), where Bacteroidetes and Firmicutes make up about 90% of healthy gut microbiome(114). The Firmicutes/Bacteroidetes ratio is a known marker of gut dysbiosis, and it had been shown to be significantly higher in obese patients due to increase in the levels of Firmicutes and a decrease in the levels of

Bacteroidetes(107, 108, 115-117). Interestingly, calorie-restricted diet (low fat, low carbohydrate diets) normalized the Firmicutes/Bacteroidetes ratio in addition to weight loss in obese individuals(108, 117-119). Gut dysbiosis has been associated with many diseases in addition to obesity and T2D such as irritable bowel syndrome (IBS), inflammatory bowel diseases (IBD), multiple sclerosis (MS), Alzheimer's and Parkinson's diseases, as well as cardiovascular diseases(112, 120-126).

Gut microbiota produces its metabolites the short chain fatty acids (SCFAs), small monocarboxylic acids made of up to six carbons, in the large intestines through anaerobic fermentation of indigestible food such as dietary fibers(127-129). The main SCFAs produced are butyrate (C4), propionate (C3), and acetate (C2) (Figure 1)(127-132). Their main function, in particular butyrate, is to provide energy for epithelial cells and maintain gut integrity(133-136) through their absorption by the colonocytes via non-ionic diffusion, H^+-dependent monocarboxylate transporters (MCTs), or sodium-dependent monocarboxylate transporters (SMCTs)(137-139) (Figure 2). SCFAs that are not metabolized in colonocytes are used as energy sources for hepatocytes after being transported through the portal vein into the liver. SCFAs can reach the systemic circulation directly by being absorbed into the inferior vena cava (132, 136, 140) (the largest vein in the human body which carries venous blood from the lower limbs and abdominopelvic regions to the heart). The systemic concentration of SCFAs relies largely on diet patterns which affects their production and absorption rates. A diet rich in fiber increases SCFAs production. Meanwhile, westernized diet consisting of high saturated fats, refined grains, high sugar, and high salt lead to gut dysbiosis and decrease in SCFAs production(141-145).

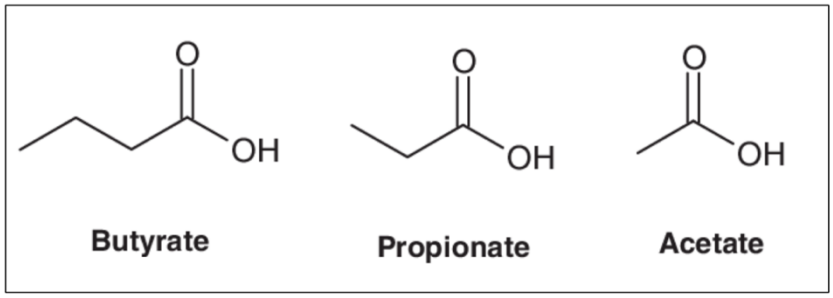

Figure 1. The Chemical Structure of the Most Abundant SCFAs Butyrate, Propionate, and Acetate.

SCFAs signaling occurs through multiple pathways such as binding to G protein-coupled receptors (GPCRs), GPR43 and GPR41 also called free fatty acid receptors FFAR2 and FFAR3, respectively (Figure 2). These receptors were found to be expressed in many tissues including the colon, white adipose tissue (WAT), skeletal muscles, and the liver(146-150). Butyrate is shown to bind to GPR109a/HCAR2 (hydrocarboxylic acid receptor) which is expressed in gut epithelial cells, immune cells, and adipocytes(151-154). Additionally, acetate and propionate bind to olfactory receptor (Olfr) 78 which is mainly found in the kidneys and blood vessels(155-157).

In addition to binding to GPCRs, SCFAs play a role in epigenetic regulation through inhibition of histone deacetylation (HDAC)(158-160). This increases the acetylation of lysine residues and transforms the chromatin from condensed to relaxed state, and in turn increases gene transcription (Figure 2). Among the SCFAs, butyrate is most known for its HDAC inhibition activity. It has been shown to change the expression of many genes involved in cell proliferation, differentiation, apoptosis, and inflammation(161-165).

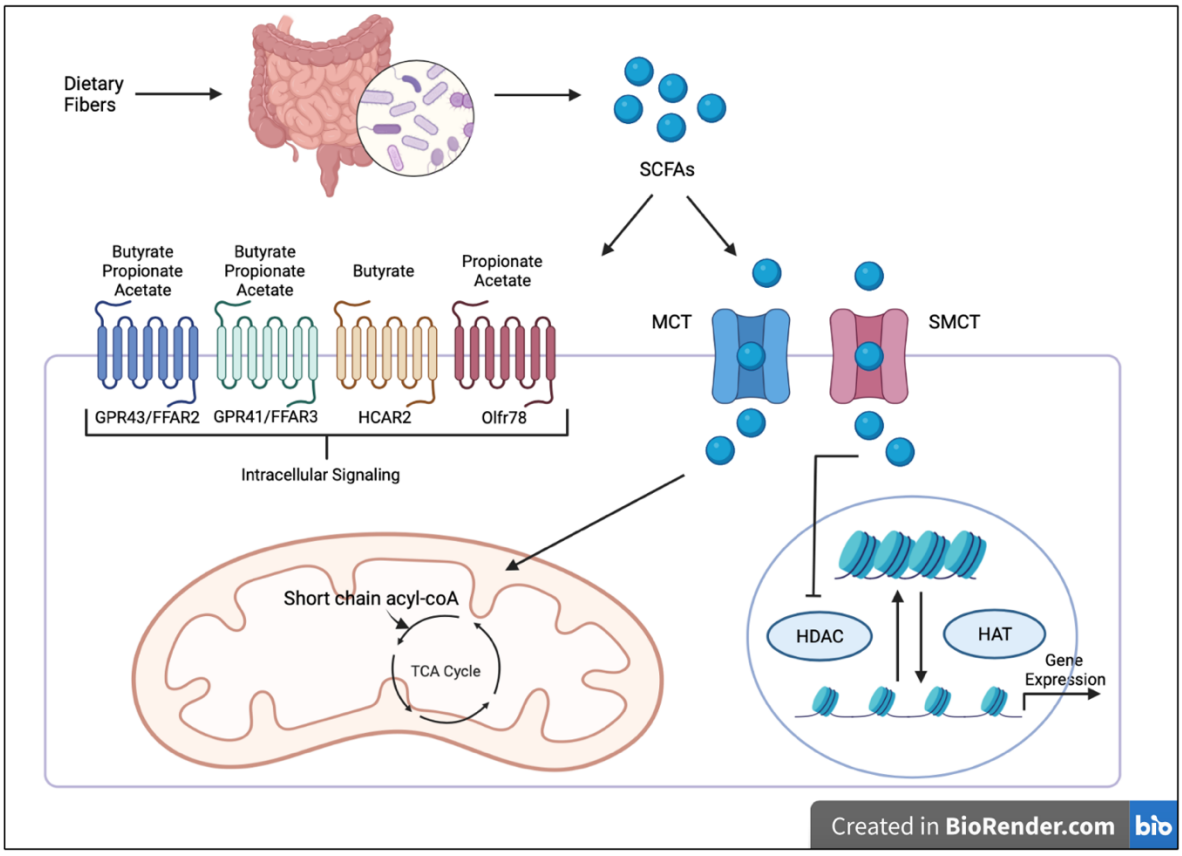

Figure 2. SCFAs Molecular Mechanisms and Functions. Dietary fibers are fermented in the intestines by the gut microbiome to produce the metabolites SCFAs (Butyrate, propionate, and acetate). SCFAs enter the cells through monocarboxylate transporters (MCTs), or sodium-dependent monocarboxylate transporters (SMCTs). In the nucleus they act as HDAC inhibitors to increase gene transcription and expression. In the mitochondrial, they participate in metabolism by undergoing β-oxidation and generating acetyl coA that enters the TCA cycle and produce energy (ATP). SCFAs bind to several GPCRs (GPR41/43, HCAR2, and Olfr78) with specific affinity leading to the activation of many intracellular signaling pathways.

Studies have shown that alterations in gut microbiome and SCFAs is involved in the development of many diseases such as metabolic syndrome (obesity, T2D, and dyslipidemia)(136, 166-169) and cardiovascular diseases including hypertension, atherosclerosis, coronary artery disease, myocardial infarction, and heart failure(123-126, 129, 170-180).

Therapeutic Interventions for Gut Dysbiosis

There are several therapeutic interventions to modulate and reconstruct the normal composition and function of gut microbiome including: 1) fecal microbiome transplantation (FMT); the introduction of fecal contents from healthy donors into the GI tract of patients. In obese/overweight individuals, FMT from lean donors led to significant decrease in insulin sensitivity and improved glucose homeostasis(167, 168). 2) Probiotics, prebiotics, and antibiotics supplementation(122, 177, 181); probiotics are live bacteria isolated from humans and cultured in a lab, while prebiotics are non-bacterial compounds that stimulate the growth and activity of 'good' bacteria. Administration of probiotics were shown to alleviate HFD-induced obesity, insulin resistance and liver lipid accumulation in mice(182). Prebiotics administrations were shown to improve gut permeability, reduce inflammation and improve glucose intolerance(183). Antibiotics are used to eliminate harmful bacteria allowing the increase of good bacteria. The use of antibiotics has been shown to reduce gut permeability, metabolic endotoxemia, and inflammation(166). However, the use of antibiotics to modulate the gut microbiome can be tricky due to inability of these antibiotics to be specific in eliminating only "bad" bacteria without affecting other types of microbiomes. Therefore, this type of intervention should be used as a last resort to other therapeutics. 3) Dietary changes; this includes the implementation of fiber-rich diet to increase the production of beneficial bacteria. A high fiber diet was shown to be beneficial by lowering blood pressure and decreasing cardiac fibrosis and hypertrophy, as well as improving insulin sensitivity(174).

Gut Microbiome and Metabolic Disorders

Metabolic syndrome (MetS) refers to a group of conditions including abdominal obesity, high blood sugar levels, and dyslipidemia (high blood triglycerides (TGs) and low high-density lipoprotein (HDL) “good” cholesterol levels). These conditions increase the risk of development coronary artery disease, stroke, and diabetes(184). A study by Vrieze A. et al, altered the gut microbiome composition by performing intestinal microbiota infusion from lean donors to patients with metabolic syndrome. They found that after 6 weeks of microbial infusion, patients with MetS had significant improvement in their insulin sensitivity (Higher insulin sensitivity permits the body reduce blood sugar levels by using blood glucose more effectively). This was associated with increase in microbial diversity and butyrate producing bacteria, which pointed to an important role for gut microbiome derived butyrate in metabolic regulation and insulin sensitivity(168).

Several studies confirmed an association between gut microbiome, diet changes, and obesity. Obese individuals were found to have significant increase in the levels of Firmicutes and a decrease in Bacteroidetes compared to lean controls(107, 108). In support of these findings, mice that developed obesity due to HFD or leptin (the hormone responsible for appetite control) deficiency (*ob/ob*) had a gut microbiome depleted of Bacteroidetes and enriched in Firmicutes(116). However, when obese mice were placed on calorie-restricted (fat-restricted or carbohydrates-restricted) diets, their Firmicutes gut microbiome levels were significantly decreased while Bacteroidetes were increased(118).

Interestingly, MetS associated gut microbiome alterations were correlated with increased inflammation and inflammatory markers. Cani et al. were first to investigate

the association between gut microbiome and metabolic endotoxemia-induced inflammation(166). Metabolic endotoxemia is known to induce systemic inflammation in HFD and *ob/ob* induced obesity due to structural changes in the intestinal epithelium that acts as a barrier to prevent the release of lipopolysaccharides (LPS) into the bloodstream(185). LPS activates Toll-like receptor 4 (TLR4) which increases the production of pro-inflammatory cytokines(186). They found HFD and *ob/ob* mice to have increase in gut permeability, LPS plasma levels, pro-inflammatory cytokines levels, and oxidative stress in visceral adipose tissue. In addition, glucose-induced insulin secretion, insulin resistance, body weight gain, total energy intake, and visceral and subcutaneous adipose weight were significantly increased in obese mice. However, they found that gut microbiome modulation with antibiotics (Ampicillin and neomycin), an approach to eliminate diseases-causing bacteria and increase “beneficial” bacteria, were able to reverse all these parameters in obese mice(185).

Another MetS condition that has been associated with gut microbiome modulation is dyslipidemia. This condition is manifested by the increase of circulating TGs, low-density lipoprotein (LDL) “bad” cholesterol, and decrease in HDL “good” cholesterol plasma levels(187). Zhang P. et al, studied the association between gut microbiome modulation and lipid metabolism in *db/db* mice, a common mouse model used to study diabetic dyslipidemia, using FMT from individuals with normal glucose tolerance (NGT). They found FMT-treated db/db mice to have significant changes in their phenotypes where they had a significant decrease in fasting blood glucose, postprandial glucose, total cholesterol, TGs, and LDL levels. Whereas there was a significant increase in HDL levels(167).

In summation, many human and animal studies show a correlation between MetS and gut microbiome composition. This includes a positive correlation between increase in gut microbiome diversity and richness and a decrease in metabolic induced inflammation, dyslipidemia, insulin resistance, weight gain and many other metabolic effects.

SCFAs and Metabolic Syndrome

One of the main proposed mechanisms on the association of gut microbiome modulation with MetS is changes in levels of the metabolites SCFAs (butyrate, propionate, and acetate). SCFAs were shown to protect against DIO by promoting weight loss through decreasing food intake, increasing fatty acid oxidation and energy expenditure(136, 188-190)(the amount of energy required to perform essential body function such as breathing, digestion, and circulation).

Butyrate acts as the main source of energy for intestinal epithelia cells which maintains the gut barrier integrity, controls gut permeability, and in turn helps in preventing the release of LPS into the circulation and decreases inflammation. In addition, butyrate has been shown to decrease the levels of pro-inflammatory markers such as VCAM, E-selectin, TNF-α as well as the expression of proinflammatory cytokines through its HDAC inhibition activity(133, 191-195). A study by Gao Z. et al, showed that butyrate supplementation of HFD fed mice increased their insulin sensitivity, decreased adiposity, and improved energy expenditure. This occurred through improvement in mitochondrial function due to induction of peroxisome proliferator–activated receptor (PPAR)-γ coactivator PGC-1 activity in skeletal muscle, brown fat, and liver(196).

Badejogbin C. et al. found that Wistar female rats fed high fat diet developed metabolic disorders indicated by dysregulation in glucose metabolism, increased levels of triglycerides, cholesterol, corticosterone, malondialdehyde (MDA), plasma and cardiac Uric Acid (UA), and lactate dehydrogenase (LDH). They also had significant increase in cardiac tissue infiltration and fibrosis. However, sodium butyrate treatment protected against the development of cardiometabolic disorders. The group identified the inhibition of UA as a possible mechanism involved in butyrate's effects on cardiometabolic changes, which in turn led to significant decrease in oxidative stress in obese Wistar female rats(197).

Propionate was found to reduce obesity-related inflammation and improve glucose uptake and lipid metabolism in visceral adipose tissue. Al-Lahham S. et al, show that propionate treatment of omental adipose tissue explants from obese individuals significantly decreased the levels of pro-inflammatory cytokines such as TNF-α, and reduced chemokines levels which leads to the decrease in the infiltration of immune cells into adipose tissue and inhibits inflammation. In addition, they found propionate to be involved in lipid and glucose metabolism where propionate treatment led to increase in lipoprotein lipase (LPL), the enzyme that degrades TGs in the blood, and Glucose transporter type 4 (GLUT4), the transporter that is responsible for insulin-regulated glucose uptake(198).

Lin H. et al, found both butyrate and propionate to reduce food intake and protect against weight gain and glucose intolerance in HFD-fed mice. These effects were independent of binding to the GPCR FFAR3 in the gut. They found butyrate and propionate supplementations to significantly increase the levels of gut hormones

Glucagon-like peptide-1 (GLP-1) and Glucose-dependent insulinotropic polypeptide (GIP), that play a key role in regulating energy and glucose metabolism(199). However, the mechanisms involved in SCFAs regulating gut hormones was dependent on FFAR3. Therefore, other signaling mechanisms might be involved in butyrate and propionate's beneficial effects such as binding to FFAR2 or HDAC inhibition activity.

In summary, many studies show positive effects of SCFAs on MetS such as obesity and T2D that occur through several mechanisms such as improvement in glucose homeostasis, lipid metabolism, energy expenditure, tissue inflammation, and skeletal muscle and liver function.

Gut Microbiome, SCFAs, and Cardiovascular Diseases

The combination of MetS (insulin resistance, impaired glucose tolerance, dyslipidemia, hypertension, and central adiposity) increase the risk of cardiovascular disease (CVD) (hypertension, atherosclerosis, myocardial infarction, and heart failure) and leads to the development of cardiometabolic disease (CMD)(200-202). Therefore, the association between gut microbiome imbalance, SCFAs, and cardiovascular disease has been an active area of research.

Gut Microbiome and SCFAs in Hypertension and Atherosclerosis

A study by Li et al. showed a direct correlation between gut microbiome and hypertension. By performing 16S sequencing analysis they found gut microbiome composition and diversity to be significantly altered in hypertensive and pre-hypertensive patients compared to control groups. In addition, they performed gut microbiome transplantation from either control or hypertensive patients into germ free mice and found hypertension recipient mice to have significant increases in their systolic

blood pressure, diastolic blood pressure and mean blood pressure compared to control recipient mice. These findings were associated with increase in inflammation, and a decrease in fatty acid oxidation and energy production(172). Similarly, a study by Yang et al. found hypertensive mice to develop gut dysbiosis where they had a decrease in microbial richness and diversity, an increase in the Firmicutes/Bacteroidetes ratio, and a decrease in acetate- and butyrate-producing bacteria. In addition, they found treatment of hypertensive mice with the anti-hypertension medication minocycline to lower blood pressure and reduce the Firmicutes/Bacteroidetes ratio. Indicating a clear direct association between gut dysbiosis and hypertension(176).

Marques F. et al, showed high fiber diet and acetate supplementation in deoxycorticosterone acetate (DOCA)–salt hypertensive mice led to significant decreases in Firmicutes/Bacteroidetes ratio, systolic and diastolic blood pressure, cardiac fibrosis, and left ventricle hypertrophy. Since SCFAs have a role in regulating gene expression, they investigated whether these improvements occurred through regulation of hypertension-causing gene transcription in the heart and kidneys. They performed RNA sequencing on cardiac and renal transcriptomes of mice fed control diet, high-fiber diet, or acetate. In the kidneys, both high fiber and acetate diets increase the expression of renin-angiotensin system protein activator-like 1 (*Rasal1*), associated with renal fibrosis, cytochrome P450 family 4 subfamily α polypeptide 14 (*Cyp4a14*), associated with regulation of fluid absorption via sodium channels, and the anti-inflammatory cholecystokinin (*Cck*) gene. In the heart, high fiber and acetate diets decreased the expression of early growth response-1 (*egr1*), which is involved in cardiovascular pathology including cardiac and renal fibrosis, cardiac hypertrophy, and

inflammation. This study shows a key role of gut microbiome and its metabolites in transcript regulation and hypertension development, through crosstalk between the gut, heart, and kidneys(174).

Alteration in autonomic nervous system (ANS) activity is one of the causes of hypertension development. This occurs due to overactivity of the sympathetic nervous system (SNS) and/or augmented parasympathetic nervous system (PNS) activity(203-208). In addition, the gut is known to be innervated by sympathetic nerves, which indicates an association between gut function and hypertension development due to SNS activity(173, 209-211). Santisteban et al. showed that both spontaneously hypertensive rats (SHR) and AngII-infused hypertensive rats had increased in gut permeability compared to controls. In addition, SHR and Ang-II infused mice had significant increase in Firmicutes, and significant decrease in Bacteroidetes indicating gut dysbiosis. To further confirm the association between gut permeability and hypertension they treated hypertensive rats with the anti-hypertension medication ACE inhibitor and found it to reduce blood pressure and gut permeability. This association between increase in gut permeability and hypertension was due to increase in the activity of the splanchnic sympathetic nerve innervating the gut in hypertensive animals(173).

In another mechanistic study on the link between gut microbiome metabolites SCFAs and blood pressure regulation, Natarajan N. et al show that SCFAs regulate blood pressure by binding to GPR41/FFAR3 located in the vascular endothelium. In another study by the same group, they found GPR41$^{-/-}$ knockout mice to have significantly higher blood pressure compared to control mice. Additionally, when they

added propionate supplementation, they found propionate's effect on lowering bloop pressure to be eliminated in GPR41$^{-/-}$ and not GPR41$^{+/-}$(178).

Furthermore, Pluznick J. et al, show that SCFAs can directly regulate blood pressure by binding to GPR41/GPR43, activating Gαi and/or Gαo and decreasing cyclic adenosine monophosphate (cAMP), thereby inducing vasodilation, and lowering blood pressure. Interestingly, SCFAs can increase blood pressure by binding to olfr78 receptors, which when activated it activates adenylate cyclase type 3 (AC3) and G_{olf} to induce cAMP production(155, 156). This opposite effect of SCFAs on blood pressure could be explained by their different affinities to different receptors based on their body levels. For example, basal concentrations of SCFAs could activate GPR41 to induce vasodilation and lower blood pressure; contrarily, higher concentrations of SCFAs could activate Olfr78 to increase renin release, induce vasoconstriction and blood pressure. However, more studies are needed to confirm these effects and to investigate whether these receptors act differently depending on the tissue type.

Another potential mechanism for SCFAs effects on blood pressure is through anti-inflammation. Bartolomaeus H. et al, showed propionate to protect against cardiac damage in hypertensive and atherosclerotic mice. Hypertension was induced in WT mice with Angiotensin II infusion while apolipoprotein E KO mice (ApoE$^{-/-}$) infused with Angiotensin II were used to develop atherosclerosis. They found propionate to decrease cardiac hypertrophy, hypertension, cardiac fibrosis, and cardiac dysfunction in both mice models. In addition, propionate reduced the atherosclerotic regions in ApoE$^{-/-}$ mice. They concluded that propionate's beneficial effects were due to its inhibition of

systemic inflammation, vascular inflammation, and reduction of immune cells infiltration in the heart(175).

Aguilar E.C. et al, looked at a direct role of SCFAs on atherosclerosis development using ApoE$^{-/-}$ mice. they found butyrate supplementation to reduce atherosclerosis in the heart by 50%. This was associated with inhibition of endothelial cells activation by decreasing proinflammatory cytokines production (TNF-α, IL-1β and IL-6) due to inhibiting the activation of nuclear factor kappa B (NF-κB). Additionally, they found butyrate supplementation to decrease the infiltration and migration of macrophages in the atherosclerotic regions by decreasing the levels of adhesion molecules VCAM-1 and chemokine (C-C motif) ligand 2 (CCL2)(195).

These studies provide insight on the association between gut microbiome and SCFAs and the development of hypertension and atherosclerosis, they also support a possible role for gut microbiome modulation and SCFAs supplementation as anti-hypertensive and atherosclerosis therapeutic agents.

Gut Microbiome and SCFAs in Postinfarction Cardiac Repair

Battson M. et al, used the *ob/ob* genetic model of obesity which has a homozygous mutation in leptin, the hormone responsible for appetite control, to investigate the association between gut microbiome composition and cardiovascular dysfunction. *ob/ob* mice were shown to have significant alterations in their gut microbiome composition compared to lean control mice. They showed a significant attenuation of infarct size in *ob/ob* mice after myocardial ischemia reperfusion injury following cecal microbial transplantation (CMT) from lean mice. Whereas they found microbial transplantation from obese mice to lean control mice to increase infarct size.

This indicates that the tendency to develop injury after ischemia reperfusion is affected by gut microbiome composition. In addition, they found aortic stiffness to be significantly reduced in *ob/ob* mice after CMT from lean mice. These cardiovascular beneficial effects after CMT were also associated with changes in the levels of SCFAs, which were increased in *ob/ob* mice after control CMT(179).

In another study by Tang W.H. et al, gut microbiome and its metabolites SCFAs were found to be associated with cardiac repair and survival rate after myocardial infarction (MI). They treated mice with antibiotic to deplete their gut microbiome prior to MI induction with left anterior descending coronary artery (LAD) ligation. They found depletion of gut microbiome to increase mortality after MI, and reconstitution of gut microbiome with fecal microbiome transplantation to improve survival rates in mice after MI by 67%. The group proposed that this effect of gut microbiome on cardiac repair and survival rate was through modulation of immune cells including myeloid cells and neutrophils, which were reduced in MI mice treated with antibiotics but restored after gut microbiome transplantation. The group found that depletion of gut microbiota decreased the levels of SCFAs acetate, butyrate, and propionate in serum and fecal samples. By supplementing mice with these SCFAs before MI, they found them to be effective in increasing the survival rate in mice by 50%. Like findings with gut microbiome depletion, SCFAs supplementation modulated immune response post-MI(180).

Gut Microbiome and SCFAs in Heart Failure

Due to the involvement of gut microbiome and SCFAs in hypertension, atherosclerosis, and MI, researchers have investigated the association of gut dysbiosis in the development of heart failure which led to the formation of “gut hypothesis of heart

failure”(212). Luedde M. et al, investigated changes in gut microbiome of HFrEF patients using 16S rRNA sequencing. They found HFrEF patients to have significant decrease in their gut microbiome diversity compared to control group(213). Cui X. et al, performed a combination of fecal and plasma metagenomic analyses from chronic heart failure (CHF) [composed of ischemic cardiomyopathy (ICM) and dilated cardiomyopathy (DCM)] and control patients. They found gut microbe composition to be significantly different between CHF patients and control groups, while being very similar between CHF subgroups. Interestingly, they found a significant reduction in butyrate producing bacteria and butyrate-acetoacetate CoA transferase, the main enzyme responsible for the generation of butyrate, in the CHF groups(214). In support of these findings, Kummen M. et al, performed 16S rRNA microbiome gene sequencing and found a significant decrease in gut microbiome diversity and richness in HF patients compared to controls. In addition, they found a significant depletion in the butyrate producing-bacteria, the *Lachnospiraceae* family(215).

Effect of SCFAs on Gut Permeability and Inflammation in Heart Failure

Many studies showed heart failure patients to have disruption in their intestinal epithelia barrier which leads to the formation of “leaky gut” that allows endotoxins and inflammatory cytokines to enter the circulation and in turn contributing to the progression of heart failure(216-219). As mentioned before, butyrate is used as a main energy for gut epithelial cells, maintaining gut integrity and promoting the intestinal barrier function. Therefore, one of the proposed mechanisms on the beneficial effects of butyrate in heart failure is its prevention of leaky gut formation and thus preventing toxins and inflammatory cytokines from entering the circulation. In addition to its effects

on gut epithelial cells, Wang Y. et al. found butyrate to suppresses inflammation by inhibiting the formation and recruitment of adhesion of monocytes VCAM-1 and E-selectin on endothelial cells by suppressing TNF-α. Which in turn reduced inflammation and oxidative stress indicated by decrease in proinflammatory cytokines IL-8 and MCP-1, and 4-hydroxynonenal (4-HNE) which is produced in oxidative stress conditions(191). Butyrate can also act directly on macrophages, the main immune cells involved in inflammation. Activated macrophages release proinflammatory cytokines (TNF-α, IL-1β and IL-6), chemokines, and nitric oxide (NO). Several studies found that incubation of macrophages with butyrate reduced the levels of TNF-α, IL-1β, IL-6, and NO(192, 193).

The main mechanism for these beneficial effects of butyrate on inflammation were due to its HDAC inhibition activity, where it modulates the expression of genes involved in many inflammatory pathways such as NF-κB(164, 220-222).

Effect of SCFAs on Cardiac Metabolism in the Failing Heart

One of the proposed mechanisms on the beneficial effects of SCFAs on the failing heart is their effects on cardiac metabolism. It is known that the heart can use many resources to produce energy (ATP), such as fatty acids (FAs), glucose, ketone bodies, and amino acids(223-226). In the normal heart, long chain fatty acids (LCFAs) are the primary metabolic substrates, providing ~60–90% of myocardial ATPs, through the process of fatty acid oxidation (FAO)(226-228). However, in heart failure FAO is significantly reduced due to impaired activity of the carnitine palmitoyltransferase (CPT1), the enzyme responsible for LCFAs entry into the mitochondria to initiate the process of FAO and ATP production, which results in an energy starved heart and cardiac dysfunction(229-233).

Studies have shown that ketone bodies, such as β-hydroxybutyrate (BHB), can be used as an alternative energy source to FAO in heart failure since they don't rely on CPT1 to enter the mitochondria but rather does so through free diffusion(234-237). However, a recent study by Carley A.N. et al, compared the efficiency of the ketone body BHB and the SCFA butyrate, which also enters the mitochondria through free diffusion bypassing CPT1, as energy substrates in a transverse aortic constriction (TAC) mouse model of heart failure. They found butyrate to be preferentially used over BHB as an energy source in the heart. When provided separately, Butyrate contributed 15% more acetyl-coA entering the tricarboxylic acid (TCA) cycle to produce energy than BHB did. In addition, when they provided a mix of butyrate and BHB, butyrate contributed 75% more acetyl-coA than BHB did(238). These findings offer a key role for butyrate as an alternative energy substrate for ketone bodies oxidation in the failing heart, and a potential therapeutic agent for cardiac dysfunctions associated with cardiac metabolism alterations and decrease in ATP production.

Gut Microbiome and SCFAs in HFpEF

Since research shows a strong correlation between gut microbiome composition, SCFAs and the development of HFpEF risk factors (obesity, T2D, MetS, and hypertension). Recent studies investigated the direct association between gut microbiome, SCFAs and HFpEF progression. Beale A.L. et al, performed bacterial 16S rRNA sequencing of HFpEF patients and control groups. They found gut microbiome diversity and richness to be significantly lower in patients with HFpEF compared to controls. As well as *Firmicutes/Bacteroidetes* ratio to be reduced in the HFpEF group. Additionally, SCFAs producing bacteria, particularly of the genus *Ruminococcus,* were

depleted in HFpEF compared with control groups(239). In support of these findings, Huan Z. et al. found the gut composition of HFpEF patients to be significantly different than that of control participants, with reduction in microbiome diversity and richness in the HFpEF group. They also identified low abundance of several bacterial at the genus level including *Butyricicoccus*, *Sutterella*, *Lachnospira,* and *Ruminiclostridium* in HFpEF patients(240). These studies provide an association between HFpEF development and gut microbiome composition, as well as an in-depth insight into which bacteria are associated with HFpEF.

As mentioned previously, HFpEF is characterized by the presence of impaired relaxation of the LV during diastole due to LV stiffness, hypertrophy, and cardiac inflammation that causes endothelial dysfunction and interstitial fibrosis. Some of the proposed mechanisms of SCFAs effects in HFpEF include: 1) Attenuating LV hypertrophy and fibrosis by inhibiting inflammation, regulating immune cells infiltration and migration, and decreasing the levels and release of proinflammatory cytokines. 2) Effects on hypertension by modulation of blood pressure via regulation of vascular tone (vasoconstriction and vasodilation of blood vessels). In addition, SCFAs can modulate the renin-angiotensin-aldosterone system (RAAS) which in turn indirectly regulate blood pressure. 3) Improvement in MetS (obesity, T2D and dyslipidemia). These effects are likely mediated either through binding to GPCRs (FFAR2/3, olfr78, and HCAR2), or through HDAC inhibition property.

Gap in Knowledge

Several reviews hypothesized SCFAs could play a key role in alleviating HFpEF symptoms and halt its progression. However, the direct effect of gut microbiome

modulation and SCFAs on HFpEF development and the molecular mechanisms involved are yet to be investigated. Studies are needed to test the outcome of gut microbiome modulation and/or SCFAs supplementation and the underlying mechanisms in HFpEF patients. In addition, one of the major gaps in knowledge is the potential therapeutic role of microbiome modulation and SCFAs supplementation in the “pre-HFpEF” stage. The previously mentioned beneficial effects of gut microbiome modulation and SCFAs in reducing obesity, T2D, dyslipidemia, inflammation, cardiac fibrosis, cardiac hypertrophy, hypertension, and improving cardiac metabolism in the failing heart, indicate their potential therapeutic role in the “pre-HFpEF” stage to prevent further progression to clinical HFpEF. Investigating the role of gut microbiome and SCFAs in “pre-HFpEF” is very important to our understanding of the disease pathophysiology and will help facilitate the development of preventative and novel therapeutics of HFpEF. In our study we focus on addressing this gap and we do so through the following approaches:

1) Development of obesity associated pre-HFpEF model of early cardiac dysfunction
2) Investigating the effect of gut microbiome modulation on microbiome composition, SCFA producing bacteria, and early cardiac dysfunction in obese pre-HFpEF mice
3) Investigating the effects of SCFA supplementation on early cardiac dysfunction in obese pre-HFpEF mice and the molecular mechanisms involved

CHAPTER THREE

GUT MICROBIOME MODULATION BY FMT IMPROVED EARLY CARDIAC DYSFUNCTION AND CARDIAC HYPERTROPHY IN OBESE PRE-HFPEF MICE

Introduction

The connection between gut microbiome and heart health has been a promising area of research where many investigators show patients with CVDs to have poor gut health(123-126, 177). This is mostly attributed to bad dietary habits that includes excessive consumption of foods high in fat and sugar and/or not enough consumption of fiber rich foods(109). Obesity is the number one cause of gut microbiome imbalance (gut dysbiosis), where many studies have established a strong association between obesity and disruption in gut health(107, 108, 116). These studies included diet induced obesity (DIO) models such as high-fat diet (HFD) and Western diet (WD) feeding, as well as genetic models of obesity such as *ob/ob* and *db/db* mice(116, 118, 119).

Since obesity is a major risk factor for many CVDs including HFpEF(1, 11, 35, 89-91, 241), defects in gut microbiome have been recently investigated as a contributor in diseases progression. Beale L.A. et al, analyzed the gut microbiome of 26 HFpEF patients and 67 controls using 16s rRNA sequencing. HFpEF patients included both men and women between 40-70 years old, with body mass index (BMI) of 19 to 30.5 kg/m^2 and did not take antihypertensive medications. Control participants were excluded if they had any type of gastrointestinal disease, type 1 or 2 diabetes, or chronic kidney disease. They found HFpEF patients to have significant decrease in the number of

microbes and the type and abundance of microbes compared to controls. HFpEF group also had a significant depletion in their SCFA producing bacteria. These results were associated with dietary and exercise habits, which showed HFpEF patients to have significantly lower dietary fiber consumption compared to controls. In addition, 73% of HFpEF patients did not perform any moderate or vigorous exercise while 75% of control did (239).

In line with these findings, Huang Z. et al. performed high-throughput DNA sequencing of stool samples from 30 HFpEF patients and 30 controls to investigate their gut microbiome composition (Table 3). They found HFpEF patients to have lower microbiome diversity compared to controls. Interestingly, they found gut microbiome composition and diversity to be altered based on different HFpEF etiologies (240).

Table 3. Demographics of HFpEF and Control Groups. Data are provided as Mean±SD or number (percentage). HFpEF; Heart failure with preserved ejection fraction, BMI; body mass index.

Characteristics	HFpEF group	Control group
Age (year)	71.20±9.36	67.03±7.43
BMI (kg/m^2)	23.83±3.04	23.85±2.95
Chronic Heart Disease	15 (50%)	-
Hypertension	25 (83.33%)	-
Hypertrophic Cardiomyopathy	6 (20%)	-

These studies provide a link between gut microbiome health and HFpEF that is associated with overweight/obesity, and unhealthy lifestyle. However, the mechanisms involved are still not know. In addition, it is still not known whether gut dysbiosis is a result of obesity and T2D that contribute to disease development, or whether gut microbiome imbalance plays a causative role in HFpEF progression. Therefore, our

study focused on understanding the role of gut microbiome imbalance caused by diet induced obesity on the progression of HFpEF. To address these questions, we developed an obesity associated pre-HFpEF mouse model that had normal systolic and diastolic function indicated by LVEF and E/A ratio measurements. LVEF refers to the percentage of blood leaving the left ventricle with each contraction (systole), normal LVEF is >50%. E/A ratio represents the LV relaxation during diastole where E wave represents the rapid passive filling of the LV while A wave represents the emptying of the LA into the LV due to atrial contraction. E>A indicates normal diastolic function and E<A means impaired relaxation of the LV to fill with blood properly. However, our pre-HFpEF mice had cardiac structural abnormalities similar to HFpEF that signify early asymptomatic changes in cardiac mechanics that occur in the absence of increased intracardiac pressure. These early changes were detected with global longitudinal strain (%GLS) measurement, which evaluates the myocardium shortening of the LV and reflects the functionality of the LV wall during systole. Previous clinical studies show GLS as a reliable measurement to detect early LV impairment (242-246). Normal %GLS in adults is >18%, where GLS<16% is considered abnormal and between 16-18% is borderline (246). Another evaluation to detect early LV dysfunction is Longitudinal strain rate reverse peak (LSRr s^{-1}), which measures the speed of myocardium deformation over time during diastole (247). GLS and LSRr evaluate early impairments of LV myocardium/wall by revealing how well it is extending to fill with blood during diastole and how well it is contracting to eject blood during systole before reaching diastolic and systolic dysfunctions (248). In addition, our obese pre-HFpEF mice LV showed cardiac hypertrophy/thickened LV muscle by our measurement of LV posterior wall thickness

during diastole (LVPWd mm) (249). Normal LVPWd measurements in mice is 0.64 ± 0.13 (mm) (250).

We further tested two of the key markers of HFpEF development, cardiac nitrosative stress and fibrosis. It is known that alteration in nitric oxide synthase (NOS) activity reduces nitric oxide (NO) availability and in turn leads to nitrosative stress development in human HFpEF hearts (11, 41, 251). The presence of cardiac fibrosis is another marker of HFpEF due to increase inflammatory cytokines infiltration causing increased deposition of collagen into the myocardial interstitial space(11, 29, 30, 252). We found no significant increase in either nitrosative stress or fibrosis markers in the heart of our obese mice further confirming our model as “pre-HFpEF”.

In this study we used our obese pre-HFpEF mice to test whether improving gut microbiome health will influence these cardiac structural changes and we provide evidence for the protective and preventative role of gut microbiome in HFpEF development. Therefore, implementing strategies to improve gut microbiome composition is an important therapeutic approach to eliminate early cardiac abnormalities and prevent further progression to systolic and diastolic dysfunctions.

Results

Diet-Induced Obesity (DIO) Leads to the Development of Early Cardiac Dysfunction and Cardiac Hypertrophy in the Absence of Cardiac Nitrosative Stress and Cardiac Fibrosis, that is Consistent with Obesity Associated Pre-HFpEF Phenotype

The epidemic of obesity in the Western World is highly driven from the excessive consumption of foods that has high saturated and trans-unsaturated fatty acids, high

sugar, and low consumption of fibers from fruits and vegetables. Therefore, the diet-induced obesity (DIO) mouse model is an essential model in studying the association between high fat/high sugar diets and the development of obesity. To induce obesity in our mice we used the Envigo Teklad (TD.88137) western diet that contains high saturated fats (61.8%) and sucrose (34% by weight), with 0.2% total cholesterol and 32% unsaturated fats. Seven-week-old male and female C57BL/6J mice were placed on Normal Chow (NC, Teklad LM-485; 17% kcal from fat, 44.3% carbohydrates by weight) or Western Diet (WD, TD88137, Teklad Diets; 42%kcal from fat, 34% sucrose by weight, and 0.2% cholesterol total) for fourteen weeks (Figure 3A). This duration of WD exposure has been previously shown to induce weight gain and insulin resistance in mice (189, 253) which are key features of diet induced obesity. Then we performed echocardiography to measure cardiac function differences between NC and WD fed mice. We evaluated systolic function by measuring LVEF and diastolic function by measuring E/A ratio. We found no alteration in either LVEF or E/A in WD fed mice compared to their NC littermates (Figures 3B, C respectively). Indicating no systolic or diastolic failure. We further evaluated systolic and diastolic functions using strain analysis by speckle-tracking echocardiography. We measured global longitudinal strain (%GLS), and longitudinal strain rate reverse (LSRr s^{-1}). Both GLS and LSRr were significantly reduced by 3.2% ± 0.99 and -2.4 s^{-1} ± 0.62 respectively in WD fed mice compared to NC (Figures 3D, E respectively). This indicates structural changes to the heart that are associated with early systolic and diastolic dysfunction. In order to evaluate cardiac hypertrophy, we measured LV posterior wall thickness in diastole (LVPWd) and found it to be significantly increased by 0.14 mm ± 0.03 in the WD group

the WD group (Figure 3F). These data indicate that obese mice had abnormal cardiac mechanical properties presented by early cardiac dysfunction and cardiac hypertrophy that has not yet escalated to clinical heart failure. Which in turn is consistent with pre-clinical HFpEF/“pre-HFpEF” phenotype.

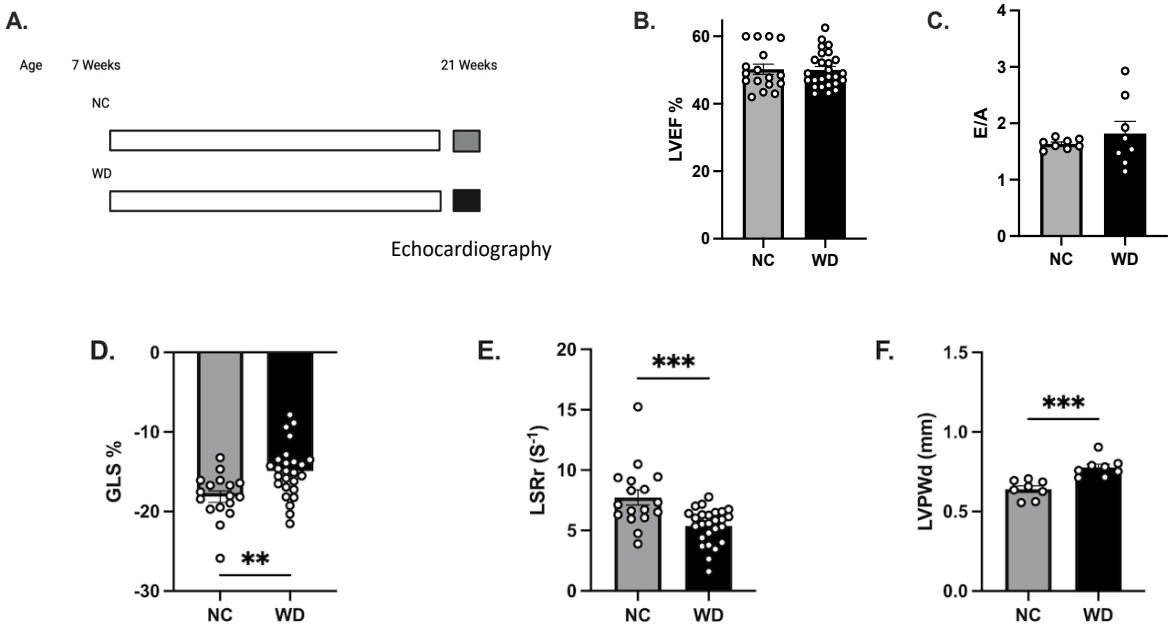

Figure 3. Mice Fed Western Diet (WD) Developed Early Cardiac Dysfunction and Cardiac Hypertrophy. A) experimental paradigm. Normal chow group was fed NC (Teklad LM-485), while the western diet group was fed WD (TD88137, Teklad Diets; 42% kcal from fat, 34% sucrose by weight, and 0.2% cholesterol total; Envigo) for 14 weeks, starting at 7 weeks of age. Echocardiography measurements were performed at 21 weeks of age, B) echocardiography measurement of left ventricle ejection fraction (LVEF), C) ratio between early to atrial diastolic trans mitral flow velocity (E/A), D) global longitudinal strain (%GLS), E) longitudinal strain rate reverse (LSRr) (s-1), F) left ventricle posterior wall diameter during diastole (mm). Statistical analysis was done using unpaired student’s t-test. Data are mean ± S.E.M. (*p<0.05, **p<0.005, ***P<0.0005).

To further validate the pre-HFpEF phenotype, we performed qPCR analysis on mice hearts to measure the gene levels of *nos2* and *col1a2,* the indicators of nitrosative

stress and fibrosis development which are in turn the two distinctive HFpEF markers. We found no changes in the levels of either *nos2* or *col1a2* between WD and NC fed mice (Figure 4A, B respectively). Indicating no development of nitrostive stress or fibrosis at that time point. Overall, this data confirms that WD fed mice developed LV remodeling and abnormalities that are consistent with obesity associated pre-HFpEF phenotype but not a complete HFpEF phenotype.

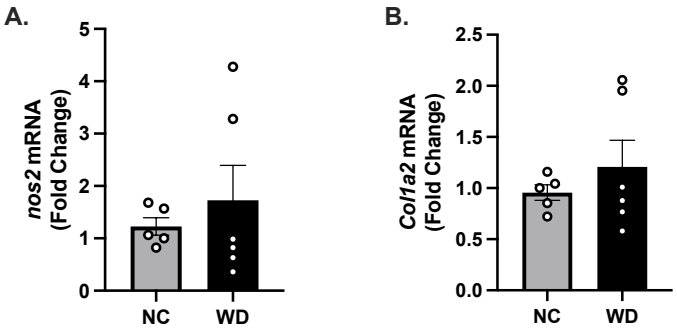

Figure 4. Mice Fed Western Diet (WD) had not Developed Nitrosative Stress or Fibrosis. mRNA levels of A) *nos2* and B) *col1a2* in hearts of mice treated with NC or WD. Statistical analysis was done using unpaired student's t-test.

Fecal Microbiome Transplantation of Obese Pre-HFpEF from Lean Mice Significantly Altered Their Gut Microbiome Composition

It has previously been shown that western diet leads to gut dysbiosis where beneficial bacteria is decreased, and harmful bacteria is increased (107, 118). Which is why obesity and T2D are both associated with the development of gut microbiome imbalance. In support of these findings, previous research has shown that mice fed WD following the previous experimental paradigm (Figure 3A) had significant decrease in their gut microbiome diversity and composition, as well as a reduction in SCFA butyrate-producing bacteria of the genera *Lactobacillus* (189, 253). In addition, recent microbiome analysis showed HFpEF patients to have significant decrease in their gut

microbiome diversity and SCFAs producing bacteria compared to control groups. Therefore, we sought to investigate the effect of gut microbiome alteration on obese pre-HFpEF mice. We used fecal microbiome transplantation (FMT) strategy to modulate the gut microbiome composition(167, 168, 253). C57BL/6J mice were given WD for 12 weeks, followed by three-days antibiotics treatment to deplete their gut microbiome and a diet switch to NC to help colonize the gut with bacteria that grows in NC conditions. Then we subjected the mice to fecal microbiome transplantation of fecal slurry from obese mice (Sham FMT) or from lean mice (FMT) for two weeks (Figure 5A). To characterize the gut microbiome composition of these mice, we collected their cecal contents and performed 16S rRNA sequencing. We found obese mice gavaged with FMT from lean mice to have significant increase in their microbiome diversity by 39.76 ± 12.48 compared to those gavaged with FMT from obese mice (Figure 5B). In addition, we identified butyrate-producing bacteria '*Lactobacillus'* as one of the main SCFA producing bacteria to be significantly increased with lean FMT treatment (Figure 5C, D). In addition, we performed Sparse Correlations for Compositional data (SparCC) network analysis and identified *Lactobacillus* as a key marker of the FMT microbiome landscape as its presence was correlated with other genera that were significantly altered with FMT treatment compared to sham FMT (Figure 5E). These data reflect the beneficial effects of FMT from lean mice on gut bacteria composition and specifically butyrate producing bacteria *Lactobacillus* in WD-fed mice.

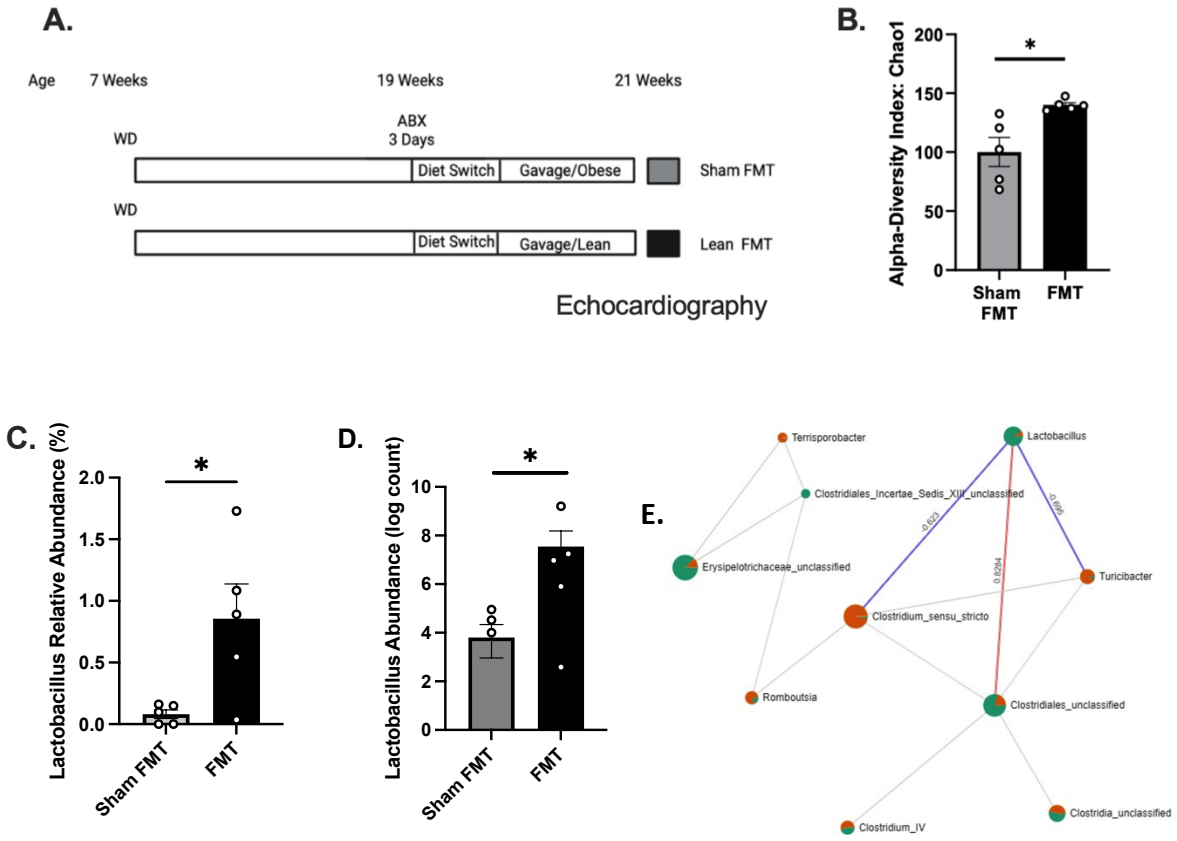

Figure 5. FMT Treatment from Lean Mice Altered Gut Microbiome Composition in Obese Pre-HFpEF Mice. A) Experimental paradigm, C57BL/6J mice fed WD for 12 weeks, followed by broad-spectrum antibiotic treatment for 3 days, brief diet switch to NC, then gavage daily for 2 weeks with fecal slurry either from obese mice (sham FMT group) or from lean mice (FMT group). 16S rRNA microbiome gene sequencing from cecal contents where B) alpha diversity index (Chao1), C) Lactobacillus relative abundance (%), D) Log-transformed Lactobacillus relative abundance (count), E) SparCC analysis between sham FMT and Lean FMT group (correlation threshold > 0.5, p <0.05)

Gut Microbiome Modulation with Fecal Microbiome Transplantation (FMT) from Lean Mice Improved Cardiac Dysfunction and Cardiac Hypertrophy in Obese Pre-HFpEF Mice

To investigate the association between FMT's improvement in microbiome composition and cardiac mechanics, we performed echocardiography measurements at the end of the experimental paradigm (Figure 5A). We found no significant changes in either LVEF or E/A between sham FMT and FMT groups (Figure 6A, B respectively). However, strain analysis measurement GLS was significantly increased by -2.1% ± 0.92 with FMT compared to sham FMT treatment (Figure 6C). LSRr measurement had a trend towards improvement with FMT treatment compared to sham FMT however it did not reach statistical significance (*P*=0.1075, Figure 6D). Additionally, LVPWd measurement was significantly decreased with FMT treatment by -0.12 mm ± 0.04 in obese pre-HFpEF mice (Figure 6E). These data indicate the ability of FMT treatment from lean mice to improve early cardiac dysfunction and LV hypertrophy observed in obesity associated pre-HFpEF. Looking at the levels of *nos2* and *col1a2* in the hearts of sham FMT and FMT treated mice, we found no significant changes in the levels of both genes between the different groups (Figure 6F, G respectively). This indicates that FMT's effect on cardiac dysfunction and hypertrophy is independent of nitrosative stress and fibrosis.

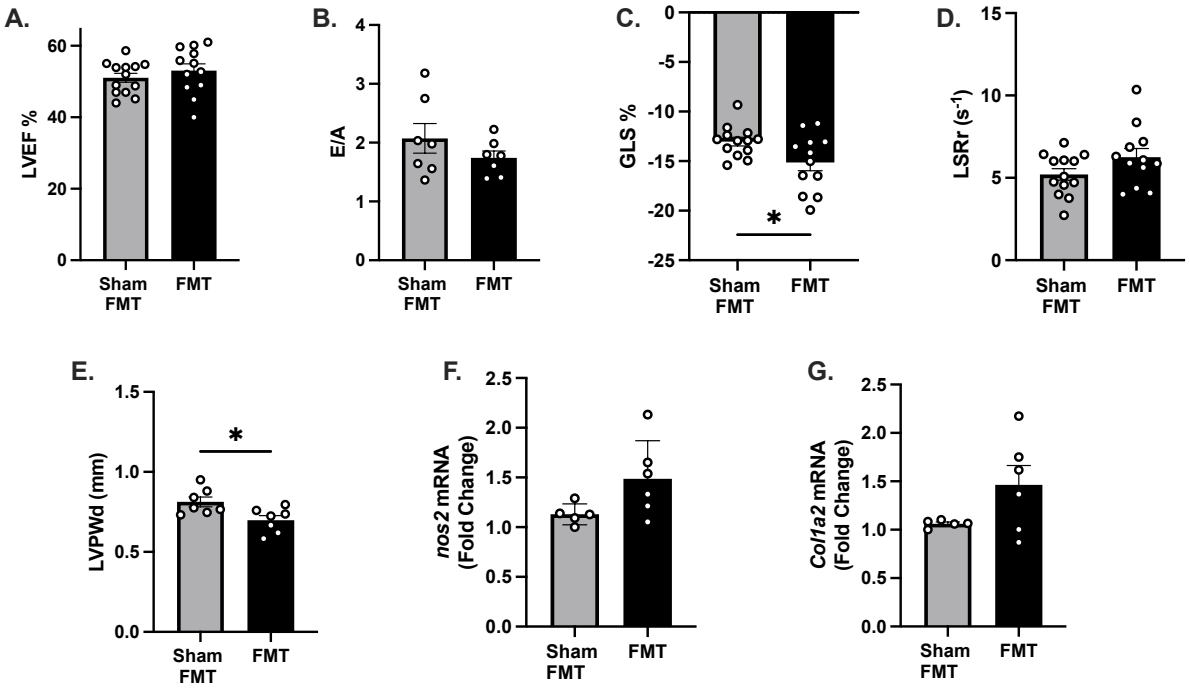

Figure 6. FMT from Lean Mice Improved Early Cardiac Dysfunction and LV Hypertrophy with No Changes in Cardiac Nitrosative Stress and Fibrosis in Obese Pre-HFpeF Mice. Representative Echocardiography measurements of sham FMT and FMT treated obese pre-HFpEF mice. A) LV ejection fraction (%LVEF), B) E/A ratio, C) Global longitudinal strain (%GLS), D) longitudinal strain rate reverse (LSRr, s^{-1}), E) left ventricle posterior wall diameter during diastole (LVPWd, mm). mRNA expression levels of F) *nos2* and G) *col1a2* in the hearts of sham FMT and FMT treated mice. Statistical analysis was done using unpaired student's t-test. Data are mean ± S.E.M. (*$p<0.05$).

Overall, these data show that diet induced obesity leads to the development of preclinical-HFpEF phenotype represented by early dysfunction in cardiac mechanics and structure that has not progressed to clinical HFpEF. DIO caused gut microbiome imbalance and reduced production of SCFA producing bacteria. However, this was reversed with FMT treatment from lean mice. Additionally, lean FMT was able to improve early cardiac dysfunction and hypertrophy in obese pre-HFpEF mice. Therefore, our data indicate that correction of gut microbiome imbalance improves

cardiac mechanics and can be used as a potential preventative treatment strategy that can halt obesity associated pre-HFpEF progression to clinical HFpEF.

Discussion

Gut microbiome imbalance/dysbiosis is a hallmark of obesity. The association between gut microbiome imbalance and the development of cardiovascular diseases has been an active area of research with many studies focusing on microbiome composition in patients with CVDs such as hypertension and HFrEF(172-174, 176, 213, 214). Only recently were there a couple of studies that looked at gut microbiome composition in HFpEF patients. They found significant alterations in gut microbiome composition and a decrease in its diversity in HFpEF patients compared to control groups, as well as a decrease in the SCFAs producing bacteria(239, 240). These studies provide a connection between HFpEF and gut microbiome composition. However, mechanistic studies on the effect of gut microbiome imbalance and HFpEF progression are still lacking. In this study, we investigated the direct association between gut microbiome imbalance, caused by obesity, and cardiac dysfunction in obese pre-HFpEF mice and asked whether improving gut microbiome in the pre-HFpEF stage would improve cardiac dysfunction and prevent further progression to clinical HFpEF. We developed an obesity associated pre-HFpEF mouse model that had early cardiac dysfunction in the absence of systolic and diastolic dysfunction. In addition, the mice developed cardiac hypertrophy (Figure 3). This occurred in the absence of the two key markers of HFpEF development, nitrosative stress and cardiac fibrosis (Figure 4). This data led us to believe that these mice are in the preclinical stage of HFpEF. To confirm that these mice will develop HFpEF, they would need to have another

comorbidity in addition to obesity. For example, the aging factor can be included where mice would be left on WD until they reach an old age of >24 months, which equals to >70 years old in humans. Another comorbidity that can be included is the induction of hypertension using the NO synthase inhibitor L-NAME as shown in Schiattarella G.G. et al. HFpEF mouse model (41). Another model of HFpEF that can be used is the 3-hit mouse model developed by Deng Y. et al. which includes aging, obesity, and hypertension (70). However, since our main goal is to test whether targeting cardiac changes in the preclinical HFpEF stage can prevent the progression to clinical HFpEF, we performed our studies using the pre-HFpEF model.

Previous work, following the same experimental paradigm in figure 3, has shown that mice after 14 weeks of WD feeding developed gut microbiome imbalance and had significant reduction in their butyrate producing bacteria (253) .Therefore, we asked whether this obesity induced microbiome imbalance is directly linked to early cardiac dysfunction and hypertrophy seen in obese pre-HFpEF mice. We used FMT from lean mice to treat gut microbiome imbalance where mice had significant improvement in microbial diversity and increase in butyrate producing bacteria. In addition, we found lean FMT treated mice to have significant improvements in their early cardiac dysfunction and hypertrophy compared to their littermates treated with FMT from obese mice. These data show that improving gut health can reverse heart dysfunction, indicating that gut microbiome plays a causative role in disease development and worsening of disease outcomes rather than being a consequence of cardiac dysfunction.

Our studies were performed using only male mice because it was previously shown that female mice are resistant to metabolic changes induced by WD (such as insulin resistance and glucose intolerance). However, future studies must include both male and female mice to better understand any sex differences that might arise with gut microbiome modulation.

CHAPTER FOUR

GUT MICROBIOME MODULATION IMPROVEMENTS OF EARLY CARDIAC DYSFUNCTION AND CARDIAC HYPERTROPHY WAS INDEPENDENT OF AUTONOMIC REGULATION

Introduction

Gastrointestinal (GI) function is controlled by the autonomic nervous system (ANS) which includes sympathetic nervous system (SNS), parasympathetic nervous system (PNS), and enteric nervous system (ENS) regulation(254). The sympathetic nervous system is responsible for the body's "fight or flight" response. The signals transmitted through the SNS require preganglionic and postganglionic neurons. The preganglionic neurons arise from the thoracolumbar region while the postganglionic neurons will synapse at the target organ. Preganglionic neurons release the neurotransmitter acetylcholine (ACh) that activates the nicotinic acetylcholine receptors (nAChRs) on postganglionic neurons which in response will release the neurotransmitter norepinephrine (NE) that activates the adrenergic receptors on target organs. This regulation occurs in collaboration with the parasympathetic nervous system (PNS) which is responsible for the body's "rest and digest" response. The preganglionic neurons of the PNS arise from the brain stem or sacral spinal cord and they release acetylcholine (ACh) that activates the nicotinic acetylcholine receptors (nAChRs) on postganglionic neurons which in response will release ACh to stimulate the muscarinic receptors (mAChRs) on target organs (255). PNS and SNS work

opposite each other to regulate many functions in several different organs (Table 4).

Table 4. Effects on Parasympathetic and Sympathetic Nervous System on the Function of Different Organs.

Target Organ	Parasympathetic Regulation	Sympathetic Regulation
Heart	Decreases heart rate (negative chronotropy) and myocardial contractility (negative inotropy), accelerate cardiac relaxation (negative lusitropy), accelerate atrioventricular conduction (negative dromotropy)	Increases heart rate (positive chronotropy), increase myocardial contractility (positive inotropy), accelerate cardiac relaxation (positive lusitropy), accelerate atrioventricular conduction (positive dromotropy)
GI Tract	Increases GI activity by increasing peristalsis and gastrointestinal secretion	Decreases GI activity by inhibition of gastrointestinal secretion and motor activity
Blood Vessels	Increases blood vessels dilation; lowers BP	Increases blood vessels constriction; Increases BP
Lungs	Increases bronchioles constriction	Increases bronchioles dilation

The enteric nervous system's (ENS) main function is the regulation of the GI tract either dependently or independently of the PNS and the SNS regulation. ENS contains a combination of sensory and motor neurons that innervate the wall of the GI tract. It mainly senses chemical and mechanical changes in the gut, where it regulates the GI hormone secretion, like gastrin and secretin through the vagus nerve activity, and peristalsis (the contraction and relaxation of GI tract muscles) (211).

The connection between ENS and CNS also known as the gut-brain axis refers to the communication between the brain and the GI tract which occurs mainly through the vague nerve(256). It carries afferent signals from different organs such as gut, heart,

liver, and lungs to the brain and efferent signals from the brain to different organs to generate a specific response(257-259). The vagus nerve has a parasympathetic effect where in the gut that leads to increase in GI activity by increasing motility and secretion. It also affects many intestinal cells such as immune cells, epithelial cells, enteric neurons, smooth muscle cells, and enterochromaffin cell(260). The gut-brain communication is evident in several studies investigating the effects of gut microbiome alterations on the brain and mood disorders like depression and anxiety(261, 262). Studies have shown an association between GI disorders like IBS and IBD and the development of mood disorders(263), where it was shown that probiotics treatment led to reduction in anxiety and stress in IBS and IBD disorders(264, 265). This occurs either through a decrease in the levels of BDNF(Brain-derived neurotrophic factor), shown to be involved in depression and anxiety(266), or through alteration in $GABA_A$ and $GABA_B$ receptors that are also associate with mood disorders development(267).

In addition to their effects on mood and behavior, gut microbiome and their metabolites SCFAs were shown to be responsible for regulating feeding behavior, food intake, energy balance, and glucose homeostasis through the vagus nerve(268-271). Butyrate was shown to control appetite and reduce food intake that prevented diet-induced obesity, hyperinsulinemia, hypertriglyceridemia, and hepatic steatosis through increasing fatty acid oxidation in brown adipose tissue (BAT) due to vagal nerve activation(271). Additionally, both butyrate and propionate supplementation were found to protect against diet induced obesity, improve glucose tolerance and insulin sensitivity in HFD-fed mice. This occurred due to increase in the release of the gut hormones glucagon-like peptide-1(GLP-1) and peptide tyrosine tyrosine (PYY) that are associated

with reduced food intake. However, these effects were independent of FFAR3 activation(199). In contrast, other studies have shown that FFAR3 whole body KO reduced energy expenditure and increased their body fat content(272, 273). More specifically, FFAR3 KO in vagal sensory neurons increased food intake and body weight. It also eliminated the positive effects of the SCFA propionate on reducing food intake(189). These conflicting findings indicate the presence of different mechanisms by which gut microbiome and SCFAs supplementation regulate feeding behavior and energy homeostasis. These might include the activation of other receptors like FFAR2, HCAR2, and Olf78.

The autonomic nervous system is known to play a key role in regulating heart function through balanced activities of SNS and PNS. The SNS is responsible for increasing myocardial contractility, heart rate and vasoconstriction to raise blood pressure(274, 275). While the PNS slows heart rate, decrease cardiac contractility, and vasodilation to lower blood pressure via the vagal nerve(276). The SNS releases norepinephrine and epinephrine that binds to adrenergic receptors (ARs), this includes α- and β-receptors(274, 277). Among the β-receptors, β1 is the most involved in cardiac activity. When activated it leads to increase in cardiac output by increasing heart rate (positive chronotropic effect) and heart muscle contraction (positive inotropic effect). The PNS release acetylcholine that binds to muscarinic receptors (mAChRs), this includes M1-M5 receptors. The predominant muscarinic receptors in the heart are M2 and M3 where they act after SNS activation to bring the heart function back to normal and reduce heart rate and cardiac muscle contractility(278).

Disruption in the homeostasis between SNS and PNS contributes to the development of cardiac dysfunction and heart disease(279). For example, autonomic dysfunction is known to be involved in the development of hypertension due to increase in sympathetic activity and decrease in parasympathetic vagal cardiac tone(203, 280-282). Increase in sympathetic activity is indicated by increase in norepinephrine plasma levels and muscular sympathetic tone(283, 284). Whereas parasympathetic vagal tone reduction can be measured by change in heart rate variability (HRV) and heart rate recovery (HRR) measurements(284, 285). Disruption in SNS and PNS activity has also been implicated in heart failure, where it is characterized by hyperactivity of the SNS and decrease in responsiveness of the PNS(274, 277, 278). Studies in HFrEF show overactivation of SNS to increase in epinephrine and norepinephrine levels that leads to chronic activation of β-receptors, and in turn causing cardiomyocyte remodeling, hypertrophy, and LV enlargement(286). It has been shown that HF patients have significant reduction in β1-receptors and uncoupling of both β1 and β2 -receptors(287-289). In addition to changes in β-receptors, G-protein–coupled receptor kinases GRK2 and GRK5 were elevated in HF(290-292). In HFpEF, autonomic regulation is still under investigation. Some studies demonstrate HFpEF to show similar autonomic dysregulation as HFrEF where hyperactivity of the SNS and downregulation of PNS contribute to LV diastolic dysfunction(293-295). Although the use of β-blockers, the therapeutic strategy used for HFrEF and hypertension(296-298), has shown no improvement in HFpEF.

Autonomic regulation therapy (ART) in heart failure has been proposed to improve cardiac function and reduce disease progression using vagal nerve stimulation,

that increases parasympathetic tone and reduces sympathetic overactivity. Increase in vagal nerve stimulation leads to activation of muscarinic receptors in cardiomyocytes which in turn improves muscle contraction and relaxation(299, 300). The effect of ART has been studied in HFrEF and HFpEF patients in the ANTHEM-HFrEF and ANTHEM-HFpEF randomized clinical studies. However, results were inconclusive on whether ART can be used as a therapeutic for HF(301, 302).

Autonomic dysregulation has been involved in the development of chronotropic incompetence (CI), the inability to increase heart rate during exercise and high energy demand, causing exercise intolerance which is common in patients with HF(303, 304). Exercise intolerance is a decrease in cardiac output (CO), decrease in blood volume pumped from the heart that does not meet the body's needs during exercise. This is assessed by measuring oxygen consumption rate at peak exercise (pVO_2), the maximum rate of oxygen consumption during exercise where oxygen uptake increases to meet energy demands(305). pVO_2 is dependent on increase in CO during exercise(306). pVO_2 has been shown to be significantly decreased in HF patients compared to control groups(307, 308). In HFpEF patients, decrease in exercise capacity and pVO_2 are very common due to chronotropic incompetence observed through decrease in contractility, impaired vasodilation, and lower heart rate during exercise compared to controls(7, 309). HFpEF patients also had decrease in their cardiac β-receptors responsiveness compared to controls which may be a contributor to chronotropic incompetence and exercise intolerance(310).

These findings show an association between the brain, gut, and heart function which led to the development of the gut-brain-heart axis that refers to the effects of the

gut on autonomic regulation of the heart, and in turn its contribution to the development of CVDs. Therefore, in this study we hypothesize that FMT's improvement of early cardiac dysfunction in our obese pre-HFpEF (Ch.3, Fig.6) might be due to alterations in autonomic function. To test this hypothesis, we measured changes in HR, CO and the levels of β- and muscarinic receptors in the heart to see whether there are any changes in SNS and PNS activity with FMT treatment.

Results

Muscarinic Receptors Expression Levels were not Altered in Obesity Associated Pre-HFpEF Mice.

Our previous results have shown WD fed mice to have early cardiac dysfunction and cardiac hypertrophy that has yet to progress to systolic and diastolic dysfunction. Impairment in parasympathetic activity (decrease in vagal tone) is involved in the development of CVDs including hypertension and heart failure that is associated with decrease in the expression of cardiac muscarinic receptors. Activation of these receptors by acetylcholine leads to muscle relaxation, and defects in their expression and activity might be a main contributor to impaired LV relaxation seen in HFpEF. Therefore, detecting and targeting PNS dysfunction in preclinical HFpEF might present a therapeutic approach to prevent further progression to systolic and diastolic dysfunction and HFpEF development. Using the obese pre-HFpEF mouse model developed in Ch.3 Fig.3 we measured the levels of muscarinic receptors that are known to be expressed in the heart M1, M2, and M3 using RT-qPCR analysis. We found no significant changes in the gene expression levels of M1, M2 and M3 in the heart of obese pre-HFpEF mice compared to NC fed mice (Figure 7). This indicates that the

development of early cardiac dysfunction was independent of changes to muscarinic receptors expression.

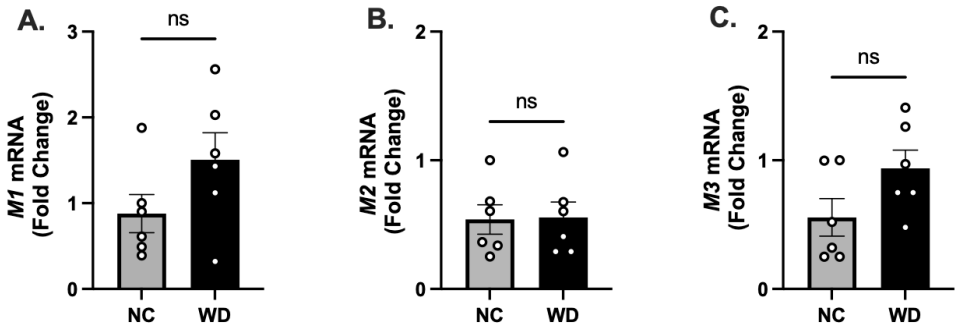

Figure 7. mRNA Gene Expression of Muscarinic Receptors in the Heart was not Changed Between NC and WD Fed Mice. mRNA expression levels of A) *M1,* B) *M2* , C) *M3* in the hearts of NC and WD fed mice. Statistical analysis was done using unpaired student's t-test. Data are mean ± S.E.M.

Muscarinic Receptors Expression Levels were not Altered with Lean FMT Treatment.

The gut-brain axis role in autonomic regulation suggests a potential role for the gut microbiome to modulate autonomic regulation of the heart by affecting the PNS activity. Therefore, we measured the levels of muscarinic receptors in the heart of obese pre-HFpEF following FMT treatment (Ch.3, Fig.5) using RT-qPCR analysis. We found no changes in the levels of M1, M2, and M3 in the heart in mice treated with lean FMT compared to sham FMT treatment (Figure 8). This further indicates that improvement in early cardiac dysfunction and hypertrophy in obese pre-HFpEF mice due to gut microbiome modulation was independent of changes to muscarinic receptors and PNS activity.

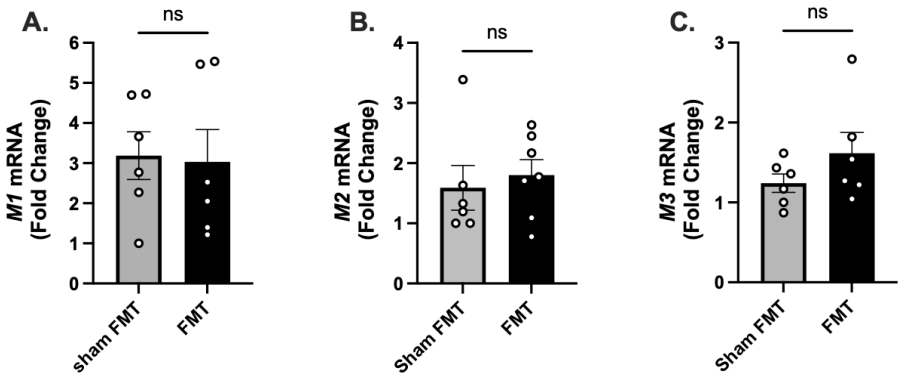

Figure 8. mRNA Gene Expression of Muscarinic Receptors in the Heart was not Changed Between Lean FMT and Sham FMT Treated Obese Pre-Hfpef Mice. mRNA expression levels of A) *M1,* B) *M2*, C) *M3* in the hearts of obese mice treated with FMT or sham FMT. Statistical analysis was done using unpaired student's t-test. Data are mean ± S.E.M

β2 but not β1-Adrenergic Receptor Gene Expression was Altered in the Hearts of Obese Pre-HFpEF Mice.

Dysfunction in autonomic regulation is caused by impaired activity of the parasympathetic nervous system (PNS) and hyperactivity of the sympathetic nervous system (SNS). We have previously shown that early cardiac dysfunction in obese pre-HFpEF mice and improvements seen with FMT treatment were independent of changes to muscarinic receptor expression. Therefore, we investigated whether SNS activity was involved in these improvements by measuring changes in the expression levels of cardiac β-adrenergic receptors (β1 and β2) using RT-qPCR analysis. We found no changes in the gene levels of β1 receptor between NC and WD fed mice (Figure 9A). However, β2 receptor levels were significantly upregulated in WD fed mice compared to NC fed mice (Figure 9B).

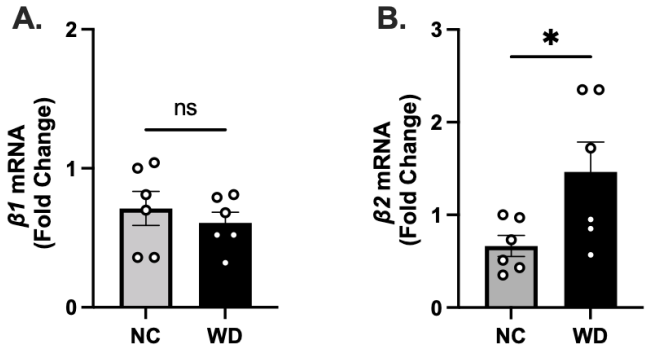

Figure 9. β1 mRNA Gene Expression was not Changed Between NC and WD Fed Mice while β2 Gene Expression was Significantly Increased in Obese Mice. mRNA expression levels of A) *β1,* B) *β2* in the hearts of obese mice. Statistical analysis was done using unpaired student's t-test. Data are mean ± S.E.M. (*p<0.05)

β-Receptors Expression Levels were not Changed with Lean FMT Treatment.

To test whether improving gut microbiome improves SNS activity by altering the expression of β-adrenergic receptors in the heart (β1 and β2), we measured their expression levels in obese pre-HFpEF mice following FMT treatment using RT-qPCR analysis. We found no significant changes in the levels of either β1- or β2- receptors in the hearts of obese pre-HFpEF mice treated with lean FMT compared to sham FMT (Figure 10). This indicates that improvement in early cardiac dysfunction and hypertrophy seen in obese pre-HFpEF mice with FMT treatment was independent of changes in β-adrenergic receptors and in turn SNS activity in the heart.

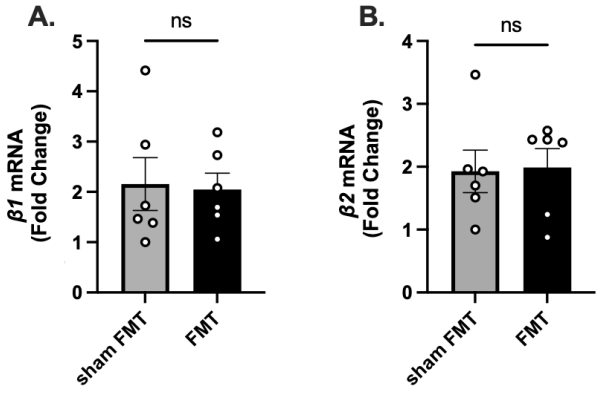

Figure 10. β-Adrenergic Receptors Gene Expression was not Changed in the Hearts of Obesity Associated Pre-HFpEF Mice Following FMT Treatment. mRNA expression levels of A) *β1,* B) *β2* in the hearts of obese mice treated with FMT or sham FMT. Statistical analysis was done using unpaired student's t-test. Data are mean ± S.E.M.

Obese Pre-HFpEF Mice and Those Treated with FMT had No Changes in Their Cardiac Output and Heart Rate Measurements.

Parasympathetic and sympathetic nervous branches of the autonomic nervous system are responsible for regulating heart rate (HR) and cardiac output (CO) and maintaining normal cardiac function (Cardiac Output=Heart Rate x Stroke Volume). Therefore, to further investigate the role of autonomic regulation in the development og early cardiac dysfunction in our obese pre-HFpEF mice, and whether gut microbiome dysbiosis leads to autonomic dysfunction, we measured HR and CO using M-mode echocardiography. We found no significant changes in either CO or HR in obese pre-HFpEF mice compared to the control NC fed mice (Figure 11A, B respectively). Similarly, we found no significant difference in CO and HR measurements between sham FMT and lean FMT obese pre-HFpEF mice (Figure 11C, D respectively). This further indicate that early cardiac dysfunction seen in obese pre-HFpEF mice and its

improvement following gut microbiome modulation with lean FMT treatment is independent of changes in autonomic system regulation.

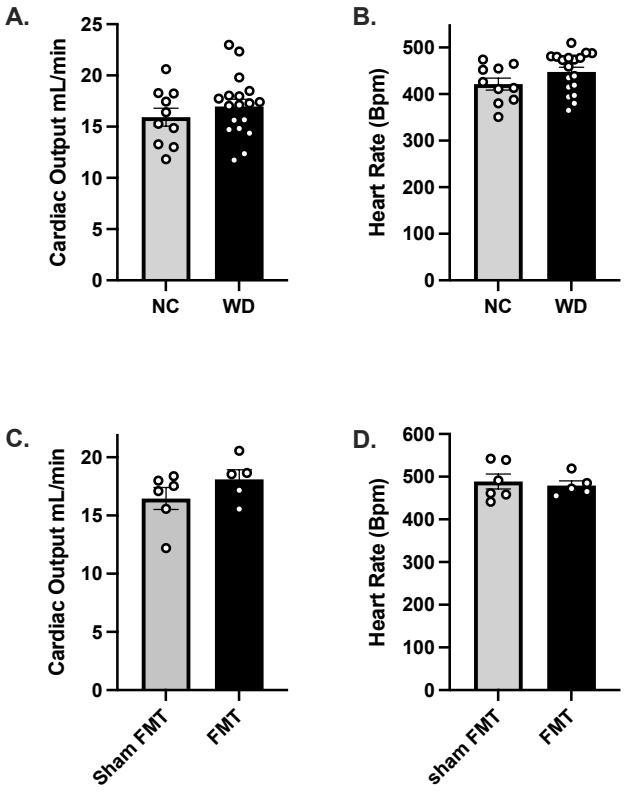

Figure 11. Early Cardiac Dysfunction in Obese Pre-HFpEF and its Improvement with FMT Treatment is Independent of Changes to Autonomic Regulation. M-mode echocardiography measurements of A) cardiac output and B) heart rate in obese pre-HFpEF mice compared to their littermates fed NC diet. M-mode echocardiography measurements of C) cardiac output and D) heart rate in obese pre-HFpEF mice treated with sham FMT or FMT. Statistical analysis was done using unpaired student's t-test. Data are mean ± S.E.M.

Discussion

Autonomic regulation involves sympathetic, parasympathetic, and enteric nervous systems (SNS, PNS, ENS). Sympathetic and parasympathetic systems counteract each other in their regulation of many cardiac responses. For example, sympathetic nervous system increases heart rate and contractility of cardiac muscle, while parasympathetic

nervous system decreases heart rate and cardiac contractility. The sympathetic system effects occur through activation of β-adrenergic receptors via epinephrine/norepinephrine neurotransmitter. While parasympathetic system effects occur through activation of muscarinic receptors via the neurotransmitter acetylcholine. Impairment in the sympathetic-parasympathetic (hyperactivity of SNS and deficiency in PNS activity) homeostasis is involved in the development of many CVDs including hypertension and heart failure.

The enteric nervous system is responsible for regulation of GI functions including GI hormones secretion and peristalsis either independently or in association with central nervous system (CNS) through the gut-brain axis. The association between the gut and the brain is shown in gut microbiome's effects on mood disorders and feeding behavior. Disruption in gut microbiome composition and diversity as well as its metabolites SCFAs has been shown to be associated with increase anxiety, depression, food intake, and disruption in glucose homeostasis and energy balance.

To determine whether improvements in early cardiac dysfunction and cardiac hypertrophy in obese pre-HFpEF mice after gut microbiome modulation with FMT was due to changes in autonomic regulation, we measured the levels of muscarinic and β-adrenergic receptors in the heart. We found no changes in the gene expression levels of muscarinic receptor M1, M2, and M3 in the hearts of obese pre-HFpEF mice as well as no changes in their expression between sham FMT and lean FMT treated mice. This indicates that parasympathetic activity was not affected in the pre-HFpEF stage and that improvement in cardiac function was independent of PNS. Similarly, we found no changes in the gene expression levels of β1-receptors in obese pre-HFpEF mice

compared to NC fed mice, and no changes in its levels after sham FMT or FMT treatments. β2-receptor levels, which increases cardiac muscles contraction and heart rate, were significantly upregulated in the obese pre-HFpEF mice. However, there was no significant changes in β2-receptor levels after FMT treatment compared to sham FMT. In addition, we measured CO and HR which are used to test the autonomic system regulation of cardiac function and we found them to be unchanged between NC and WD-fed pre-HFpEF mice as well as unaltered between sham FMT and FMT treated mice. This indicates that PNS and SNS activity were not responsible for early cardiac dysfunction detected at that specific pre-HFpEF stage. However, we must take into consideration that these measurements were recorded when the mice were under anesthesia which is known to suppress heart rate and cardiac output based on the type, duration, and the level of anesthetic exposure(311, 312). Therefore, other methods to record HR and CO in conscious mice might provide a more accurate representation. This includes the use of implanted PA-C10 pressure transmitter device that measures HR(313) or ETA F-10 transmitter for ECG and HR recordings(314). However, these require the mice to undergo surgery for device implantation and a recovery period afterwards before taking any recordings. Other methods can include non-invasive ECG but it requires the mice to be restrained, or tethered ECG in conscious mice which gives the mice more freedom to move around but the wires can be detached with increased movement(314). Additionally, protein levels of each receptor must be measured since RNA expression does not always reflect protein levels in the tissue.

CHAPTER FIVE

TRIBUTYRIN TREATMENT REPLICATES FMT'S IMPROVEMENTS IN EARLY DYSFUNCTIONS IN CARDIAC MECHANICS AND STRUCTURE IN OBESE PRE-HFPEF MICE

Introduction

Gut microbiome produces metabolites short chain fatty acids (SCFAs) from the fermentation of dietary fibers in the GI tract(315). The most abundant SCFAs produced acetate, propionate, and butyrate are present in the colon in a 60:20:20 ratio(132, 316, 317). Excess SCFAs get transported by the portal vein to the liver and get released into the circulation(132). SCFAs have been shown to be involved in improving CVDs such as atherosclerosis, hypertension, and heart failure. These effects are mediated either through binding to GPCRs to activate downstream signaling pathways, regulating gene expression through HDAC inhibition, or improving cellular metabolism (Figure 2). Among the three SCFAs, butyrate was shown to have many physiological effects, it plays an essential role in preventing leaky gut development by being the main fuel source for colonocytes and maintaining the gut barrier integrity(133, 134, 136, 192, 194, 222). Indicating a crucial role for butyrate in gut microbiome health.

By preserving the gut barrier, butyrate prevents the entry of endotoxins such as Lipopolysaccharide (LPS) and the infiltration of proinflammatory cells and cytokines into the system. A study by Wang F. et al. found butyrate to protect the heart in an endotoxemia (sepsis) mouse model induced by LPS injection. They found butyrate

treatment to improve LV function and attenuate myocardial injury after LPS injection. This was associated with butyrate's inhibition of inflammation and oxidative stress in the myocardium(194). In addition, gut barrier dysfunction has been linked to the development of hypertension. Kim S. et al. performed taxonomic analysis of gut microbiome in hypertensive patients where they found an increase in the abundance of species linked to gut barrier dysfunction and inflammation. This was associated with reduction in butyrate producing bacteria and plasma butyrate levels in hypertensive groups. Treating AngII induced hypertensive mice with butyrate led to significant improvement in gut barrier function and decreased inflammation. Butyrate also improved cardiac function in hypertensive mice that was associated with decrease in cardiac oxidative stress and inflammation(133). These data support the importance of maintaining gut barrier integrity by butyrate on cardiac health.

Another potential mechanism by which SCFAs were shown to improve blood pressure is through binding to GPCRs. Natarajan N. et al. studied the effect of FFAR3(GPR41) KO in mice on blood pressure. They found GPR41 KO mice to have significant increase in their systolic blood pressure compared to their WT littermates. Several studies also showed SCFAs to regulate appetite and energy expenditure through binding to FFAR2/3. SCFAs can activate their receptors in peripheral organs (adipose tissues, gut, and pancreas) to modulate CVDs indirectly, and/or can directly activate receptors on cardiac cells to modulate cardiovascular function(178).

Butyrate also improves metabolism by being utilized in the mitochondria to produce energy through β-oxidation. Panagia M. et al. showed mice fed high fat high sucrose diet (HFHS) to have improved ATP synthesis rate after butyrate

supplementation(318). Carley N.A. et al. also showed butyrate to be a preferred source of energy over the ketone body B-hydroxybutyrate in the failing heart(238). Butyrate also has been shown to have many beneficial effects on cardiac function, Patel M. B. showed sodium butyrate (NaB) treatment to reduce LV wall thickness, collagen levels, and oxidative stress in a partial abdominal aorta constriction (PAAC)-induced cardiac hypertrophy rat model(319). This was supported by the work of Zhang L. et al. where they found NaB to reduce AngII induced hypertension and cardiac hypertrophy(320). As well as the work of Chen Y. et al. where Streptozotocin (STZ)-induced diabetic mice treated with NaB had improved cardiac function and hypertrophy(321). The main molecular mechanisms of butyrate's beneficial effects in these studies were attributed to butyrate's HDAC inhibition activity. Alternative to HDAC inhibition, a recent study by Thomas P.S. and Denu M.J. showed butyrate to affect gene transcription through increasing histone acetylation (HATs). They found butyrate to metabolize into acyl-coA (butyryl-coA) which in turn activates acetyltransferase p300 and increases histone acetylation(322).

The role of butyrate was explored in heart failure, where several studies conducted 16s rRNA sequencing analysis on HF patients and found butyrate producing bacteria of the genera *F. prausnitzii* (214) and of the genera *Lachnospiraceae* (215) to be significantly reduced compared to control groups. Furthermore, butyrate producing bacteria of the genera *Lachnospiraceae* and *Lactobacillus* were significantly decreased in WD-fed mice, meanwhile butyrate serum levels were significantly increased with lean FMT treatment (189, 253). Moreover, our data show that FMT's improvement in cardiac mechanics and structure in obese pre-HFpEF mice to be associated with improving gut

microbiome composition and the increase in butyrate producing bacteria *Lactobacillus* (Figures 5C, D).

Collectively, these findings provide strong evidence for the involvement of butyrate in FMT's improvements. Therefore, we hypothesized that FMT's improvement in early cardiac dysfunction and hypertrophy in obese pre-HFpEF mice was due to the SCFA butyrate. We tested this hypothesis by treating obese pre-HFpEF mice with butyrate's prodrug, tributyrin, which consists of 3 butyrate molecules linked to a glycerol backbone. Tributyrin has slower metabolization rate compared to sodium butyrate (NaB), which allows butyrate to be absorbed easily, increasing its concentration in the circulation. Following tributyrin administration, we performed echocardiography measurement to test its effects on cardiac function. We predicted tributyrin to replicate FMT's improvements in cardiac dysfunction and hypertrophy.

Results

Tributyrin Treatment Improved Early Systolic and Diastolic Dysfunction, and LV Hypertrophy in Obese Pre-HFpEF Similar to FMT Treatment

We placed seven-weeks old C57BL/6J mice on either NC or WD for fifteen weeks to develop pre-HFpEF. Then we treated them with tributyrin using oral gavage (needle feeding) following a two-days on, two-days off strategy for two weeks (Figure 12A). To confirm that WD-fed mice had developed pre-HFpEF prior to the tributyrin treatment, we performed echocardiography at week fifteen of WD feeding.

Similar to our previous data (Ch.3, Fig.3) we found WD fed to develop early cardiac dysfunction and cardiac hypertrophy that is consistent with obese pre-HFpEF phenotype. WD-fed mice had no changes in their LVEF, and E/A compared to NC fed

mice (Figure 12B, C respectively). However, they had significant decrease in their early systolic and diastolic functions indicated by GLS and LSRr measurements, where GLS was decreased by 3% ± 0.97 and LSRr was decreased by -1.8 s^{-1} ± 0.62 in WD fed mice compared to NC fed control mice (Figure 12D, E respectively). In addition, mice on WD developed cardiac hypertrophy shown by increase in LVPWd by 0.14 mm ± 0.04 compared to mice on NC (Figure 12F).

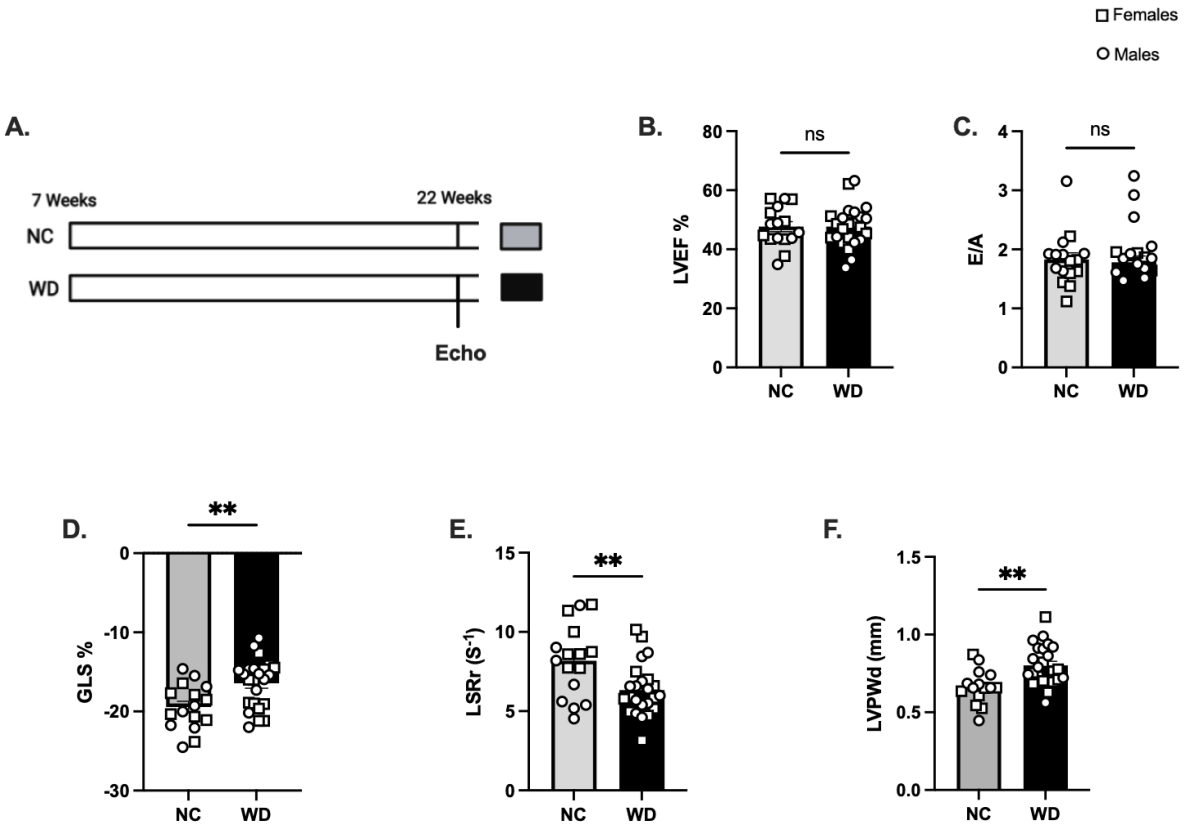

Figure 12. Mice Fed WD Prior to Tributyrin Treatment Developed Early Cardiac Dysfunction and Cardiac Hypertrophy that is Consistent with Obesity Associated Pre-HFpEF Phenotype. A) Experimental paradigm of mice fed WD, or NC for fifteen weeks followed by echocardiography measurements of B) %LVEF, C) E/A ratio, D) %GLS, E) LSRr (s^{-1}), F) LVPWd (mm), prior to Tributyrin administration. (n=20 per group). Statistical analysis was done using unpaired student's t-test. Data are mean ± S.E.M. (*p<0.05, **p<0.005).

Following the confirmation that WD-fed mice had developed obesity associated pre-HFpEF, we treated them with tributyrin (5g/kg dose) or vehicle for two weeks, while treating NC-fed mice with vehicle. Then we performed echocardiography measurements to assess changes to their cardiac function (Figure 13A). We found no changes in either LVEF and E/A between NC+Vehicle, WD+Vehicle, and WD+Tributyrin treated mice (13B, C respectively). However, we found tributyrin treatment to significantly improve GLS by -10.4% ± 1.9 and LSRr by 4 s^{-1} ± 1.6 in WD fed mice compared to vehicle treatment (Figure 13D, E respectively). Similarly, we found the increase in LVPWd by -0.13 mm ± 0.05 in WD-fed mice to be obliterated after tributyrin treatment (Figure 13F). Additionally, to make sure our tributyrin treatment was administered correctly and that the specific dose was able to sustain the levels of butyrate in circulation, we measure butyrate serum levels of tributyrin treated mice with mass spectrometry. We found butyrate levels to be significantly increased in tributyrin treated mice compared to vehicle treatment by 228.5 μM ± 55.1 (Figure 13G). This data show that butyrate's prodrug, tributyrin, was able to replicate FMT's improvements in early systolic and diastolic dysfunction and cardiac hypertrophy seen in obese pre-HFpEF mice. Which in turn points to changes in the SCFA butyrate as a potential mechanism by which FMT improves cardiac mechanics in obesity associated pre-HFpEF.

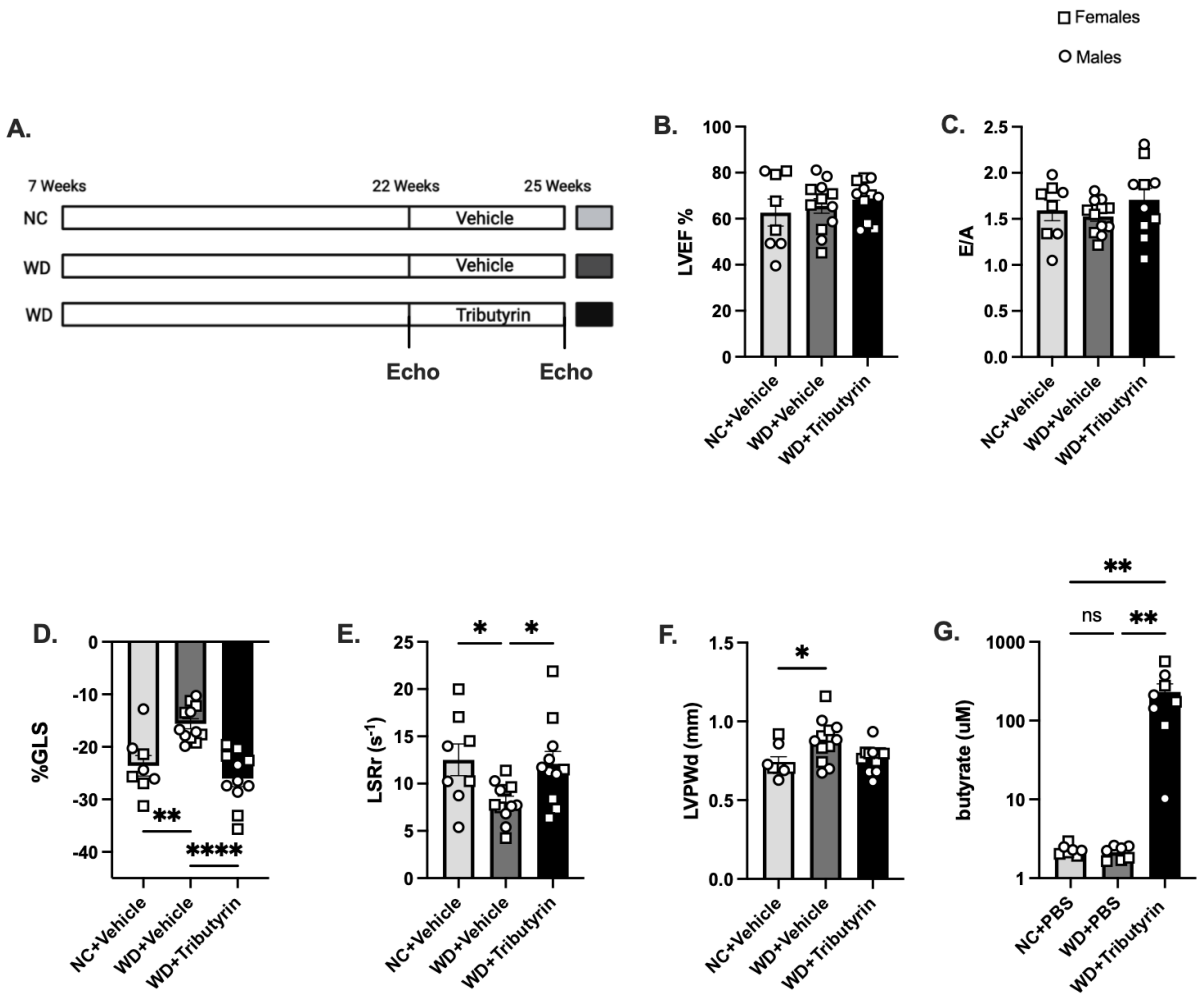

Figure 13. Obese Pre-HFpEF had Significant Improvement in Early Cardiac Dysfunction and Cardiac Hypertrophy After Tributyrin Treatment. A) Experimental paradigm continuation of figure 12A, where NC-fed mice were treated with vehicle while WD-fed mice were treated with either vehicle or Tributyrin (5g/kg body weight) for two weeks followed by echocardiography measurements of B) %LVEF, C) E/A ratio, D) %GLS, E) LSRr (s^{-1}), F) LVPWd (mm). G) levels of butyrate in the serum measure by mass spectrometry(μM). (n=8-12 per group). Statistical analysis was done using one-way ANOVA followed by Tukey's multiple comparison test. Data are mean ± S.E.M. (*p<0.05, **p<0.005).

Tributyrin Improves Exercise Capacity Independently of Effects on Heart Rate and Cardiac Output

As mentioned previously, exercise intolerance due to chronotropic incompetence (CI) is very common in HFpEF patients and is one of the main symptoms that correlates with HFpEF severity and progression. Exercise training was shown to have improve autonomic dysfunction in both HFpEF and HFrEF patients with CI, where it led to significant improvement in their HR recovery (improved vagal tone), peak HR, and pVO_2 (323-326). However, the molecular mechanism involved in this improvement is still not know. Interestingly, exercise training has also been shown to improve gut microbiome diversity and composition and was associated with increase in the levels of SCFA producing bacteria(327, 328). In particular, the SCFA butyrate levels and butyrate producing bacteria were shown to be increased in individuals that exercise regularly(329). This improvement was also associated with reduced gut permeability, preventing toxins from entering the gut and causing inflammation(330). Gut microbiome modulation also influenced exercise capacity. Fecal microbiome transplantation from normal fed mice to HFD obese mice led to significant improvement in their exercise capacity as well as a decrease in fasting glucose levels and inflammatory cytokines levels(331). Gut microbiome modulation improvement of exercise capacity was also associated with effects on skeletal muscle function. It was shown that depletion of gut microbiome with antibiotics led to reduction in running capacity and skeletal muscle contraction. These changes were associated with increase inflammation and decrease in glucose homeostasis (332). A reduction in exercise capacity, especially in obese HFpEF patients, can reduce the beneficial effects of using exercise training as a

preventative/treatment strategy to improve quality of life. It is still not known whether exercise intolerance is a consequence of cardiac dysfunction in heart failure or secondary to obesity and increase in body weight. In our obese pre-HFpEF mice we saw a significant reduction in their exercise capacity by 87.5 m ± 31.6 compared to NC-fed mice, indicated by decrease in running distance. However, this decrease was eliminated after tributyrin treatment (Figure 14A). As expected, mice fed WD had significant increase in their body weight compared to NC-fed mice ($p<0.0001$, Figure 14B). However, obese mice treated with tributyrin had no significant change in their body weight compared to WD treated with vehicle ($p=0.2296$) but were still significantly higher compared to NC group ($p<0.0001$, Figure 14C). Therefore, the improvement in exercise capacity was independent of body weight or weight loss. Exercise intolerance in HFpEF patients is associated with reduction in cardiac output (CO), and chronotropic incompetence (CI), that is related to decrease in cardiac β–receptors. From our echocardiography measurements, we found no significant changes in CO or heart rate (HR) between NC, WD and WD+Tributyrin mice (Figure 14D, E respectively). In addition, we performed cardiac RNA sequencing analysis, and we found no alteration in genes involved in autonomic nervous system regulation such as adrenergic or muscarinic receptors (Figure 14F). These data indicate that tributyrin's effect on exercise capacity is independent of effects on autonomic regulation of CO and HR.

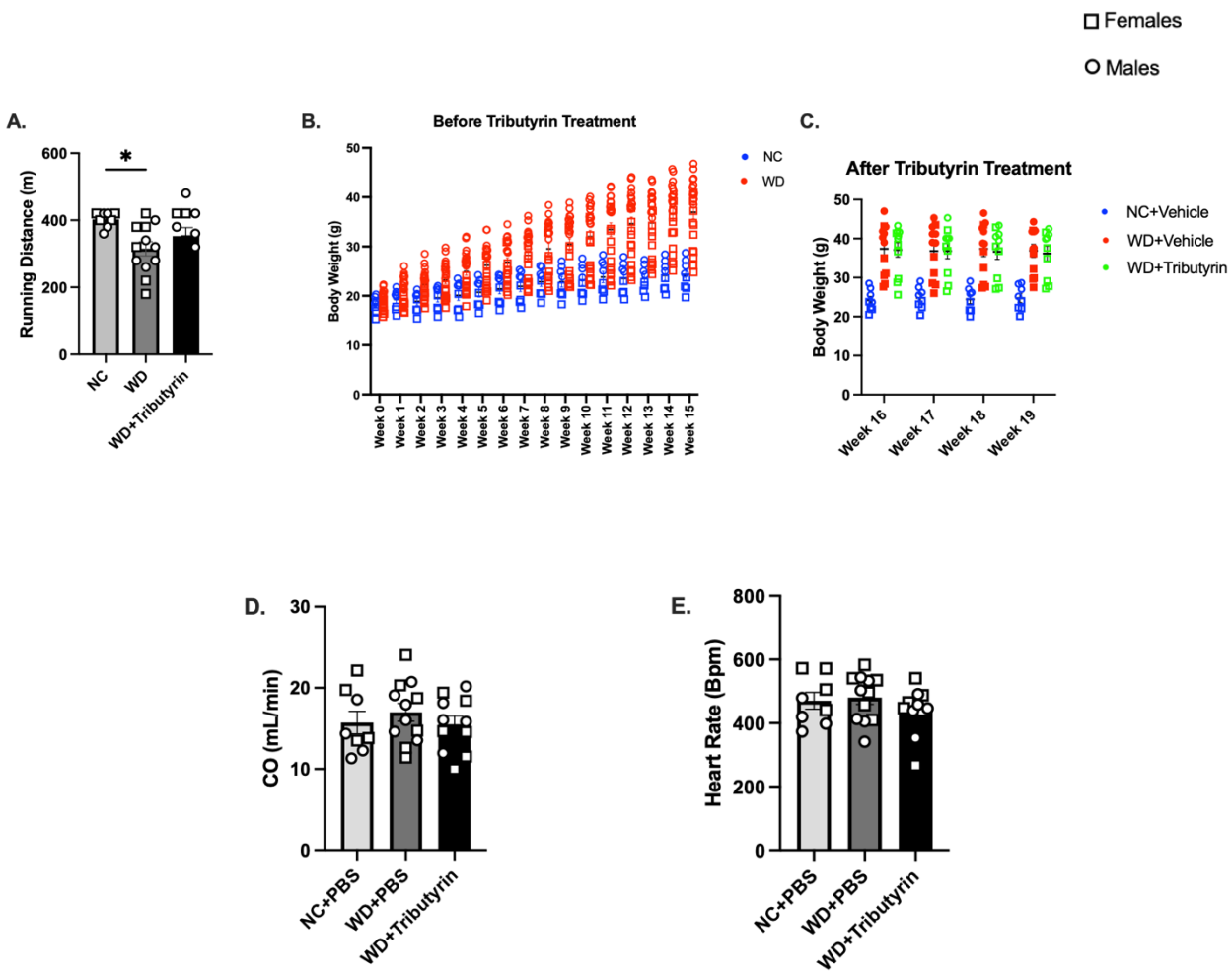
Females
Males
A.
Running Distance (m)
600
400
200
0
*
NC
WD
WD+Tributyrin
B.
Before Tributyrin Treatment
Body Weight (g)
50
40
30
20
10
0
NC
WD
Week 0
Week 1
Week 2
Week 3
Week 4
Week 5
Week 6
Week 7
Week 8
Week 9
Week 10
Week 11
Week 12
Week 13
Week 14
Week 15
C.
After Tributyrin Treatment
Body Weight (g)
50
40
30
20
10
0
NC+Vehicle
WD+Vehicle
WD+Tributyrin
Week 16
Week 17
Week 18
Week 19
D.
CO (mL/min)
30
20
10
0
NC+PBS
WD+PBS
WD+Tributyrin
E.
Heart Rate (Bpm)
800
600
400
200
0
NC+PBS
WD+PBS
WD+Tributyrin

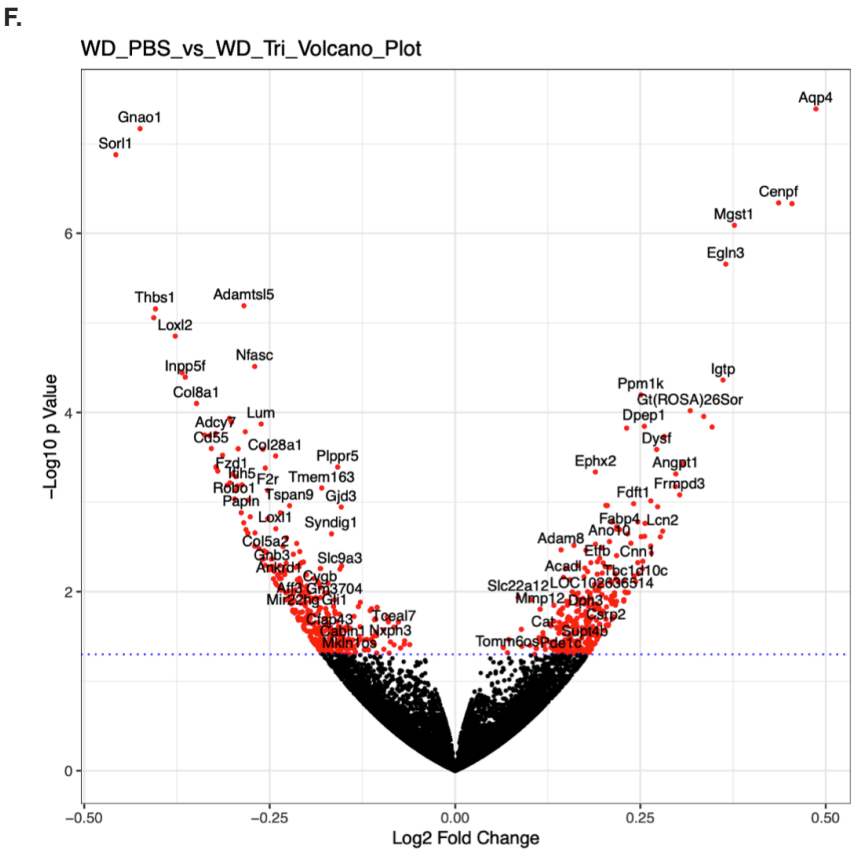

Figure 14. Tributyrin's Improvement in Exercise Capacity in Obese Pre-HFpEF Mice is Independent of Weight Loss, and Autonomic Regulation of Cardiac Output and Heart Rate. A) Running distance during exercise exhaustion test (m). Body weight measured weekly of B) NC and WD fed mice before tributyrin treatment and C) after vehicle or tributyrin treatment. Echocardiography measurements of D) cardiac output (mL/min) and E) heart rate (Bpm) between NC+vehicle, WD+vehicle and WD+Tributyrin groups. F) Volcano plot showing significantly altered genes in the heart of WD fed mice with vehicle or tributyrin. Statistical analysis was done using one-way ANOVA followed by Tukey's multiple comparison test. Data are mean ± S.E.M. (*p<0.05).

Tributyrin's Improvement in Exercise Capacity is Likely Independent of Changes in Mitochondrial Fatty Acid Oxidation in Muscle Cells

Another proposed mechanism for improvement in exercise capacity is the increase in skeletal muscles' fatty acid oxidation (FAO). It has been shown that skeletal muscle biopsies from HFpEF patients displayed mitochondrial dysfunction due to

deficiency in muscle oxidation and energy production. Therefore, we investigated whether butyrate's increase in exercise capacity is due to increase in FAO and mitochondrial function by measuring oxygen consumption rate (OCR) with the Seahorse XF assay, utilizing C2C12 (mouse myoblast) cells *in-vitro* approach. We treated C2C12 with sodium butyrate (NaB) or vehicle for 24 hours in low glucose media. Then we treated the cells with palmitate (LCFA) to further push the cells into utilizing FAO over glycolysis for energy production. We found significant decrease in the respiration rate (OCR) in response to the LCFA oxidation inhibitor etomoxir compared to media injection. This suggests that C2C12 cells preferred the utilization and oxidation of fatty acids under these experimental conditions. However, we found no significant changes in OCR with butyrate treatment compared to vehicle in either basal respiration (no changes in oxygen consumption to meet ATP demands under baseline conditions), or maximal respiration (no changes in oxygen consumption after adding FCCP which mimics physiological energy demand) (Figures 15A, B). In addition, we found no changes in spare respiratory capacity between vehicle and NaB treated cells indicating no changes in the cells' flexibility and the ability to respond to increase energy demand with butyrate (Figure 15C). These data show that butyrate's effects on increase in exercise capacity in mice is likely independent of its effects on mitochondrial function and fatty acid oxidation.

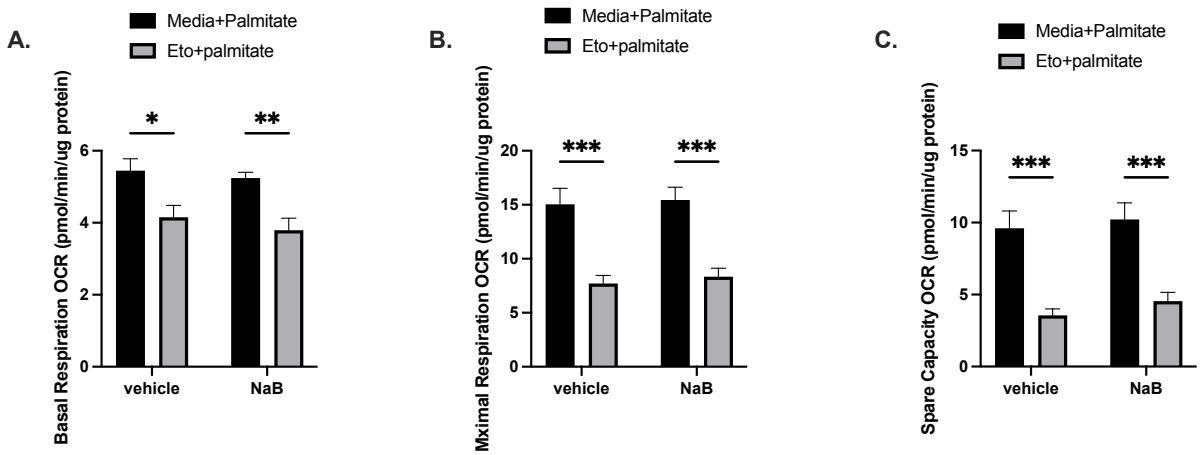

Figure 15. Butyrate does not Affect Mitochondrial Respiration and Fatty Acid Oxidation in C2C12 Cells. A) Basal mitochondrial respiration, B) Maximal mitochondrial respiration, C) Spare capacity (maximal - basal) mitochondrial respiration of OCR in C2C12 cells treated with palmitate and either vehicle or NaB. OCR readings were normalized to total protein concentration in each well after assay run. Statistical analysis was done using two-way ANOVA followed by Tukey's multiple comparison test. Data are mean ± S.E.M. (*p<0.05, **p<0.005, ***p<0.0005).

Discussion

Gut microbiome imbalance and changes in its composition has recently gained attention in HFpEF. A couple of studies show gut diversity and composition to be altered in HFpEF patients with decrease in the SCFA producing bacteria compared to control groups (239, 240). However, the mechanisms involved and whether reversing these changes will affect HFpEF progression is still not known. We have shown that gut microbiome modulation using FMT from lean mice into obese pre-HFpEF mice improved early cardiac dysfunction and hypertrophy. Additionally, obese mice show imbalance in their gut microbiome diversity and composition that is accompanied with decrease in butyrate producing bacteria. However, lean FMT intervention in obese mice led to significant increase in the circulating levels of the SCFA butyrate(253). Furthermore, our results showed that lean FMT treatment of obese pre-HFpEF mice

significantly improved their gut microbiome diversity and increased the abundance of butyrate producing bacteria. Our results demonstrated a preventative therapeutic role for gut microbiome in HFpEF progression and point to the SCFA butyrate as the potential mechanistic link between gut microbiome caused by diet induced obesity and cardiac changes seen in the pre-HFpEF stage.

Butyrate has been extensively studied in CVDs such as hypertension, myocardial infarction, and HFrEF. Where studies demonstrate its effectiveness in eliminating gut dysbiosis and improving cardiac function. However, to this day the effect of butyrate in HFpEF is not investigated. In this study, we aimed to test whether butyrate supplementation will replicate FMT's improvements in obese pre-HFpEF mice. Our results showed tributyrin treatment to have the same improvements of GLS, LSRr and LVPWd as lean FMT treatment. Unlike FMT study that included only male mice, we included both male and female mice in this study to investigate whether there are any sex differences in butyrate's effects on cardiac function and hypertrophy. We found no differences in tributyrin treatment's effects on GLS, LSRr and LVPWd between male and female obese pre-HFpEF mice. Butyrate treatment was able to better improve GLS and LSRr compared to FMT's improvements. For example, FMT improved GLS by -2.1% ± 0.92 compared to sham FMT. While tributyrin improved GLS by -10.4% ± 1.928 compared to vehicle treatment. FMT improved LSRr by 1.04 s^{-1} ± 0.62, whereas tributyrin improved LSRr by 4 s-1 ± 1.6. These data suggest that a more concentrated supplementation of Butyrate rather than FMT treatment provides better improvements in cardiac function.

In our tributyrin study we included both male and female mice to investigate whether there are any sex differences in tributyrin's effects on early cardiac dysfunction and cardiac hypertrophy. Even though male mice were more prone to body weight increase with WD than female mice, there were no significant differences in the effects of tributyrin between male and female obese pre-HFpEF mice.

Additionally, we found tributyrin to improve exercise capacity in obese pre-HFpEF that was independent of changes on heart rate (HR) or cardiac output (CO). The decrease in running distance correlated with an increase in body weights, however the improvement seen with tributyrin treatment was independent of changes in body weight. The effect of tributyrin on exercise capacity was also not different between male and female mice. Future studies should include further measurements of CO and HR in conscious mice during and immediately after exercise training such as heart rate recovery (which indicates how well the heart recovers after exercise/stress). Methods that could be used include those mentioned in chapter four discussion. Additionally, extracardiac effects on exercise capacity must also be considered such as cardiopulmonary changes which can be measured by assessing pVO_2.

Studies show butyrate to affect exercise capacity via improving mitochondrial metabolism and fatty acid oxidation in skeletal muscles(333, 334). Therefore, we analyzed the effect of butyrate supplementation on a mitochondrial function *in-vitro* using Seahorse XF assay. However, we found no changes in mitochondrial function (indicated by oxygen consumption rate) after butyrate treatment. Additionally, in the presence of the carnitine palmitoyltransferase-1 (CPT-1) inhibitor Etomoxir, butyrate supplementation was not efficient in increasing mitochondrial function and energy

production. However, more experiments must be performed in order to conclude the effect of butyrate on mitochondrial oxidation and metabolism. For example, other cell types must be considered in these measurements such as isolated mitochondria from mice skeletal muscle tissue, or a more human relative cells such as primary human skeletal muscle cells (HSkMC) or iPSC (induced pluripotent stem cells) differentiated skeletal muscle cells. In addition, the effect of butyrate on cardiac metabolism must also be tested to investigate whether butyrate affects cardiac mitochondrial function. This can be done using isolated cardiomyocytes from treated mice, iPSC differentiated cardiomyocytes, or mitochondria isolated from treated mice heart tissue. Exercise intolerance is a key clinical feature of HFpEF development. Understanding the physiology involved and targeting the specific abnormalities is critical for developing effective therapies that will help improve patient outcomes.

Collectively, these data indicate butyrate as a better alternative to FMT treatment in improving early cardiac dysfunction and cardiac hypertrophy. In addition, butyrate was also efficient in improving exercise capacity in obese pre-HFpEF mice. Finally, the advantage of using butyrate supplementation over FMT helps avoid the risk of infection, endotoxin transfer and rejection risks that are associated with FMT.

CHAPTER SIX

TRIBUTYRIN IMPROVES BRANCHED CHAIN AMINO ACIDS METABOLIC PATHWAY IN THE HEART

Introduction

In our previous data we show that improving gut microbiome health by FMT and tributyrin supplementation have similar effects on early cardiac dysfunction and cardiac hypertrophy in obese pre-HFpEF mice. However, the molecular mechanisms involved are still not known. It is critical to identify the molecular mechanisms involved in pre-HFpEF progression in order to develop targeted and preventative therapeutic strategies. Therefore, we sought to identify the molecular pathways that are altered in the heart and might be contributing to these effects by performing cardiac RNA sequencing analysis. This technique helped us identify several genes that are being upregulated/downregulated in the heart due to butyrate. By analyzing these genes and the molecular pathways they are involved in, we were able to identify the branched chain amino acids (BCAAs) catabolism pathway that is involved in obesity, metabolism, and heart function.

BCAAs include Valine, Leucine, and Isoleucine. They are essential amino acids that are not synthesized in the body but are obtained from diet, and they provide building blocks for protein synthesis(335-338). In addition to being involved in protein synthesis and turnover, they are involved in many metabolic processes such as glucose

metabolism and energy production via TCA cycle, and physiological processes like insulin signaling, cell growth regulation and apoptosis(339-345). BCAAs bypass the liver and are oxidized in peripheral tissues like skeletal muscles, heart, adipose tissue, and other organs(336, 339, 346-349). Their uptake into cells occur through L-type amino acid transporter 1 (LAT1) and/or L-type amino acid transporter 2 (LAT2) also known as SLC7A5 and SLC7A8 respectively(350-352) (Figure 16).

BCAAs metabolism begins with the reversible transamination reaction by branched-chain amino acid transferase (BCAT) to produce branched-chain α-keto acid (BCKA)(336). Valine is converted to α-ketoisovaleric acid (KIV), Leucine is converted to α-ketoisocaproic acid (KIC), and Isoleucine is converted to 3-methyl-2-oxovaleric acid (KMV)(353). BCKAs are then irreversibly catabolized by the rate limiting enzyme BCKA dehydrogenase complex (BCKDH) to produce final metabolites(354-356). Valine metabolism yields succinyl-CoA, leucine yields acetoacetate and acetyl-CoA, while isoleucine yields propionyl-CoA and acetyl-CoA. All of which contribute to energy production(336, 352, 357). The rate limiting enzyme BCKDH is regulated by the activity of the protein phosphatase (PP2Cm) and kinase (BDK) When BCKDH is phosphorylated by BDK it becomes inactive, meanwhile it gets activated when dephosphorylated by PP2Cm(354, 356, 358) (Figure 16). The PP2Cm/BDK regulation of BCKDH is what controls the catabolism of BCAAs.

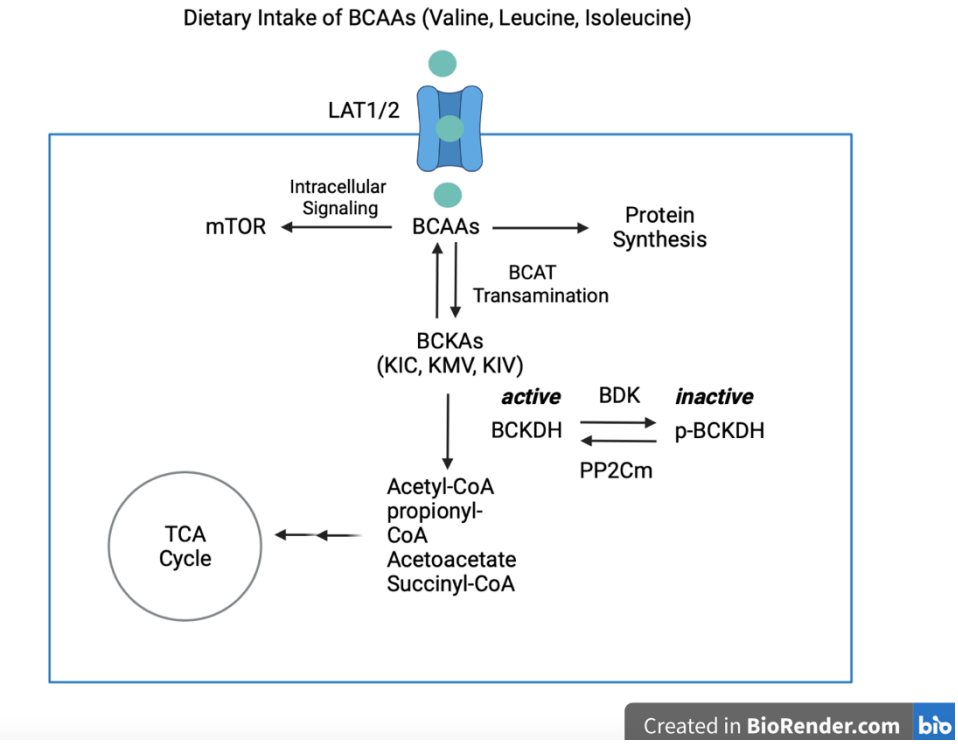

Figure 16. BCAAs Catabolic Pathway. BCAT; branched-chain amino acid transferase. BCKAs; branched-chain α-keto acid. BCKDH; BCKA dehydrogenase complex. KIV; α-ketoisovaleric acid. KMV; 3-methyl-2-oxovaleric acid. KIC; α-ketoisocaproic acid. PP2Cm; protein phosphatase 2Cm. BDK; branched-chain α-ketoacid dehydrogenase kinase

PP2Cm was identified by Lu G. et al. (2007) as a protein of the Serine/Threonine phosphatase (PP2C) family that was exclusively located in the mitochondria. They found it to be highly expressed in the heart and further determined its expression profile in TAC induced heart failure in mice where it was significantly reduced compared to control hearts. This indicates a potential role for PP2Cm in cardiac function(359). Furthermore, Lu G. et al. (2009) performed biochemical purification and identified BCKDH as the protein substrate of PP2Cm. Using both *in-vitro* and *in-vivo* models they demonstrate the importance of PP2Cm in dephosphorylating and activating BCKDH enzyme and in turn activating BCAA catabolism. They show PP2Cm KO ($PP2Cm^{-/-}$)

mice to have significant upregulation in BCAA and BCKA levels compared to WT mice. In addition, loss of PP2Cm led to increase in reactive oxygen species (ROS) levels indicating a direct link between PP2Cm activity and oxidative stress. This data further confirms the importance of protein phosphatase 2Cm (PP2Cm) as a key regulator of BCAAs catabolism, oxidative stress, and cardiac dysfunction(360).

Since dietary food is the main source for BCAAs production and gut microbiome plays a key role in food digestion to produce important metabolites, several studies have suggested a role for gut microbiome in the synthesis of BCAAs. Studies have reported an association between gut microbiota composition alteration and biosynthesis/degradation of BCAAs in both human and animal models of obesity/T2D. Liu R. et al. performed metagenomic and metabolomic analysis of obese and lean individuals and found gut microbiome of obese individuals to have microbiome species associated with increased production of BCAAs and decrease in their degradation(361). Pedersen K.H. et al. investigated gut microbiome composition in patients with insulin resistance and metabolic syndrome and they identified a positive correlation between *Prevotella Copri (p.copri)* and increasing levels of BCAAs. They validated these findings experimentally by placing mice on HFD and oral gavage with either *p.copri* or sham (1% glycerol in PBS). obese mice with *p.copri* gavage had significant increase in their BCAAs levels compared to sham gavaged mice. In addition, *p.copri* treated mice developed insulin resistance and glucose intolerance compared to sham mice. Indicating a direct effect of gut microbiome on BCAAs metabolism and the development of metabolic syndrome(362). Several other groups investigated the association between gut microbiome and BCAAs in animal models of obesity (HFD fed mice) (363) and

diabetes (HFD+STZ injection)(364). Researchers found serum levels of BCAAs to be upregulated in both animal models in addition to gut dysbiosis. Based on gut microbiome changes, pathway analysis identified BCAAs synthesis pathway to be increased in obese mice(363) while their degradation pathway was decreased(365).These data indicate that gut microbiome modulation provide a promising therapeutic target for obesity associated defects in BCAAs catabolism and the effects of their accumulation in the body on cardiac function.

Defects in BCAA catabolism causes accumulation of circulating BCAAs levels and has been shown to be associated with development of metabolic syndrome like obesity, T2D, insulin resistance as well as CVDs including heart failure. Sun H. et al. performed transcriptomic and metabolomic analysis on TAC induced HF in mice and found the BCAA catabolic enzymes (BCAT, BCKDH, and PP2Cm) to be significantly reduced. This was accompanied with significant increase in the levels of BCKAs (KIV, KIC, and KMV) but not BCAAs in the failing hearts. They observed similar results in failing human hearts where BCAT, BCKDH, and PP2Cm were significantly reduced, while BCKAs but not BCAAs were increased in HF patients compared to controls. To test a direct association between BCAA catabolism and heart function, they performed PP2Cm KO ($PP2Cm^{-/-}$) that led to significant accumulation in cardiac BCAAs and BCKAs, as well as impairment in cardiac function indicated by a decrease in LV ejection fraction and cardiac contractility accompanied with elevated wet lung weights (pulmonary congestion). These data further show an association between BCAAs catabolism defects and the development of heart failure. To investigate the upstream molecular mechanisms involved in the regulation of BCAAs catabolism, they performed

regulator analysis and identified Krüppel-like factor 15 (KLF15) transcription factor as a main regulator of BCAA catabolism. Overexpressing KLF15 in cultured cardiomyocytes led to upregulation in BCAT, BCKDH, and PP2Cm. Meanwhile, KLF15 KO ($KLF15^{-/-}$) in the heart reduced the expression of BCAT, BCKDH and PP2Cm. They also investigated the possible mechanisms involved in BCAAs and BCKAs accumulation effects on cardiac function and found their accumulation to increase the production of superoxide that is associated with increased oxidative stress in the failing hearts. Therefore, they conclude that deficiency in BCAAs catabolism due to deficiency in the upstream transcriptional regulator KLF15 leads to cardiac dysfunction and heart failure due to their downstream effects on superoxide production and oxidative stress(366).

Similarly, Uddin M.G. et al. studied BCAAs metabolism in dilated cardiomyopathy patients (DCM) and TAC induced heart failure mouse model. In DCM patients they found cardiac PP2Cm and BCAT levels to be significantly reduced, and this was associated with significant increase in p-BCKDH and cardiac BCAAs levels. Similarly, they found cardiac BCAAs and p-BCKDH to be significantly increased in TAC mice. However, treating TAC mice with BT2 (pharmacological inhibitor of BDK) significantly improved BCAAs catabolism indicated by decreased in cardiac BCAAs and p-BCKDH levels. This improvement was associated with improved LV ejection fraction and attenuation of cardiac hypertrophy seen in TAC mice indicating an association between BCAAs catabolism impairment and the development of cardiac dysfunction. Like previous findings, they found the decrease in BCAA catabolism to be associated with decrease in KLF15 expression. However, they further identified upstream regulation of KLF15 where they found its downregulation to be due to increase in the activation of

TAK1 and p38MAPK. Furthermore, they identified the activation of mTOR pathway and its subsequent impairment in insulin signaling as a potential mechanism by which BCAAs catabolism defects contribute to cardiac dysfunction in the failing heart(367).

Wang W. et al. found BDK, inactive p-BCKDH, and cardiac BCAAs levels to be significantly upregulated, while PP2Cm levels were significantly reduced in MI mice hearts. This was associated with increased inflammation, fibrosis, and cardiac remodeling due to activation of mTOR signaling(368). Similarly, Lian K. et al. found PP2Cm to be significantly reduced but p-BCKDH, cardiac BCKAs and BCAAs to be significantly increased in diabetic mice (HFD+STZ injection) compared to WT mice. Overexpression of PP2Cm (using PP2Cm-expressing adenovirus injection) in diabetic mice followed by MI induction led to significant decrease in infarct size, while PP2Cm whole body KO ($PP2Cm^{-/-}$) significantly increased infarct size in MI mice compared to sham mice indicating an association between BCAA catabolism and myocardial injury. To investigate this association further, they treated diabetic + MI mice with BT2 (a pharmacological inhibitor of BDK), which significantly reduced cardiac BCKAs, BCAAs, and p-BCKDH levels. BT2 treatment also reduced myocardial infarct size in both diabetic + MI mice and $PP2Cm^{-/-}$ +MI mice. These data confirm that improving BCAAs catabolism, either by activating PP2Cm or inhibiting BDK, attenuates myocardial injury in diabetic mice. Similar to Sun H. et al, they found the association between BCAAs catabolism defects and cardiac dysfunction to be mediated through increase in oxidative stress(369).

Furthermore, the association between BCAAs catabolism defects and oxidative stress were directly studied by Zhenyukh O. et al. using an *in-vitro* cell model. They

found cultured human peripheral blood mononuclear cells (PBMC) and endothelial cells (ECs) treated with high BCAAs to increase oxidative stress and inflammation through the activation of the mTOR pathway(370). These data indicate that defective BCAAs catabolism pathway is involved in both metabolic and cardiac dysfunctions, and the associated mechanisms include transcriptional regulation by KLF15 and increase in oxidative stress, inflammation, fibrosis, and cardiac remodeling that occurs through activation of many downstream signaling pathways such as mTOR signaling.

Several research papers show BCAAs to be accumulated in HF patients and animal models of HFrEF due to defects in the catabolic enzymes PP2Cm and active BCKDH(366-368, 371). Meanwhile, increasing BCAAs oxidation/metabolism in HFrEF animal models led to significant improvements in cardiac dysfunctions(369). Additionally, recent transcriptomic analysis by Gibb A.A. et al. on early and late HFpEF cat model showed elevated BCAAs levels and defects in its catabolic pathway in both stages(224). These findings indicate a potential role for BCAAs in HFpEF development, and improving their metabolism provides a promising preventative therapeutic for HFpEF progression. However, studies that address these concepts are still lacking.

Our study shows defects in BCAAs catabolism in the early stage of obesity associated HFpEF and provides for the first time a role for gut microbiome metabolites in improving BCAAs metabolism that is linked to improvements in early cardiac changes at the pre-HFpEF stage. These results present a novel molecular mechanism involved in obesity associated HFpEF and open new avenues for the development of preventative therapeutics involving the gut microbiome.

Results

Tributyrin Treatment Altered Gene Expression in the Heart.

To investigate the molecular mechanisms by which butyrate improves cardiac function and hypertrophy in obese pre-HFpEF, we turned to metagenomic analysis to identify changes in cardiac gene expression of WD-fed mice treated with vehicle or tributyrin (Chapter five). By performing RNA sequencing analysis, we identified 23,564 transcripts in the heart. Using a 5% false discovery rate (FDR) we found sixteen genes to be significantly changed with tributyrin treatment (Figure 17A). Out of the sixteen altered genes, nine were significantly downregulated while seven were significantly upregulated with tributyrin (Figure 17B). Of the nine downregulated genes many are involved in collagen formation and extracellular matrix (ECM) which in turn is involved in cardiac fibrosis and hypertrophy. For example, *Loxl2* (encodes lysyl oxidase homolog 2) is involved in collagen crosslinks formation and increase in fibrosis(372-374). *Col16a1*(encodes collagen type XVI alpha 1 chain) which is associated with the formation of collagen type I and type II(375). *Thbs1* (encodes thrombospondin 1) is involved in cell adhesion, and ECM expression where it activates TGF- β (which is involved in fibrosis by activating myofibroblasts activation and increases collagen secretion and deposition into the ECM) in multiple cell types like endothelial cells and cardiac fibroblasts(376, 377). *Nfasc* (encodes Neurofascin) is involved in the formation of cell adhesion molecules that in turn induces fibrosis (increase in cell adhesion molecules is known to increase inflammatory cell recruitment and infiltration)(378, 379).

On the other hand, the upregulated genes are involved in the regulation of cellular and metabolic processes (Figure 17C) such as *mgst1* (Microsomal glutathione

S-transferase 1) which plays a role in the protection of mitochondria from oxidative stress(380). *Ppm1k* (protein phosphatase Mg2+/Mn2+ Dependent 1K) encodes PP2Cm (protein phosphatase 2Cm) which is involved in activation of branched chain amino acids (BCAAs) catabolic pathway(359, 360). *Aqp4* (Aquaporin 4) which is involved in cardiac contractility through regulation of SERCA pump (sarco-/endoplasmic reticulum Ca^{2+} ATPase)(381, 382), a regulator of muscle relaxation by facilitating calcium transport from the cytosol into the sarcoplasmic reticulum (SR) during diastole(383, 384). It was shown that Aqp4-KO mice had SERCA downregulation, resulting in increased diastolic $[Ca^{2+}]_i$, and in turn increased risk in cardiac arrhythmias and heart failure(385). *Cacng6* (Calcium Voltage-Gated Channel Auxiliary Subunit Gamma 6) encodes voltage gated calcium channels gamma subunit which in turn stabilizes calcium channels in the closed (inactive) state giving muscle cells enough time to relax properly before the next contraction(386). *Igtp* (interferon-gamma induced GTPase) which is involved in the protection from bacterial infections(387). *Egln3,* a member of the alpha-ketoglutarate-dependent hydroxylases that have several roles including biosynthesis, post-translational modifications, epigenetic regulation, and cell energy metabolism(388). *CenpF* (encodes Centromere protein F) which plays a role in proper mitosis and cell division(389, 390).

A.

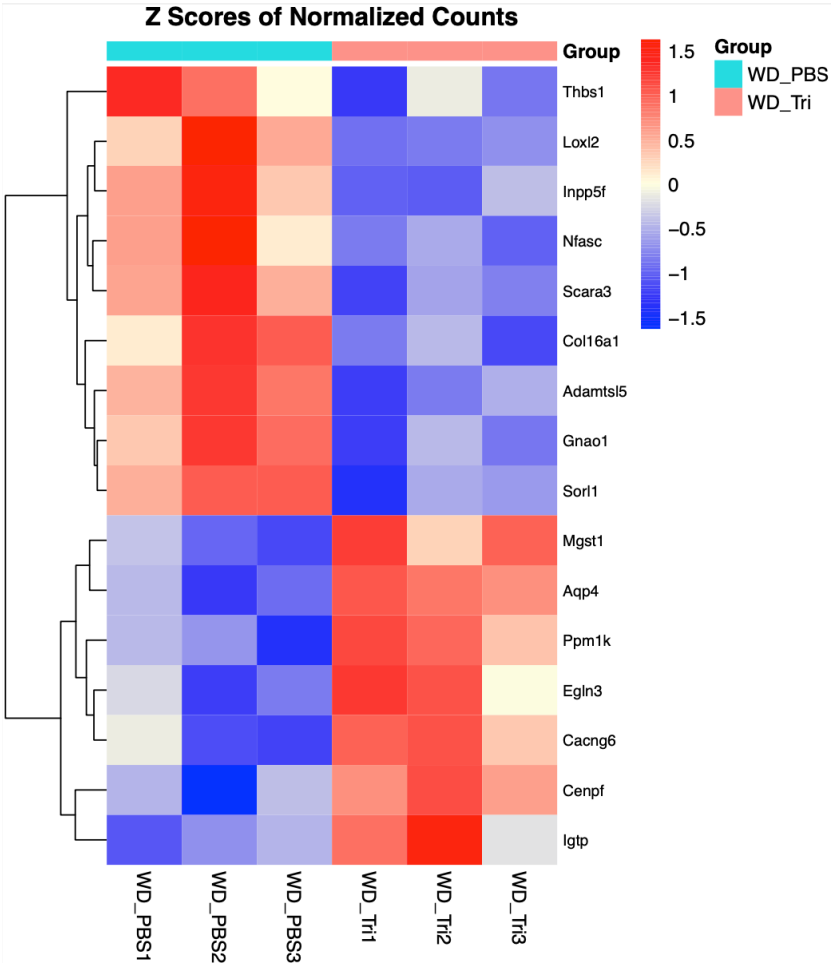
Z Scores of Normalized Counts
Group
WD_PBS
WD_Tri
1.5
1
0.5
0
−0.5
−1
−1.5
Thbs1
Loxl2
Inpp5f
Nfasc
Scara3
Col16a1
Adamtsl5
Gnao1
Sorl1
Mgst1
Aqp4
Ppm1k
Egln3
Cacng6
Cenpf
Igtp
WD_PBS1
WD_PBS2
WD_PBS3
WD_Tri1
WD_Tri2
WD_Tri3

B.

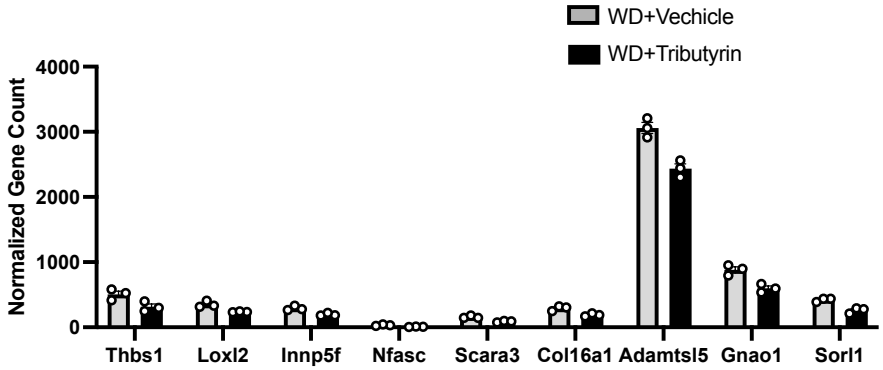
WD+Vechicle
WD+Tributyrin
Normalized Gene Count
4000
3000
2000
1000
0
Thbs1
Loxl2
Innp5f
Nfasc
Scara3
Col16a1
Adamtsl5
Gnao1
Sorl1

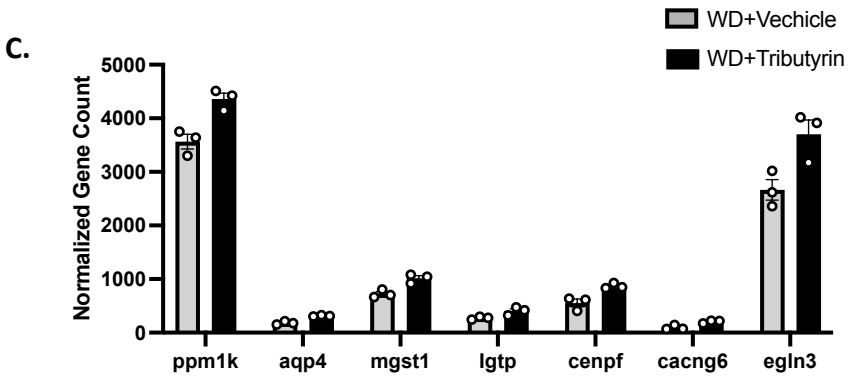

Figure 17. Tributyrin Treatment Altered Gene Expression in the Hearts of Obese pre-HFpEF Mice. A) heat map showing topmost regulated transcripts after tributyrin or vehicle treatment in the hearts of obese pre-HFpEF mice (5% FDR-adjusted P<0.05), B) Normalized gene count of downregulated genes after tributyrin compared to vehicle treatment, C) Normalized gene count of upregulated genes after tributyrin compared to vehicle treatment.

Tributyrin Modulates the Expression of Enzymes Involved in Branched Chain Amino Acids Catabolic Pathway

Of the 16 significantly altered genes with tributyrin treatment, *ppm1k* was of particular interest to us because it is highly involved in metabolism, mitochondrial function, obesity, and CVDs. As indicated from the previous RNAseq data (Figures 17A, C), tributyrin significantly upregulates the expression of *ppm1k* in the heart, which encodes the enzyme PP2Cm that dephosphorylates and activates the rate limiting enzyme, branched-chain α-keto acid dehydrogenase (BCKDH), in the BCAAs catabolic pathway. Therefore, we investigated whether tributyrin affects BCAAs catabolism by altering the expression of the enzymes PP2Cm and BCKDH. By performing western blot analysis, we measured the protein levels of PP2Cm in the hearts of obese pre-HFpEF mice after vehicle or tributyrin treatments. We found tributyrin to significantly

increase the levels of PP2Cm compared to vehicle treatment (Figure 18A, B). From this result we expected the increase in PP2Cm levels to cause a decrease in the levels of the inactive p-BCKDH. Therefore, we measure the levels of p-BCKDH in the hearts and we found it to be significantly decrease after tributyrin treatment (Figure 18C, D). This data indicate that butyrate plays a role in enhancing the catabolism of BCAAs in the heart through modulation of the metabolic enzymes involved. Therefore, we measured the serum and cardiac BCAAs levels. However, we found no significant changes in either measurement between tributyrin and vehicle treated obese mice (Figure 18E, F). In addition, since BCKDH is directly involved in the catabolism of BCKAs (KIV, KMV, KIC) we measured serum levels of BCKAs in our tributyrin treated mice. However, we found no significant difference in either BCKA between WD+Vehicle and WD+Tributyrin treated mice.

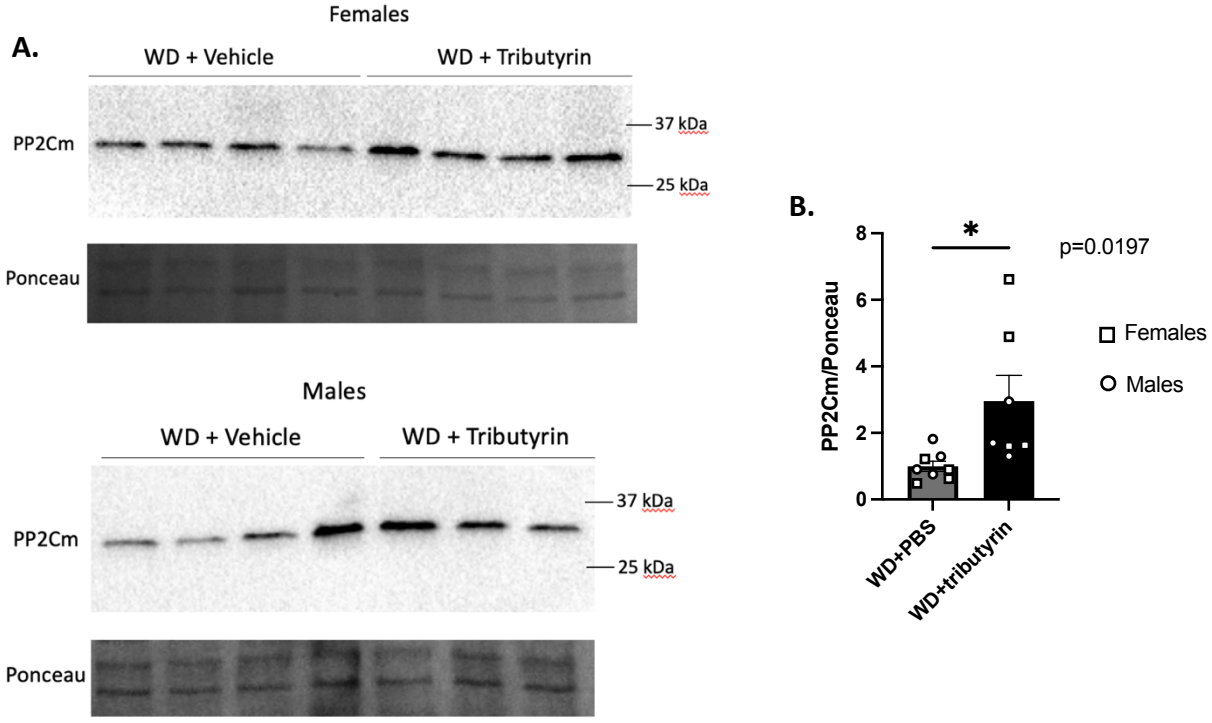

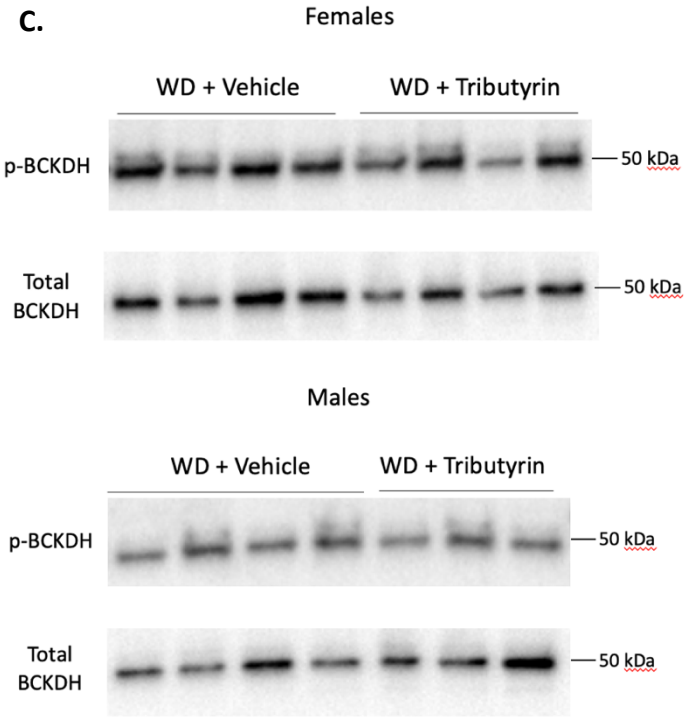
C.
Females
WD + Vehicle
WD + Tributyrin
p-BCKDH
50 kDa
Total BCKDH
50 kDa
Males
WD + Vehicle
WD + Tributyrin
p-BCKDH
50 kDa
Total BCKDH
50 kDa

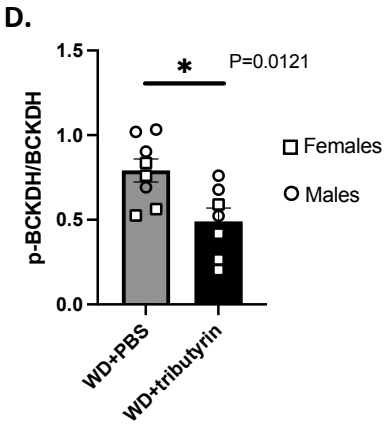
D.
p-BCKDH/BCKDH
1.5
1.0
0.5
0.0
*
P=0.0121
Females
Males
WD+PBS
WD+tributyrin

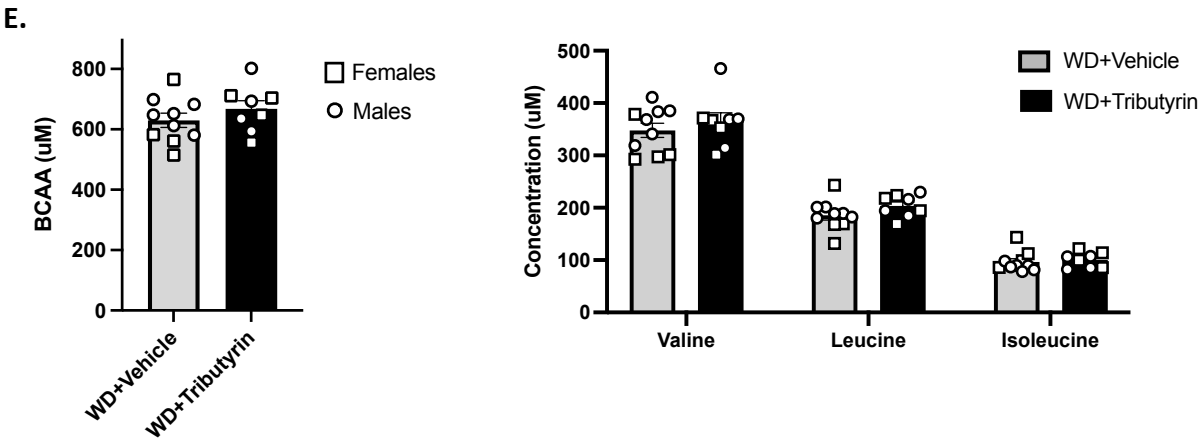
E.
BCAA (uM)
800
600
400
200
0
Females
Males
WD+Vehicle
WD+Tributyrin
Concentration (uM)
500
400
300
200
100
0
WD+Vehicle
WD+Tributyrin
Valine
Leucine
Isoleucine

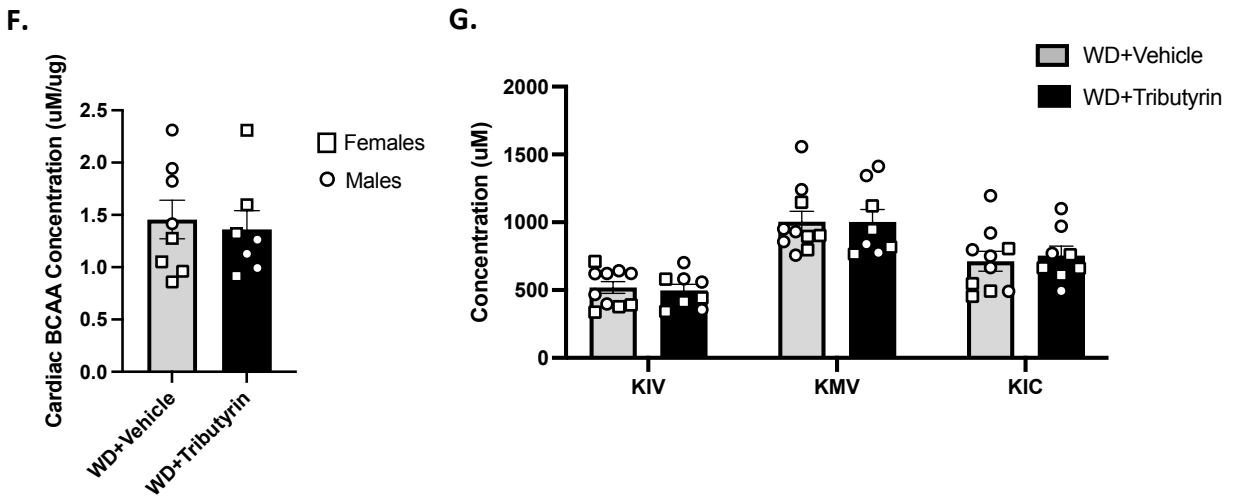

Figure 18. Tributyrin Alters Protein Expression of BCAAs Catabolic Enzymes PP2Cm and p-BCKDH. A) Immunoblot images of PP2Cm protein and total protein staining (ponceau) from WD-fed mice treated with Tributyrin or vehicle, B) Densitometric analysis of the ratio of PP2Cm to total protein staining (ponceau) bands, C) Immunoblot images of p-BCKDH and total BCKDH from hearts of WD-fed mice treated with Tributyrin or vehicle, D) Densitometric analysis of the ratio of p-BCKDH/BCKDH protein bands, E) Concentration of combined and separate BCAAs in serum of WD+vehicle and WD+Tributyrin treated mice, F) Cardiac BCAAs levels in WD vehicle and WD+Tributyrin treated mice normalized to total protein concentration, G) BCKAs serum concentration levels. Statistical analysis was done using unpaired student's t-test. Data are mean ± S.E.M. (*p<0.05).

Fecal Microbiome Transplantation and Tributyrin Treatments Share Similar Effects on BCAAs Catabolic Pathway in the Heart of Obese Pre-HFpEF Mice

The data in chapter three showed tributyrin treatment to replicate FMT's effects on early cardiac dysfunction and cardiac hypertrophy in obese pre-HFpEF mice. Therefore, we sought to investigate whether FMT has similar effects as tributyrin on BCAAs catabolic enzymes PP2Cm and p-BCKDH. We measure the levels of *pp1mk* gene expression in the heart using RT-qPCR. In WD-fed mice we found *ppm1k* levels to have a trend towards decreasing compared to NC-fed mice (Figure 19A), while *ppm1k* showed opposite trend towards increasing in mice treated with FMT compared to sham

FMT (Figure 19B). However, these results did not reach statistical significance. Furthermore, we measured the levels of PP2Cm protein expression by western blot analysis. Similar to *ppm1k* results, we found PP2Cm protein levels to trend towards decrease in WD-fed mice compared to NC-fed mice (Figures 19C, D), while PP2Cm had a trend towards increase with FMT compared to sham FMT treated obese mice (Figures 19E, F). For further analysis of FMT's effect on BCAA catabolism pathway, we measured the levels of p-BCKDH protein, and we found it to be significantly increased in WD-fed mice (Figures 19G, H), and that to be significantly decreased with lean FMT treatment (Figures 19I, J). These data further confirm that tributyrin and FMT share common molecular mechanism in improving cardiac dysfunction and hypertrophy in obese pre-HFpEF, and that is likely through the modulation of enzymes involved in BCAAs metabolic pathway.

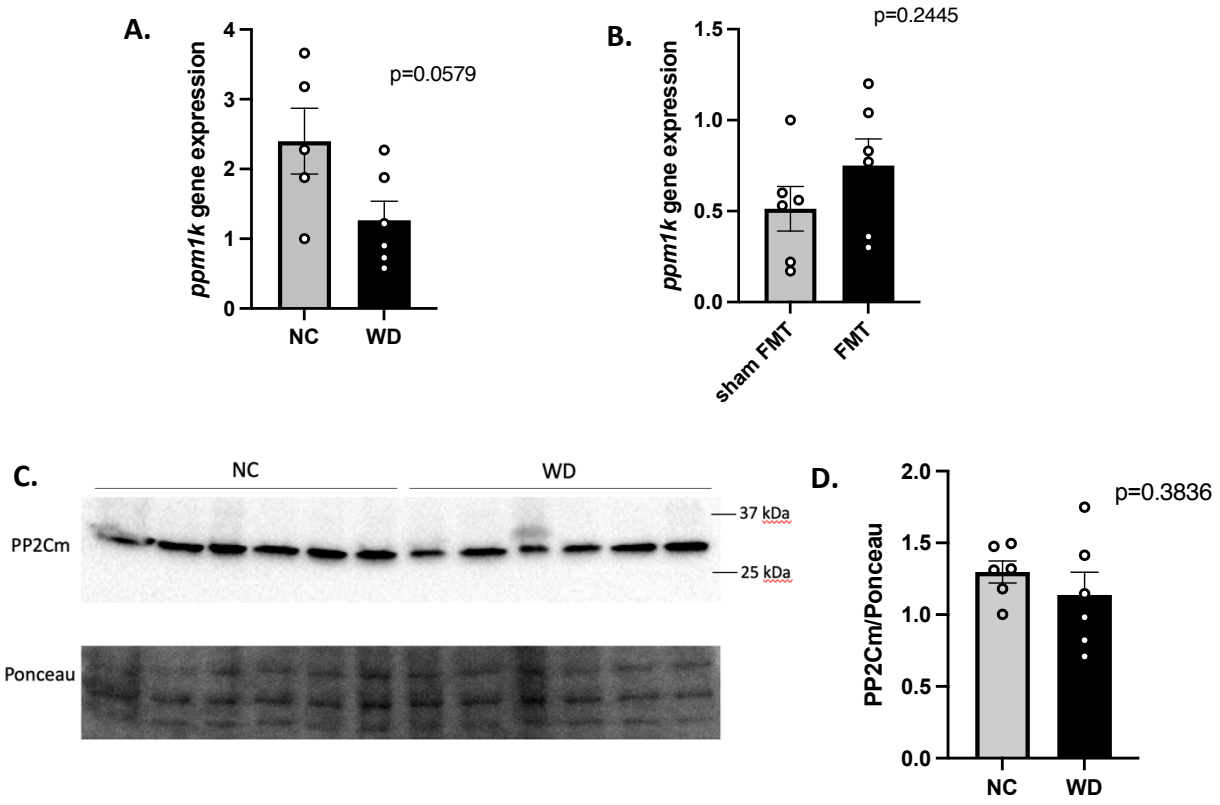

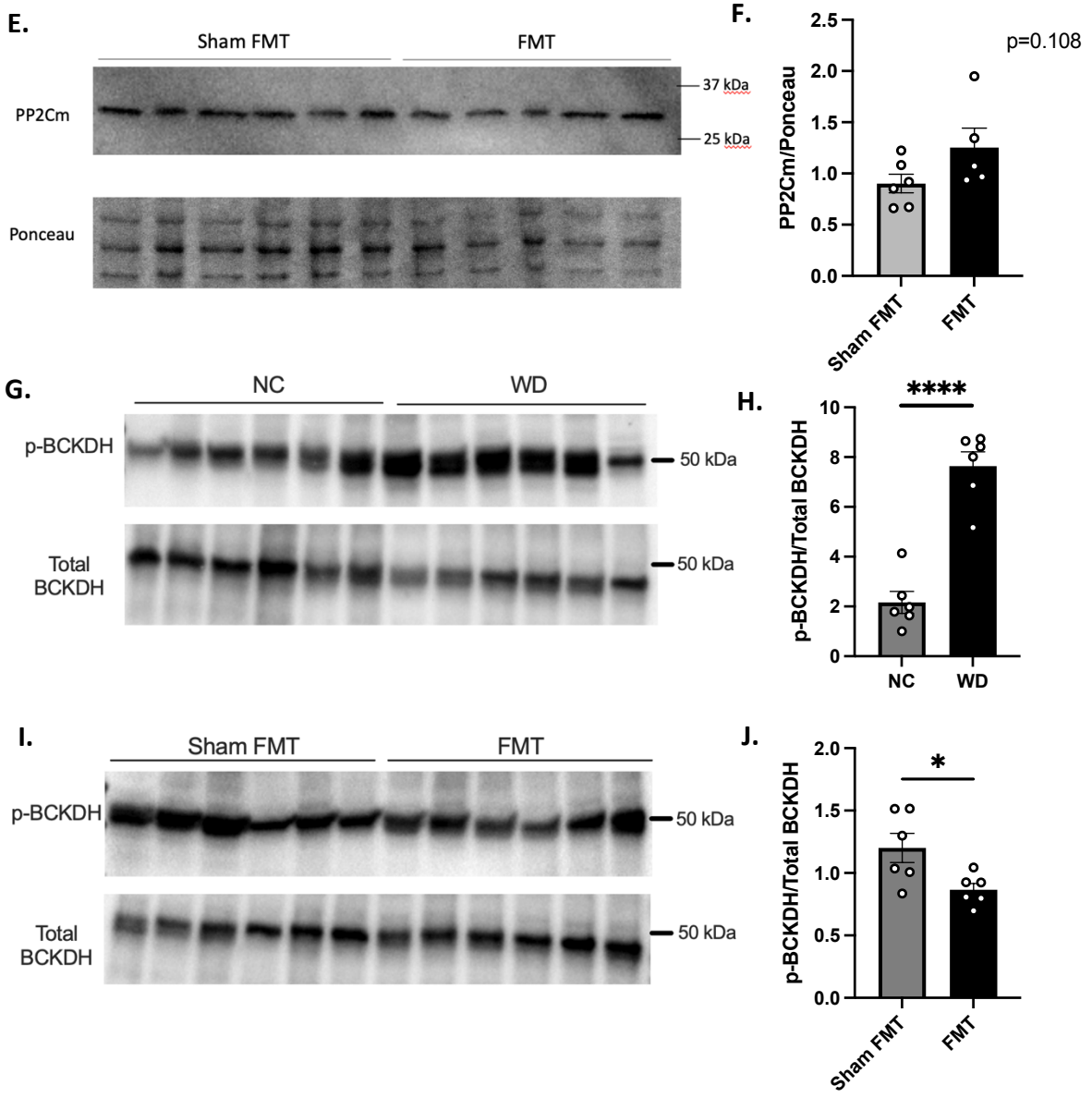

Figure 19. FMT Treatment has Similar Effects as Tributyrin on BCAAs Catabolism Enzymes. mRNA levels of *ppm1k* using RT-qPCR analysis from A) NC and WD fed mice, B) sham FMT and FMT treated obese mice, C) Immunoblot images of PP2Cm and total protein staining from NC and WD fed mice, D) Densitometric analysis of the ratio of PP2Cm to total protein staining (ponceau) bands, E) Immunoblot images of PP2Cm and total protein staining from FMT and sham FMT treated mice, F) Densitometric analysis of the ratio of PP2Cm to total protein staining (ponceau) bands, G) Immunoblot images of p-BCKDH and total BCKDH from hearts of NC and WD fed mice. H) Densitometric analysis of the ratio of p-BCKDH/BCKDH protein bands, I) Immunoblot images of p-BCKDH and total BCKDH from hearts of WD fed mice treated with sham FMT or FMT, J) Densitometric analysis of the ratio of p-

BCKDH/BCKDH protein bands. Statistical analysis was done using unpaired student's t-test. Data are mean ± S.E.M. (*p<0.05, ****p<0.00005).

Tributyrin's Increase in *ppm1k* Gene Expression was in Part Due to its Histone Deacetylase Inhibition (HDACi) Activity

Following butyrate's increase in *ppm1k* gene expression and the encoded protein PP2Cm in the heart, which in turn decreased the phosphorylated (inactive) rate limiting enzyme p-BCKDH, we wanted to investigate the molecular mechanisms by which butyrate caused these effects. As mentioned previously in chapter two (Figure 2), SCFAs effects are mediated either by binding to their GPCRs, participating in mitochondrial metabolism and ATP generation, inhibiting HDAC/increasing HAT activity that leads to upregulation in gene expression. In order to test whether butyrate increases *ppm1k* by binding to its GPCRs, we performed *in-situ* hybridization of FFAR2/3 in heart tissue sections. We found both receptors to have very low expression in the heart (Figure 20A, B) compared to positive control tissue nodos ganglia, which is known to have very high expression of FFAR2/3 (Figure 20C). Which indicates that butyrate's effects in the heart are independent of binding to GPCRs and the subsequent activation of intracellular signaling pathways. From our results in chapter five (Figure 15), we saw that butyrate does not affect mitochondrial respiration or energy production therefore, butyrate's effects on BCAAs catabolism are independent of its effects on mitochondrial metabolism. Lastly, we tested whether butyrate's effects were mediated by its HDAC inhibition activity using *in-vitro* assay. We treated C2C12 mouse myoblasts with NaB or vehicle followed by RT-qPCR to make sure we see similar effects on *ppm1k* gene expression *in-vitro.* We saw significant increase in *ppm1k* gene expression with NaB treatment as early as six hours of treatment (Figure 21A). After this

confirmation, we treated C2C12 cells with the pharmacological HDAC inhibitor, Trichostatin A (TSA), or vehicle followed by RT-qPCR to test for *ppm1k* gene expression. Similar to our findings with NaB treatment, we found *ppm1k* expression to be significantly increased with TSA compared to vehicle treatment (Figure 21B). Therefore, this indicates that butyrate's increase in *ppm1k* levels and BCAA metabolic pathway is due to its HDAC inhibition activity.

A.

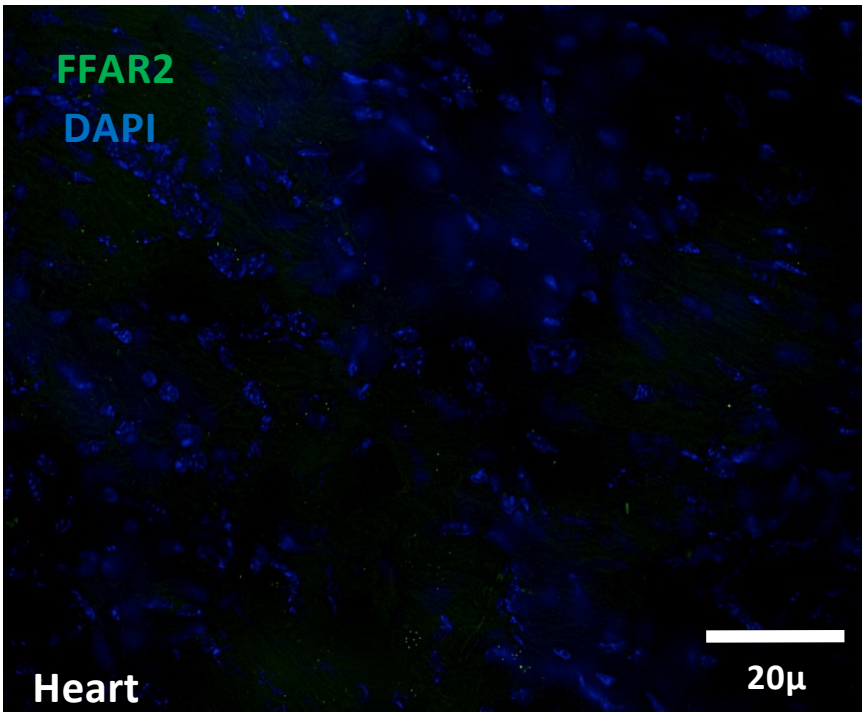

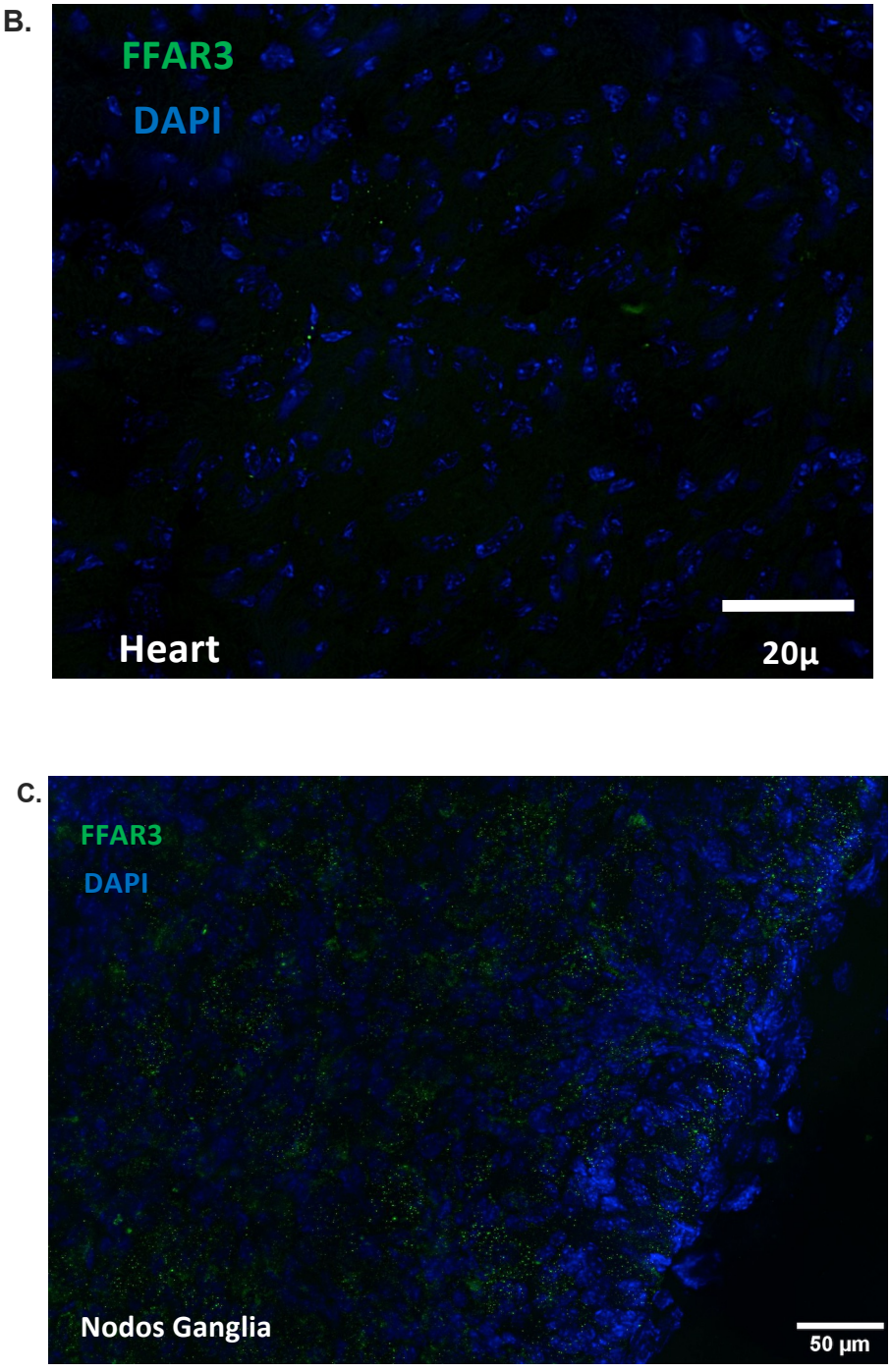

Figure 20. Tributyrin's Effects on *ppm1k* is Independent of Binding to its GPCRS FFAR2/3. Chromogenic *in-situ* hybridization staining of A) *ffar2* mRNA (green) and B) *ffar3* mRNA (green) in heart sections. C) Chromogenic *in-situ* hybridization staining of *ffar3* mRNA (green) in nodose ganglia (NG) (positive control).

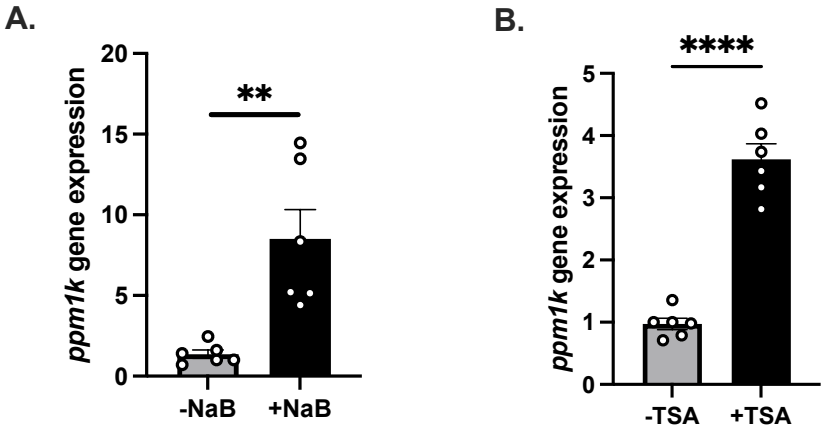

Figure 21. Tributyrin's Increase in *ppm1k* Gene Expression is Due to its HDAC Inhibition Activity. A) mRNA levels of *ppm1k* in C2C12 treated with 5mM sodium butyrate (NaB) or vehicle for 6 hours. b) mRNA levels of ppm1k in C2C12 cells treated with 1μM HDAC inhibitor Trichostatin A (TSA) or vehicle for 6 hours. *ppm1k* gene expression is normalized to β-actin levels. Statistical analysis was done using unpaired student's t-test. Data are mean ± S.E.M. (**p<0.005, ***p<0.0005).

Tributyrin Treatment Reduced Oxidative Stress in the Hearts of Obese Pre-HFpEF Mice.

Defects in BCAAs catabolism due to deficiency in catabolic enzymes PP2Cm and BCKDH lead to the accumulation of BCAAs which has been associated with increase in superoxide production and increase in oxidative stress(25,31,34,35). Additionally, oxidative stress is known to be increased in CVDs such as hypertension, , HFrEF, and HFpEF(53, 54, 88, 391, 392). Therefore, we tested whether butyrate decreases oxidative stress in the hearts. We measured the levels of oxidative stress marker 4-hydroxynonenal (4-HNE), the product of lipid peroxidation and an oxidative stress marker (36, 393), in the hearts of obese pre-HFpEF mice before and after tributyrin treatment. We found 4-HNE levels to be significantly reduced in the hearts of obese pre-HFpEF mice after tributyrin treatment compared to vehicle treatment (Figure 22).

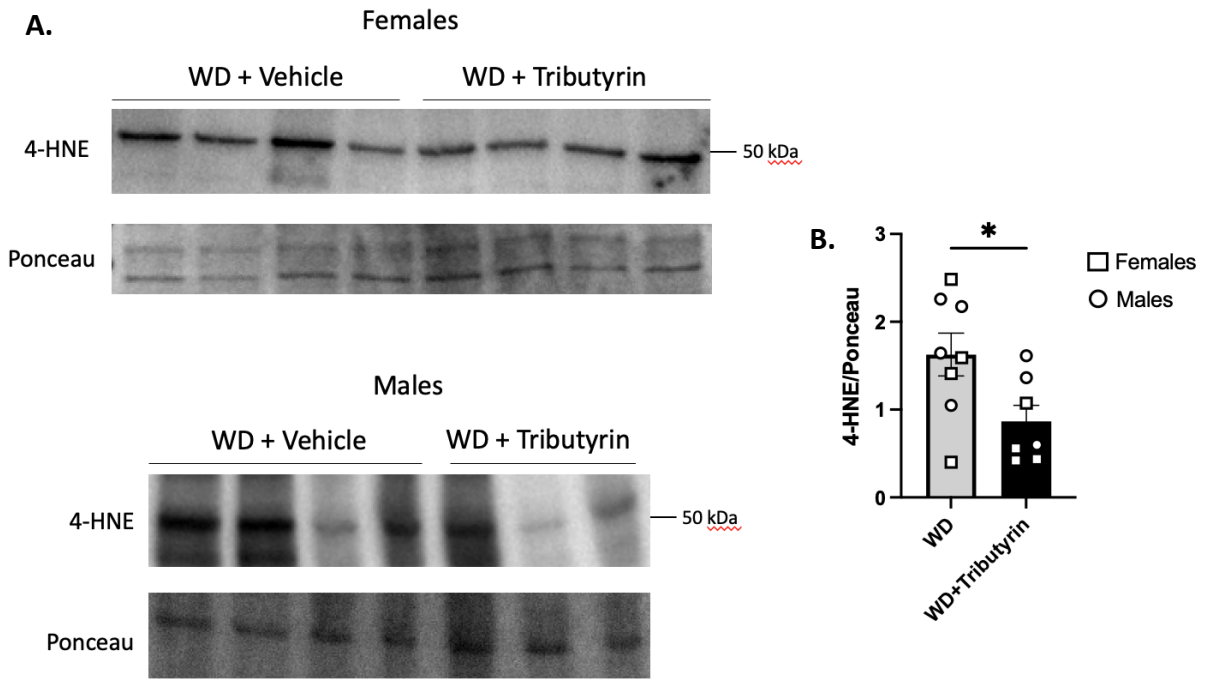

Figure 22. Tributyrin Reduced the Levels of Oxidative Stress Marker 4-HNE in the Hearts of Obese Pre-HFpEF Mice. A) Immunoblot images of 4-HNE and total protein staining from hearts of obese pre-HFpEF mice treated with Tributyrin or vehicle, B) Densitometric analysis of the ratio of 4-HNE/total protein bands. Statistical analysis was done using unpaired student's t-test. Data are mean ± S.E.M. (*p<0.05)

Discussion

Studies have shown an association between gut microbiome modulation in obesity and deficiency in BCAAs degradation. In addition, defects in BCAAs catabolism have been linked to cardiac dysfunction and hypertrophy in many cardiovascular diseases including heart failure. In agreement with these findings, our data indicate a decrease in BCAAs catabolic pathway in obese pre-HFpEF mice that is improved with gut microbiome modulation using FMT and the SCFA butyrate supplementation. In obese pre-HFpEF mice hearts we show a decreasing trend in *ppm1k* and its encoded protein PP2Cm, while FMT treatment from lean mice showed an increasing trend in *ppm1k* and

PP2Cm expression compared to sham FMT treatment. Additionally, we found the inactive rate limiting enzyme p-BCKDH to be significantly increased in obese pre-HFpEF mice, while lean FMT treatment significantly reduced its levels compared to obese FMT. In correspondence with these findings, we show an improvement in BCAAs catabolic enzymes after tributyrin in obese pre-HFpEF mice hearts. This was shown by cardiac RNAseq analysis which revealed an increase in *ppm1k* gene after tributyrin treatment. This increase was also associated with increase in the levels of the encoded protein PP2Cm as well as a decrease in the levels of the inactive p-BCKDH enzyme.

However, improvements in BCAAs catabolic enzymes were not associated with decrease in either serum BCAAs, serum BCKAs, or cardiac BCAAs levels. This inability to detect any changes in BCAAs and BCKAs levels could be attributed to the treatment does/duration we used, which might have resulted in small differences that could not be accurately measured in circulating or whole organ. Another possible explanation is that BCAAs and BCKAs changes could be occurring in a cell specific manner. Therefore, further experiments must be performed to measure the levels of BCAAs and BCKAs in certain cell types such as cardiomyocytes. Additionally, dose-response studies should be done to identify the best tributyrin dose and treatment duration that will induce changes in the circulatory BCAAs and BCKAs levels. Alternatively, BCAAs supplementation can be included in the experimental strategy prior to tributyrin treatment. This will further help test the direct effect of butyrate on BCAAs circulating levels.

We sought to determine butyrate's mechanisms of action that are contributing to its effects on *ppmk1*. We excluded butyrate's binding to its GPCRs *ffar2/3* and activation

of intracellular signaling pathways using *in-situ* hybridization in heart sections, where we found both *ffar2/3* to be very lowly expressed. However, we identified butyrate's epigenetic regulation through its HDAC inhibition activity as a possible mechanism. Using *in-vitro* treatment we found both butyrate and the HDAC inhibitor TSA to significantly upregulate *ppm1k* expression levels. In addition to its HDAC inhibition activity, butyrate can also increase histone acetylation (HATs) by activating the acetyltransferase p300(322). Therefore, future work should also investigate whether butyrate's increase in *ppm1k* is due to its increase in HAT activation.

One of the potential beneficial effects of tributyrin's activation of BCAAs catabolic enzymes is the decrease in oxidative stress. We found the oxidative stress marker 4-hydroxynonenal (4-HNE) to be significantly decreased in obese pre-HFpEF hearts following tributyrin treatment indicating an effective role for butyrate in decreasing cardiac oxidative stress associated with obesity and cardiac dysfunction. The decrease in 4-HNE could be due to butyrate's effect on BCAAs catabolism since defects in this pathway has been associated with increase oxidative stress. However, further studies must be done to test this direct association. This can be done using *in-vitro* treatment with BCAAs followed by NaB/vehicle treatment and ROS levels can be measured using MitoSOX live-cell imaging assay. In addition, since BCAAs accumulation contributes to mitochondrial dysfunction through increasing oxidative stress, *in-vitro* studies following the previously proposed experimental conditions can be used to identify the effect of butyrate's reduction of oxidative stress on mitochondrial function using the Seahorse Mitostress assay. Furthermore, as seen in Figure 17A, butyrate upregulates the expression of *mgst1* which plays a role in the protection of mitochondria from oxidative

stress(47). Therefore, future studies should investigate whether this decrease in oxidative stress by butyrate is through the upregulation of *mgst1.*

Finally, in our tributyrin study we included both male and female mice to investigate whether there are any sex differences in our results. However, we found no significant differences in catabolic enzyme levels PP2Cm and p-BCKDH, plasma and cardiac BCAAs levels, or 4-HNE levels between males and females.

Identifying the molecular mechanisms involved in tributyrin's improvement of cardiac dysfunction and hypertrophy in pre-HFpEF is paramount to understanding the role of gut microbiome and its metabolite butyrate in HFpEF development. In this study, we identified the BCAAs catabolic pathway and cardiac oxidative stress as a potential molecular mechanism involved in tributyrin's improvements, that occurred due to its HDAC inhibition property. Future studies should investigate the effect of using butyrate supplementation on obesity associated HFpEF animal models to test whether it would have similar beneficial effects in improving cardiac dysfunction, and whether that is mediated through BCAAs metabolism and oxidative stress reduction. This will give insight on whether tributyrin can be used as a therapeutic agent to treat HFpEF in addition to being able to halt the progression of pre-HFpEF to clinical HFpEF. Furthermore, future studies should investigate whether improving BCAAs catabolism can be used to treat cardiac dysfunction in HFpEF mice besides being a preventative therapeutic.

CHAPTER SEVEN

SUMMARY & FUTURE DIRECTIONS

Summary of Thesis Work

HFpEF remains one of the most critical cardiovascular diseases that requires extensive research and studies to understand its complex pathophysiology(8-10). Its heterogeneity gives rise to several specific disease phenotypes that require different treatment approaches(9, 13). This hindered the efficacy of many therapeutic approaches and conventional medications that are used in improving HFrEF patient outcomes such as β-blockers and ACE inhibitors(11, 20, 42, 63). Recent clinical research showed the effectiveness of SGLT2 inhibitors in reducing the risk of hospitalization of HFpEF patients, but more studies are needed to understand the mechanisms involved in these improvements (77, 78, 83). The progression of HFpEF involves many comorbidities such as obesity, T2D, hypertension, aging, pulmonary and kidney failure(4, 9, 11-13, 19, 24, 25). However, the two main comorbidities seen in patients are obesity and T2D(89-94). This led to the identification of a separate group called obesity associated HFpEF (91) in which obesity induces systemic inflammation, increases the infiltration of immune cells, and collagen production in the interstitial space between the endothelium and cardiomyocytes. Additionally, systemic inflammation increases ROS production, reduces NO and PKG(11, 106). These lead to the development of cardiac fibrosis and hypertrophy which in turn contributes to the decrease in LV relaxation and stiffness that is seen in HFpEF(11, 106).

Obesity remains a global epidemic that evolves from excess consumption of westernized diets that are composed of processed foods high in fat and sugar, decrease intake of food rich in fibers, and decrease in physical activity which reduces quality of life and present a significant risk for development of several CVDs including HFpEF(47, 89, 92, 394). More than 80% of HFpEF patients are obese, thus it is critical to focus on and target mechanisms involved in obesity associated HFpEF to reduce morbidity and mortality of patients(89-94).

One possible approach to reduce morbidity and mortality of advanced HFpEF is developing preventative therapies that halts the progression of the disease by targeting early pathophysiological alterations in the pre-clinical stage of HFpEF that are involved in the transition to advanced HFpEF. This stage was recently identified as a new pathological entity where patients present with no symptoms of HF like shortness of breath, fatigue, pulmonary edema, and many others. However, these patients have changes to their heart structure that resemble those found in advanced HFpEF(19, 85). Studies investigating the transition from preclinical to advanced HFpEF stage are still lacking, thus the need to focus on them and the mechanisms involved are crucial to halt further progression of HFpEF.

In chapter three, we developed an obesity associated pre-HFpEF mouse model where mice had reduction in GLS and LSRr measurements that point to decreased relaxation of the LV to properly fill with blood in diastole and decrease in the rate of contraction to pump blood during systole. However, the mice had normal LVEF and E/A ratio indicating what they have is early systolic and diastolic dysfunction that hasn’t yet evolved to advanced cardiac dysfunction. We further confirmed the model as pre-

HFpEF by detecting no development of nitrosative stress or cardiac fibrosis , which are two key markers of HFpEF development(41).

Obesity due to excess consumption of westernized diets is associated with the development of gut dysbiosis which decreases the production of beneficial microbiome, increases harmful bacteria, and reduced gut microbiome diversity(107, 108, 115). This modulation of gut microbiome has been associated with the development of many CVDs including hypertension(172, 173, 176), HFrEF(213-215), and atherosclerosis (124, 126)where many studies attributed it to the decrease in the production of gut microbiome metabolites SCFAs (Acetate, Butyrate, Propionate)(174, 175, 178, 395). Only recently was gut microbiome composition investigated in HFpEF patients, where studies performed 16S rRNA sequencing and identified a difference in gut microbiome composition between HFpEF and control groups(239, 240). Interestingly, studies also found a significant reduction in butyrate-producing bacteria in HFpEF patients which points to a potential connection between the SCFA butyrate and HFpEF development(239, 240). However, no mechanistic links were investigated.

In line with these findings, we found significant reduction in microbiome diversity in our obese pre-HFpEF mice (chapter three) as well as a reduction in the butyrate-producing bacteria *Lactobacillus.* Therefore, we sought to investigate the effect of improving gut microbiome composition using FMT and butyrate supplementation in our obesity associated pre-HFpEF mice. By treating obese pre-HFpEF mice with FMT from lean NC-fed mice we found a significant improvement in early cardiac dysfunction, which further reinforced the potential association between gut microbiome and cardiac function in the pre-HFpEF stage. In chapter five, we treated obese pre-HFpEF mice

with tributyrin, butyrate prodrug, and we found it to recapitulate FMT's amelioration of early cardiac dysfunction which suggested that FMT's improvements are due to butyrate. tributyrin supplementation was able to better improve GLS and LSRr compared to FMT thus further supporting the fact that butyrate is mainly responsible for augmentation of early cardiac dysfunction in obese pre-HFpEF mice.

In chapter six, we further explored the molecular mechanisms involved in butyrate's effects on cardiac function by performing cardiac RNA sequencing analysis. We identified 16 genes to be significantly altered with tributyrin treatment in obese pre-HFpEF mice. Among the altered genes we focused on *ppm1k* since it was associated with obesity and CVDs. *ppm1k* encodes PP2Cm, the main regulator of the rate limiting enzyme BCKDH that is involved in the catabolism of BCAAs. Accumulation of BCAAs occurs due to deficiency in the catabolic enzymes PP2Cm and BCKDH which was shown to be associated with the development of many pathologies including obesity and heart failure(366, 367, 371). We found tributyrin to increase *ppm1k* , PP2Cm , and decrease the inactive p-BCKDH in the hearts of obese pre-HFpEF mice. Indicating the efficiency of butyrate in improving the catabolic activity of BCAAs in the heart. Furthermore, we measure the levels of BCAAs and BCKAs, but we found them to be unaltered with tributyrin treatment. This might be due to the short duration of tributyrin treatment and/or the dose used. Furthermore, the change in BCAAs and BCKAs levels could occurring in cell specific manner thus future measurements should take that into consideration.

Next, we investigate butyrate's mechanisms of action that could be involved in butyrate's upregulation of *ppm1k* including binding to GPCRs or HDAC inhibition. We

confirmed that butyrate's receptors FFAR2/FFAR3 have very low expression in the heart using RNAscope analysis which means that butyrate's increase of ppm1k is independent of binding to tis GPCRs. Then, we found treatment with pharmacological HDAC inhibitor TSA to increase *ppm1k* levels *in-vitro* using RT-qPCR similarly to NaB treatment. This implies that butyrate increases *ppm1k* likely through its HDAC inhibition activity. However, further studies must be done to further explore how HDAC inhibition is leading to gene expression regulation.

One of the main effects of BCAAs accumulation on cardiac function is increasing oxidative stress and ROS production(369, 396). Therefore, we measured the levels of oxidative stress marker 4-HNE in the heart and found it to be significantly reduced with tributyrin treatment. However, this could also be due to increase in the levels of *mgst1,* one of the genes that is upregulated with tributyrin and has a role in mitochondrial protection from oxidative stress. Therefore, future studies should be performed to determine whether tributyrin's effects on oxidative stress are directly related to increase in BCAAs catabolism or through other mechanisms.

Contraction and relaxation of the LV are known to be controlled by the ANS through a balance between the functions of parasympathetic and sympathetic nervous systems. The PNS is responsible for "rest and digest" while the SNS is responsible for "fight and flight" response. Dysregulation/imbalance between PNS and SNS is known to be associated with development of heart failure, hypertension, and chronotropic incompetence (274- 279). Moreover, ANS controls gastrointestinal function and activity through the PNS, SNS and enteric nervous system which led to the formation of gut-brain-heart axis(254). Therefore, in chapter four we sought to determine whether early

cardiac dysfunction in obese pre-HFpEF and improvements seen after gut microbiome modulation with FMT occurs via autonomic regulation. However, we detected no changes in either HR or CO in obese pre-HFpEF compared to NC controls, or in those treated with lean FMT compared to FMT from obese mice. Furthermore, we detected no changes in the levels of GPCRs of the PNS and SNS, muscarinic and β-adrenergic receptors between different treatment groups. Therefore, the effects of gut microbiome on cardiac function in obese pre-HFpEF mice is independent of changes to autonomic regulation.

Tributyrin's effects on obese pre-HFpEF included improvements in exercise capacity in addition to cardiac function. First, we thought this occurred due to enhancement in cardiac function. However, we found no alteration in either CO or HR after tributyrin treatment. Next, we speculated that the increase in exercise capacity was due to decrease in body weights, however tributyrin treated mice had no changes in the body weights compared to their vehicle treated littermates. Lastly, we tested whether tributyrin's amelioration of exercise intolerance was due to improvements in mitochondrial metabolism. By performing seahorse analysis, we measured changes in mitochondrial metabolism after butyrate treatment in mouse myoblasts cell line. We detected no changes in mitochondrial oxygen consumption rate after butyrate treatment. However, to further confirm these results future seahorse measurements should be done using other relevant cell types such as IPSC derived cardiomyocytes, isolated skeletal muscle cells, isolated adult cardiomyocytes.

Sex differences is a critical component in obesity and HFpEF research. Several studies indicate that women are more prone to developing HFpEF and obesity than

men(397-400). However, in mice studies females are more resistant to developing cardiometabolic changes with WD feeding than males(401, 402). Therefore, we included both males and females in our tributyrin study and analysis. We found no difference in any of the measurements between male and female obese pre-HFpEF mice. The only difference we noticed was that males were gaining weight at a higher rate than females on the WD.

Future Directions

Our data indicate an association between the gut microbiome, its metabolite butyrate, and the development of obesity associated pre-HFpEF. In our results, we identify improving gut microbiome composition, and more directly butyrate supplementation to be able to reverse early cardiac dysfunction indicated by decrease relaxation and contraction efficiency of the LV in obese pre-HFpEF mice. This points to a causative role of gut microbiome imbalance in HFpEF development, rather than a side effect of disease progression. Our findings in turn open new avenue of preventative therapeutics that can be applied during the preclinical stage of HFpEF prior to progression to advanced HFpEF. In addition to its preventative role, the use of butyrate supplementation could provide further improvement in obesity associated HFpEF. Therefore, future studies investigating the role of tributyrin on cardiac function using a HFpEF mouse model such as the HFD+L-NAME model (41) would provide further insights on the potential therapeutic role of butyrate in advanced HFpEF. Important molecular mechanisms that could be involved are butyrate's effects on cardiac fibrosis, inflammation, and oxidative stress.

Our study mainly focused on the role of gut microbiome and butyrate in the heart. However, since HFpEF is a heterogenous diseases that include extra-cardiac abnormalities, it would be interesting to further explore the effect of butyrate on skeletal muscle function especially after our findings of improved exercise capacity with butyrate treatment, as well as effects on vascular system/hypertension, adipose tissue, kidney and pulmonary functions.

Moreover, the direct association between BCAAs catabolism, oxidative stress, and cardiac function in HFpEF should also be investigated using a pharmacological activator of BCAAs catabolism in HFpEF mouse models followed by echocardiography and oxidative stress measurements. This will allow for further understanding of the role of BCAAs metabolism in obesity associated HFpEF and whether it can be used as a potential therapeutic target. We identified HDAC inhibition as a potential mechanism by which butyrate upregulates *ppm1k* gene expression, but more studies should investigate how this HDAC inhibition activity occurs such as through the recruitment of butyrate by a specific transcription factor on *ppm1k* promoter region. Additionally, further experiments should investigate butyrate's increase in gene expression through the increase in the acetylation of a specific histone on *ppm1k* promoter region. Another potential mechanism in which butyrate can be improving the catabolic pathway of BCAAs is through the activation of the transcription factor KLF15 that is an upstream regulator of BCAAs metabolism(366). This can be done *in-vitro* by KD of KLF15 using siRNA followed by NaB or vehicle treatment and RT-qPCR to measure the changes in *ppm1k* expression levels. As well as western blot analysis to measure the levels of PP2Cm, p-BCKDH expression after KLF15 with and without butyrate treatment.

Lastly, in our studies we focused on the effect of Tributyrin on *ppm1k* and its associated pathway. However, our RNA sequencing results reveal other genes that are being altered (upregulated or downregulated) with butyrate. Therefore, future studies should also consider *mgst1* which has a protective role against mitochondrial oxidative stress, *Aqp4* which regulates cardiac contractility through regulation of SERCA pump, *Loxl2* and *Col16a1* which are involved in cardiac fibrosis and hypertrophy by increasing collage formation and deposition in the interstitial space, *Thbs1* and *Nfasc* that are involved in increased immune cells infiltration and inflammation. These pathophysiological effects have all been described as part of obesity associated HFpEF paradigm and the proposed molecular mechanisms for the development of therapeutic targets.

Concluding Remarks

This dissertation explored the effect of gut microbiome modulation and butyrate supplementation on cardiac function in obesity associated pre-HFpEF progression and the molecular mechanisms involved. We knew from previous research and studies that obesity is linked to the development of gut microbiome imbalance, and the reduction of SCFA producing bacteria(107, 108, 166). Additionally, we knew that gut imbalance is linked to cardiac dysfunction in many CVDs(123, 124, 126, 170-172, 176). Most importantly, we knew that HFpEF patients display a significant reduction in gut microbiome diversity and butyrate-producing bacteria compared to controls (239, 240).Therefore, we hypothesized that gut microbiome and SCFA butyrate play a key role in the development of obesity associate HFpEF, and we focused on studying the pre-HFpEF stage to explore the avenue of preventative therapeutics to halt further

progression to advanced HFpEF. To explore these hypotheses, we began testing the effect of FMT treatment and butyrate supplementation on cardiac function in diet induced obese mice, and to determine the molecular mechanisms involved. Upon completion of our studies, we conclude that improving gut microbiome composition as a successful approach to improve early cardiac dysfunction and hypertrophy. Moreover, we conclude that butyrate supplementation provided a similar but a better improvement in early cardiac dysfunction and hypertrophy than FMT. Additionally, we identified BCAAs catabolism as a novel molecular mechanism that links obesity to cardiac dysfunction in pre-HFpEF. A more detailed understanding of this association between obesity, butyrate, BCAA catabolism and cardiac dysfunction in HFpEF might lead to the development of not only for prevention of disease progression but also a potential therapeutic target for advanced obesity associated HFpEF.

CHAPTER EIGHT

GENERAL METHODS

Animals

Animal experiments were conducted in accordance with the guidelines set by the Loyola University Chicago Institutional Animal Care and Use Committee (IACUC), and in adherence with the recommendations set in the Guide for Care and Use of Laboratory Animals of the US National Institutes of Health. Experimental protocols were approved by the Loyola University Chicago Health Science Division IACUC, and all proper actions were taken to minimize pain and suffering. Mice were kept in 12:12 hour light/dark cycles and had unrestrained access to food and water.

Diet-Induced Obesity (DIO)

Wild type C57BL/6J (#000664) mice were obtained from Jackson Laboratories (Maine, USA). Mice were placed on Normal Chow (NC) diet (Teklad LM-485) or Western Diet (WD) (TD88137, Teklad Diets; 42% kcal from fat, 34% sucrose by weight, and 0.2% cholesterol total; Envigo) starting at 7 weeks of age for 14 weeks. Body weights were collected weekly.

Fecal Microbiome Transplantation (FMT)

For the FMT study, Wild type C57BL/6J mice were place on WD (TD88137, Teklad Diets; 42% kcal from fat, 34% sucrose by weight, and 0.2% cholesterol total; Envigo) for 12 weeks, starting at 7 weeks of age. At the end of week of 12 on WD, mice

Life Technologies) for 3 days in drinking water. Mice were then subjected to diet switch and placed on NC (Teklad LM-485) diet for 5 days. Then they were switched back to were given antibiotic mixture of penicillin (2,000U/Kg) and streptomycin (2mg/kg: Gibco, WD and were orally gavaged with feces from NC-fed mice or with feces from WD-fed mice (Bacterial load in all mice: 0.04 mg/mL in 0.9% saline solution). The gavage was done daily for 2 weeks with 2-day breaks between each week (5 days on, 2 days off, 5 days on).

Echocardiography

Echocardiography was performed using a Visual Sonics Vevo 3100 system equipped with MX550D transducer (Visual Sonics). Anesthesia was induced by isoflurane and measurements were obtained from short-axis M-mode scans. Parameters collected include heart rate, stroke volume, LVEF, left ventricular fractional shortening, left ventricular end-diastolic diameter, left ventricular end-systolic diameter, left ventricular end-diastolic posterior wall, peak Doppler blood inflow velocity across the mitral valve during early diastole. In addition, B-mode traces were acquired and used to calculate global longitudinal strain and longitudinal strain rate reverse peak using Vevo Strain software (Visual Sonics) and a speckle-tracking algorithm. At the end of the procedures all mice recovered from anesthesia without difficulties.

16S Sequencing and Microbiome Diversity Analysis

Cecal content was collected, and equal amounts were homogenized, and DNA isolated using the QIAamp Powerfecal DNA Kit (Qiagen) as described previously(189, 253). qPCR was performed with universal 16S primers. The Loyola Genomic Core performed PCR of 16S rRNA V4-5 regions sequenced by the Illumina HiSeq4500

platform, as done previously(403);16S sequences were aligned using the Silva Taxonomy Annotation, and files were uploaded to Microbiome Analyst for analysis(404). (https://www.microbiomeanalyst.ca/).

RNA Extraction and cDNA Synthesis

Total RNA was extracted from mice hearts and C2C12 cells using TRIzol reagent (Invitrogen). A total of 1ug was used for reverse transcription using the High-Capacity cDNA Reverse Transcription Kit (Applied Biosystems), according to manufacturer instructions.

Reverse Transcription Quantitative Polymerase Chain Reaction (RT-qPCR)

Quantitative PCR (qPCR) was performed in triplicate for each sample using diluted cDNA (1:10), SYBR Green (Roche, Cat.04913850001), and 10μM of forward and reverse primers specific for each gene of interest. The $2^{-\Delta\Delta Ct}$ relative quantification method was used to estimate the amount of target mRNA in samples, using 18S for normalization, and fold ratios were calculated relative to mRNA expressions levels from control samples. Samples were cycled 50 times as following (95°C 15 sec, 60°C 1 min, measure fluorescence), using CFX96 Real-Time System (Bio-Rad, Cat.1855196). PCR amplification was followed by a melt curve analysis to verify uniformity of amplicon product. The following PCR primer list includes primer sequences including forward and reverse sequences used for each gene:

Gene Name	Forwards Sequence	Reverse Sequence
18S mouse	AGGACCGCGGTTCTATTTTGTTGG	ATGCTTTCGCTCTGGTCCGTCTTG
Nos2 mouse	GAGACAGGGAAGTCTGAAGCA	CCAGCAGTAGTTGCTCCTCTTC
Col1a2 mouse	TTCTGTGGGTCCTGCTGGGAAA	TTGTCACCTCGGATGCCTTGAG
M1 mouse	TCAGGACTCCTCTGGCTTC	CCGGGTTTCACTCTCTGTCT
M2 mouse	CCGGTGTCTCCCAGTCTAGT	CAGACGTGGAGTCATTGGAG
M3 mouse	ACCAAGCTACCCTCCTCAGA	GACAGTTGTCACGGTCATCC
β1 mouse	CTCATCGTGGTGGGTAACGTG	ACACACAGCACATCTACCGAA
β2 mouse	GGTTATGGTCCTGGCCATCGTGTTTG	TGGTTCGTGAAGAAGTCACAGCAAGTCTC
β-actin mouse	ACCTTCTACAATGAGCTGCG	CTGGATGGCTACGTACATGC
ppm1k mouse	GAGTTATGCCCACCTGTCTGCA	CTGTCTCCAACACTGGCTACCA

Tributyrin Treatment

Male and Female mice were fed NC (Teklad LM-485) or WD (TD88137, Teklad Diets; 42% kcal from fat, 34% sucrose by weight, and 0.2% cholesterol total; Envigo) for 15 weeks. WD-fed mice were treated with Tributyrin (Sigma-Aldrich) or Vehicle, while NC-fed mice were treated with Vehicle, for 3 weeks (2 days on/2 days off) at a dose of 5g/kg of mice body weight. Body weights were measured weekly.

Butyrate and BCAAs Serum Measurement

After decapitation under anesthesia, blood was isolated from mice and collected in Sarstedt microvette blood collection tubes, and centrifuged at 2,000xg for 10 min for serum collection. The quantification and analysis of serum butyrate and BCAAs was performed by the Mass Spectrometry Core in Research Resources Center of University of Illinois at Chicago. Serum samples were stored in the -80 °C freezer prior to use and were thawed in water bath for 30 sec. 10ul of serum sample was taken for deproteinization and 40 µl methanol (MeOH) was added before vortexing for 2 min. The

samples were incubated at 4°C for 30 min and vortexed again thoroughly. The samples were then centrifuged at 14000rpm for 10 min and 30 µl of the supernatant was taken for derivatization. For derivatization, 30ul of each standard solution or sample supernatant was mixed with 15 µl of 200mM 3-NPH in 50% aqueous MeOH and 15 µl of 120mM EDC in the same solution. The reaction was allowed to proceed for 30 min at 40 °C. The reaction mix was then diluted with 350 µl of 10% MeOH. LC/MS analysis was performed on AB SCIEX 6500 QTRAP coupled with Agilent 1290 UPLC system. The LC/MS data files were processed using the AB Sciex MultiQuant software.

Exercise Exhaustion Test

After three days of pre-training for adjustment to the treadmill exercise, the exhaustion test was performed in all the experimental groups of mice. Mice ran on the treadmill starting at a speed of 5 m min^{-1} for 5 minutes. The treadmill speed was then increased by 1m min^{-1} every minute until the mouse was exhausted. Continuation of running was encouraged by delivering a mild shock using an electric-stimulus grid. Exhaustion was defined as the inability of the mouse to return to running after 10 seconds of shock delivery. Running time was measured and calculated as total minutes ran by each mouse prior to exhaustion and running distance was calculated accordingly.

RNA Isolation, cDNA Library Construction, and Illumina Sequencing.

Total RNA was extracted from mice hearts using the RNAeasy isolation kit (Qiagen). The stranded mRNA-seq was conducted in the Northwestern University NUSeq Core Facility. Briefly, total RNA examples were checked for quality using RINs generated from Agilent Bioanalyzer 2100. RNA quantity was determined with Qubit

fluorometer. The Illumina Stranded mRNA Library Preparation Kit was used to prepare sequencing libraries from high-quality RNA samples (RIN>7). The Kit procedure was performed without modifications. This procedure includes mRNA purification and fragmentation, cDNA synthesis, 3' end adenylation, Illumina adapter ligation, library, PCR amplification and validation. LIlumina HiSeq 4000 sequencer was used to sequence the libraries with the production of single-end, 50 bp reads at the depth of 20-25 M reads per sample. The quality of DNA reads, in FASTQ format, was evaluated using FastQC. Adapters were trimmed and reads of poor quality or aligning to rRNA sequences were filtered. The cleaned reads were aligned to the reference genome using STAR (Dobin et al, 2013). Read counts for each gene were calculated using htseq-count (Anders et al, 2015). Normalization and differential expression were determined using DESeq2 (Love et al, 2014). The cutoff for determining significantly differentially expressed genes was an FDR-adjusted p-value less than 0.05. A pathway analysis was performed on both gene lists using GeneCoDis (Tabas-Madrid et al, 2012; Nogales-Cadenas et al, 2009; Carmona-Saez et al, 2007) to identify pathways that are enriched with genes that are upregulated and downregulated.

Isolation of Mice Hearts and Tissue Preparation

At the endpoint of the experimental paradigm, mice were sacrificed and whole heart was isolated, washed with Phosphate Buffer Saline (PBS) to remove all blood contamination, and flash frozen with dry ice then were later stored at -80°C. Flash frozen hearts were obtained and powderized in liquid nitrogen using mortar and pestle. Powderized heart tissue was then used for RNA isolation using the protocol mentioned above (for qPCR analysis), and protein isolation for (for western blot analysis).

Protein Isolation from Frozen Heart Tissue

Protein from powdered frozen mouse hearts was extracted using ice-cold RIPA lysis buffer (ThermoFisher) containing protease and phosphatase inhibitor (ThermoFisher). Tissue was homogenized using bullet blender bead lysis kit (Next Advance), and protein concentrations were determined with Pierce BCA Protein Assay Kit (Thermofisher). 10 or 25 µg protein was boiled with 2x Laemmli buffer (BioRad) at 95°C for 5 minutes before electrophoresis.

Western Blot Analysis

Proteins were separated by sodium dodecyl sulfate polyacrylamide gel electrophoresis (SDS-PAGE) on 4-15% gradient gel (Bio-Rad) and transferred to PVDF membrane using iBlot 2 transfer system (ThermoFisher). Membranes were incubated with ponceau stain for total protein normalization and imaged with ChemiDoc imaging system (Bio-Rad), then washed with water to remove the stain. Membranes were blocked with 3%BSA+PBST solution for 1 hour at room temperature, followed by incubation with primary antibody (1:1000-1:2000) overnight with constant shaking at 4°C. Membranes were then incubated with secondary antibody (1:4000) for 1 hour at room temperature. Protein expression was visualized by chemiluminescence using ChemiDoc imaging system (Bio-Rad) and analyzed with ImageJ software. Proteins were detected with the following primary antibodies: BCKDH (ThermoFisher, cat.PA5-97248), phospho-BCKDH (S293) (abcam, ab200577), PP2Cm (abcam, ab135286), 4-hydroxynonenal (abcam, ab46545).

Cell Culture

C2C12 cells, mouse myoblasts cell line, were grown to 80-90% confluency in Dulbecco's Minimum Essential Medium (DMEM) media containing glucose, L-glutamine, sodium pyruvate, supplemented with 10% fetal bovine serum (FBS) and 1% pen/strep (Mixture of Penicillin-Streptomycin) in a humidified 5% CO2 atmosphere at 37°C

Sodium Butyrate (NaB) and Trichostatin A (TSA) Treatments

C2C12 cells were treated with 5mM sodium butyrate (NaB) dissolved in RNAse/DNAase free water for 6 hours. Then cells were lysed, and RNA was isolated using the protocol described above. C2C12 cells were treated with Trichostatin A (TSA) at a final concentration of 1μM for 6 hours. TSA was diluted with Dimethylsulfoxide (DMSO) for a stock concentration of 1mM prior to addition to the cells.

Cardiac BCAA Measurements

Branched Chain Amino Acid (Leu, Ile, Val) Colorimetric Assay Kit (Biovision) was used for the measurements of BCAAs concentrations in the heart. The kit uses an enzyme assay in which BCAAs are oxidatively deaminated, producing NADH, reducing the probe, and generating a colored product. Reaction mixture was prepared following the kit instructions and absorbance was measured at 450nM using a microplate reader. A standard curve was plotted, and the samples readings were applied to the curve. BCAAs concentrations were calculated using the following equation:

$$C = S_a/S_v \text{ (nmol/μl, or mM)}$$

Where: S_a = BCAA content of unknown samples (nmol) from standard curve,

S_v = sample volume (μl) added into the assay wells.

Seahorse Palmitate Oxidation Stress Assay

C2C12 cells were cultured in growth media (DMEM containing glucose, L-glutamine, sodium pyruvate, supplemented with 10% fetal bovine serum (FBS) and 1% pen/strep) in a humidified 5% CO_2 atmosphere at 37°C (two days prior to running assay). Cells were then switched to substrate limited growth media (DMEM (no glucose, no pyruvate, no glutamine) + 0.5mM glucose + 1mM glutamine + 1%FBS + 0.5mM L-carnitine) and treated with 0.5mM NaB or vehicle overnight (day prior to assay). Day of assay the cells were switched to seahorse assay media (without NaB) and incubated at 37°C no CO_2 for 1 hour. Immediately prior to running the assay, palmitate or BSA were added to the cells to further push the cells to utilizing FAO. The assay was run with the following final well concentrations for each reagent: Etomoxir 4μM, Oligomycin 1.5μM, FCCP 2μM, and Rotenone + antimycin A 0.5 μM. Data were analyzed using seahorse Wave software and normalized to protein concentration in each well obtained using BCA assay.

Statistics

Results are presented as mean ± SEM and were analyzed using GraphPad Prism 8.0. For comparison of two groups, data were analyzed using two-tailed unpaired student's t-test. For analysis of three groups, data were analyzed using one-way ANOVA followed by Tukey's post hoc test to determine statistically significant differences between group means. For comparison of groups with two variables, data were analyzed suing two-way ANOVA followed by Tukey's post hoc test to determine statistically significant differences between group means. Data are presented as mean ± S.E.M. and are considered significant when p value < 0.05

REFERENCE LIST

1. **Mishra S, and Kass DA**. Cellular and molecular pathobiology of heart failure with preserved ejection fraction. *Nat Rev Cardiol* 2021.

2. **Dodek A, Kassebaum DG, and Bristow JD**. Pulmonary edema in coronary-artery disease without cardiomegaly. Paradox of the stiff heart. *N Engl J Med* 286: 1347-1350, 1972.

3. **Dougherty AH, Naccarelli GV, Gray EL, Hicks CH, and Goldstein RA**. Congestive heart failure with normal systolic function. *Am J Cardiol* 54: 778-782, 1984.

4. **Dunlay SM, Roger VL, and Redfield MM**. Epidemiology of heart failure with preserved ejection fraction. *Nat Rev Cardiol* 14: 591-602, 2017.

5. **Mishra S, and Kass DA**. Cellular and molecular pathobiology of heart failure with preserved ejection fraction. *Nat Rev Cardiol* 18: 400-423, 2021.

6. **Norman HS, Oujiri J, Larue SJ, Chapman CB, Margulies KB, and Sweitzer NK**. Decreased cardiac functional reserve in heart failure with preserved systolic function. *J Card Fail* 17: 301-308, 2011.

7. **Borlaug BA, Olson TP, Lam CS, Flood KS, Lerman A, Johnson BD, and Redfield MM**. Global cardiovascular reserve dysfunction in heart failure with preserved ejection fraction. *J Am Coll Cardiol* 56: 845-854, 2010.

8. **Ussher JR, Elmariah S, Gerszten RE, and Dyck JR**. The Emerging Role of Metabolomics in the Diagnosis and Prognosis of Cardiovascular Disease. *J Am Coll Cardiol* 68: 2850-2870, 2016.

9. **Oktay AA, Rich JD, and Shah SJ**. The emerging epidemic of heart failure with preserved ejection fraction. *Curr Heart Fail Rep* 10: 401-410, 2013.

10. **Owan TE, Hodge DO, Herges RM, Jacobsen SJ, Roger VL, and Redfield MM**. Trends in prevalence and outcome of heart failure with preserved ejection fraction. *N Engl J Med* 355: 251-259, 2006.

11. **Paulus WJ, and Tschöpe C**. A novel paradigm for heart failure with preserved ejection fraction: comorbidities drive myocardial dysfunction and remodeling through coronary microvascular endothelial inflammation. *J Am Coll Cardiol* 62: 263-271, 2013.

12. **Shah SJ, Borlaug BA, Kitzman DW, McCulloch AD, Blaxall BC, Agarwal R, Chirinos JA, Collins S, Deo RC, Gladwin MT, Granzier H, Hummel SL, Kass DA, Redfield MM, Sam F, Wang TJ, Desvigne-Nickens P, and Adhikari BB**. Research Priorities for Heart Failure With Preserved Ejection Fraction: National Heart, Lung, and Blood Institute Working Group Summary.
Circulation 141: 1001-1026, 2020.

13. **Shah SJ, Kitzman DW, Borlaug BA, van Heerebeek L, Zile MR, Kass DA, and Paulus WJ**. Phenotype-Specific Treatment of Heart Failure With Preserved Ejection Fraction: A Multiorgan Roadmap. *Circulation* 134: 73-90, 2016.

14. **Chaturvedi RR, Herron T, Simmons R, Shore D, Kumar P, Sethia B, Chua F, Vassiliadis E, and Kentish JC**. Passive stiffness of myocardium from congenital heart disease and implications for diastole. *Circulation* 121: 979-988, 2010.

15. **Zile MR, Baicu CF, and Gaasch WH**. Diastolic heart failure--abnormalities in active relaxation and passive stiffness of the left ventricle. *N Engl J Med* 350: 1953-1959, 2004.

16. **Zile MR, Gottdiener JS, Hetzel SJ, McMurray JJ, Komajda M, McKelvie R, Baicu CF, Massie BM, Carson PE, and Investigators I-P**. Prevalence and significance of alterations in cardiac structure and function in patients with heart failure and a preserved ejection fraction. *Circulation* 124: 2491-2501, 2011.

17. **Phan TT, Abozguia K, Nallur Shivu G, Mahadevan G, Ahmed I, Williams L, Dwivedi G, Patel K, Steendijk P, Ashrafian H, Henning A, and Frenneaux M**. Heart failure with preserved ejection fraction is characterized by dynamic impairment of active relaxation and contraction of the left ventricle on exercise and associated with myocardial energy deficiency. *J Am Coll Cardiol* 54: 402-409, 2009.

18. **Soufer R, Wohlgelernter D, Vita NA, Amuchestegui M, Sostman HD, Berger HJ, and Zaret BL**. Intact systolic left ventricular function in clinical congestive heart failure. *Am J Cardiol* 55: 1032-1036, 1985.

19. **Withaar C, Lam CSP, Schiattarella GG, de Boer RA, and Meems LMG**. Heart failure with preserved ejection fraction in humans and mice: embracing clinical complexity in mouse models. *Eur Heart J* 42: 4420-4430, 2021.

20. **Ather S, Chan W, Bozkurt B, Aguilar D, Ramasubbu K, Zachariah AA, Wehrens XH, and Deswal A**. Impact of noncardiac comorbidities on morbidity and mortality in a predominantly male population with heart failure and preserved versus reduced ejection fraction. *J Am Coll Cardiol* 59: 998-1005, 2012.

22. **Shah AM, and Solomon SD**. Phenotypic and pathophysiological heterogeneity in heart failure with preserved ejection fraction. *Eur Heart J* 33: 1716-1717, 2012.

23. **Shah AM, and Pfeffer MA**. The many faces of heart failure with preserved ejection fraction. *Nat Rev Cardiol* 9: 555-556, 2012.

24. **Mohammed SF, Borlaug BA, Roger VL, Mirzoyev SA, Rodeheffer RJ, Chirinos JA, and Redfield MM**. Comorbidity and ventricular and vascular structure and function in heart failure with preserved ejection fraction: a community-based study. *Circ Heart Fail* 5: 710-719, 2012.

25. **Maréchaux S, Six-Carpentier MM, Bouabdallaoui N, Montaigne D, Bauchart JJ, Mouquet F, Auffray JL, Le Tourneau T, Asseman P, LeJemtel TH, and Ennezat PV**. Prognostic importance of comorbidities in heart failure with preserved left ventricular ejection fraction. *Heart Vessels* 26: 313-320, 2011.

26. **Borbély A, van der Velden J, Papp Z, Bronzwaer JG, Edes I, Stienen GJ, and Paulus WJ**. Cardiomyocyte stiffness in diastolic heart failure. *Circulation* 111: 774-781, 2005.

27. **van Heerebeek L, Borbély A, Niessen HW, Bronzwaer JG, van der Velden J, Stienen GJ, Linke WA, Laarman GJ, and Paulus WJ**. Myocardial structure and function differ in systolic and diastolic heart failure. *Circulation* 113: 1966-1973, 2006.

28. **Franssen C, Chen S, Unger A, Korkmaz HI, De Keulenaer GW, Tschöpe C, Leite-Moreira AF, Musters R, Niessen HW, Linke WA, Paulus WJ, and Hamdani N**. Myocardial Microvascular Inflammatory Endothelial Activation in Heart Failure With Preserved Ejection Fraction. *JACC Heart Fail* 4: 312-324, 2016.

29. **Westermann D, Lindner D, Kasner M, Zietsch C, Savvatis K, Escher F, von Schlippenbach J, Skurk C, Steendijk P, Riad A, Poller W, Schultheiss HP, and Tschöpe C**. Cardiac inflammation contributes to changes in the extracellular matrix in patients with heart failure and normal ejection fraction. *Circ Heart Fail* 4: 44-52, 2011.

30. **Kasner M, Westermann D, Lopez B, Gaub R, Escher F, Kühl U, Schultheiss HP, and Tschöpe C**. Diastolic tissue Doppler indexes correlate with the degree of collagen expression and cross-linking in heart failure and normal ejection fraction. *J Am Coll Cardiol* 57: 977-985, 2011.

31. **van Heerebeek L, Hamdani N, Falcão-Pires I, Leite-Moreira AF, Begieneman MP, Bronzwaer JG, van der Velden J, Stienen GJ, Laarman GJ, Somsen A, Verheugt FW, Niessen HW, and Paulus WJ**. Low myocardial protein kinase G activity in heart failure with preserved ejection fraction. *Circulation* 126: 830-839, 2012.

32. **Hamdani N, Franssen C, Lourenço A, Falcão-Pires I, Fontoura D, Leite S, Plettig L, López B, Ottenheijm CA, Becher PM, González A, Tschöpe C, Díez J, Linke WA, Leite-Moreira AF, and Paulus WJ**. Myocardial titin hypophosphorylation importantly contributes to heart failure with preserved ejection fraction in a rat metabolic risk model. *Circ Heart Fail* 6: 1239-1249, 2013.

33. **Morgan MJ, and Liu ZG**. Crosstalk of reactive oxygen species and NF-κB signaling. *Cell Res* 21: 103-115, 2011.

34. **Münzel T, Gori T, Keaney JF, Maack C, and Daiber A**. Pathophysiological role of oxidative stress in systolic and diastolic heart failure and its therapeutic implications. *Eur Heart J* 36: 2555-2564, 2015.

35. **Sorop O, Heinonen I, van Kranenburg M, van de Wouw J, de Beer VJ, Nguyen ITN, Octavia Y, van Duin RWB, Stam K, van Geuns RJ, Wielopolski PA, Krestin GP, van den Meiracker AH, Verjans R, van Bilsen M, Danser AHJ, Paulus WJ, Cheng C, Linke WA, Joles JA, Verhaar MC, van der Velden J, Merkus D, and Duncker DJ**. Multiple common comorbidities produce left ventricular diastolic dysfunction associated with coronary microvascular dysfunction, oxidative stress, and myocardial stiffening. *Cardiovasc Res* 114: 954-964, 2018.

36. **Kiyuna LA, Albuquerque RPE, Chen CH, Mochly-Rosen D, and Ferreira JCB**. Targeting mitochondrial dysfunction and oxidative stress in heart failure: Challenges and opportunities. *Free Radic Biol Med* 129: 155-168, 2018.

37. **Banerjee A, Banerjee V, Czinn S, and Blanchard T**. Increased reactive oxygen species levels cause ER stress and cytotoxicity in andrographolide treated colon cancer cells. *Oncotarget* 8: 26142-26153, 2017.

38. **Cao SS, and Kaufman RJ**. Endoplasmic reticulum stress and oxidative stress in cell fate decision and human disease. *Antioxid Redox Signal* 21: 396-413, 2014.

39. **Maamoun H, Benameur T, Pintus G, Munusamy S, and Agouni A**. Crosstalk Between Oxidative Stress and Endoplasmic Reticulum (ER) Stress in Endothelial Dysfunction and Aberrant Angiogenesis Associated With Diabetes: A Focus on the Protective Roles of Heme Oxygenase (HO)-1. *Front Physiol* 10: 70, 2019.

40. **Ochoa CD, Wu RF, and Terada LS**. ROS signaling and ER stress in cardiovascular disease. *Mol Aspects Med* 63: 18-29, 2018.

41. **Schiattarella GG, Altamirano F, Tong D, French KM, Villalobos E, Kim SY, Luo X, Jiang N, May HI, Wang ZV, Hill TM, Mammen PPA, Huang J, Lee DI, Hahn VS, Sharma K, Kass DA, Lavandero S, Gillette TG, and Hill JA**. Nitrosative stress drives heart failure with preserved ejection fraction. *Nature* 568: 351-356, 2019.

42. **Savji N, Meijers WC, Bartz TM, Bhambhani V, Cushman M, Nayor M, Kizer JR, Sarma A, Blaha MJ, Gansevoort RT, Gardin JM, Hillege HL, Ji F, Kop WJ, Lau ES, Lee DS, Sadreyev R, van Gilst WH, Wang TJ, Zanni MV, Vasan RS, Allen NB, Psaty BM, van der Harst P, Levy D, Larson M, Shah SJ, de Boer RA, Gottdiener JS, and Ho JE**. The Association of Obesity and Cardiometabolic Traits With Incident HFpEF and HFrEF. *JACC Heart Fail* 6: 701-709, 2018.

43. **Wei J, Nelson MD, Szczepaniak EW, Smith L, Mehta PK, Thomson LE, Berman DS, Li D, Bairey Merz CN, and Szczepaniak LS**. Myocardial steatosis as a possible mechanistic link between diastolic dysfunction and coronary microvascular dysfunction in women. *Am J Physiol Heart Circ Physiol* 310: H14-19, 2016.

44. **Mahmod M, Pal N, Rayner J, Holloway C, Raman B, Dass S, Levelt E, Ariga R, Ferreira V, Banerjee R, Schneider JE, Rodgers C, Francis JM, Karamitsos TD, Frenneaux M, Ashrafian H, Neubauer S, and Rider O**. The interplay between metabolic alterations, diastolic strain rate and exercise capacity in mild heart failure with preserved ejection fraction: a cardiovascular magnetic resonance study. *J Cardiovasc Magn Reson* 20: 88, 2018.

45. **Faria A, and Persaud SJ**. Cardiac oxidative stress in diabetes: Mechanisms and therapeutic potential. *Pharmacol Ther* 172: 50-62, 2017.

46. **Cavalera M, Wang J, and Frangogiannis NG**. Obesity, metabolic dysfunction, and cardiac fibrosis: pathophysiological pathways, molecular mechanisms, and therapeutic opportunities. *Transl Res* 164: 323-335, 2014.

47. **Alex L, Russo I, Holoborodko V, and Frangogiannis NG**. Characterization of a mouse model of obesity-related fibrotic cardiomyopathy that recapitulates features of human heart failure with preserved ejection fraction. *Am J Physiol Heart Circ Physiol* 315: H934-H949, 2018.

48. **Kitzman DW, Nicklas B, Kraus WE, Lyles MF, Eggebeen J, Morgan TM, and Haykowsky M**. Skeletal muscle abnormalities and exercise intolerance in older patients with heart failure and preserved ejection fraction. *Am J Physiol Heart Circ Physiol* 306: H1364-1370, 2014.

49. **Hirai DM, Musch TI, and Poole DC**. Exercise training in chronic heart failure: improving skeletal muscle O2 transport and utilization. *Am J Physiol Heart Circ Physiol* 309: H1419-1439, 2015.

50. **Weiss K, Schär M, Panjrath GS, Zhang Y, Sharma K, Bottomley PA, Golozar A, Steinberg A, Gerstenblith G, Russell SD, and Weiss RG**. Fatigability, Exercise Intolerance, and Abnormal Skeletal Muscle Energetics in Heart Failure. *Circ Heart Fail* 10: 2017.

51. **Molina AJ, Bharadwaj MS, Van Horn C, Nicklas BJ, Lyles MF, Eggebeen J, Haykowsky MJ, Brubaker PH, and Kitzman DW**. Skeletal Muscle Mitochondrial Content, Oxidative Capacity, and Mfn2 Expression Are Reduced in Older Patients With Heart Failure and Preserved Ejection Fraction and Are Related to Exercise Intolerance. *JACC Heart Fail* 4: 636-645, 2016.

52. **Tumova J, Andel M, and Trnka J**. Excess of free fatty acids as a cause of metabolic dysfunction in skeletal muscle. *Physiol Res* 65: 193-207, 2016.

53. **Hummel SL, Seymour EM, Brook RD, Kolias TJ, Sheth SS, Rosenblum HR, Wells JM, and Weder AB**. Low-sodium dietary approaches to stop hypertension diet reduces blood pressure, arterial stiffness, and oxidative stress in hypertensive heart failure with preserved ejection fraction. *Hypertension* 60: 1200-1206, 2012.

54. **Tian N, Moore RS, Braddy S, Rose RA, Gu JW, Hughson MD, and Manning RD**. Interactions between oxidative stress and inflammation in salt-sensitive hypertension. *Am J Physiol Heart Circ Physiol* 293: H3388-3395, 2007.

55. **Capasso JM, Palackal T, Olivetti G, and Anversa P**. Left ventricular failure induced by long-term hypertension in rats. *Circ Res* 66: 1400-1412, 1990.

56. **Qu P, Hamada M, Ikeda S, Hiasa G, Shigematsu Y, and Hiwada K**. Time-course changes in left ventricular geometry and function during the development of hypertension in Dahl salt-sensitive rats. *Hypertens Res* 23: 613-623, 2000.

57. **Meng Q, Lai YC, Kelly NJ, Bueno M, Baust JJ, Bachman TN, Goncharov D, Vanderpool RR, Radder JE, Hu J, Goncharova E, Morris AM, Mora AL, Shapiro SD, and Gladwin MT**. Development of a Mouse Model of Metabolic Syndrome, Pulmonary Hypertension, and Heart Failure with Preserved Ejection Fraction. *Am J Respir Cell Mol Biol* 56: 497-505, 2017.

58. **Fayyaz AU, Edwards WD, Maleszewski JJ, Konik EA, DuBrock HM, Borlaug BA, Frantz RP, Jenkins SM, and Redfield MM**. Global Pulmonary Vascular Remodeling in Pulmonary Hypertension Associated With Heart Failure and Preserved or Reduced Ejection Fraction. *Circulation* 137: 1796-1810, 2018.

59. **Olson TP, Johnson BD, and Borlaug BA**. Impaired Pulmonary Diffusion in Heart Failure With Preserved Ejection Fraction. *JACC Heart Fail* 4: 490-498, 2016.

60. **van de Wouw J, Broekhuizen M, Sorop O, Joles JA, Verhaar MC, Duncker DJ, Danser AHJ, and Merkus D**. Chronic Kidney Disease as a Risk Factor for Heart Failure With Preserved Ejection Fraction: A Focus on Microcirculatory Factors and Therapeutic Targets. *Front Physiol* 10: 1108, 2019.

61. **Agrawal A, Naranjo M, Kanjanahattakij N, Rangaswami J, and Gupta S**. Cardiorenal syndrome in heart failure with preserved ejection fraction-an under-recognized clinical entity. *Heart Fail Rev* 24: 421-437, 2019.

62. **Upadhya B, Amjad A, and Stacey RB**. Optimizing The Management of Obese HFpEF Phenotype: Can We Mind Both The Heart and The Kidney? *J Card Fail* 26: 108-111, 2020.

63. **Hunter WG, Kelly JP, McGarrah RW, Khouri MG, Craig D, Haynes C, Ilkayeva O, Stevens RD, Bain JR, Muehlbauer MJ, Newgard CB, Felker GM, Hernandez AF, Velazquez EJ, Kraus WE, and Shah SH**. Metabolomic Profiling Identifies Novel Circulating Biomarkers of Mitochondrial Dysfunction Differentially Elevated in Heart Failure With Preserved Versus Reduced Ejection Fraction: Evidence for Shared Metabolic Impairments in Clinical Heart Failure. *J Am Heart Assoc* 5: 2016.

64. **Plitt GD, Spring JT, Moulton MJ, and Agrawal DK**. Mechanisms, diagnosis, and treatment of heart failure with preserved ejection fraction and diastolic dysfunction. *Expert Rev Cardiovasc Ther* 16: 579-589, 2018.

65. **Xanthopoulos A, Triposkiadis F, and Starling RC**. Heart failure with preserved ejection fraction: Classification based upon phenotype is essential for diagnosis and treatment. *Trends Cardiovasc Med* 28: 392-400, 2018.

66. **Borlaug BA, and Paulus WJ**. Heart failure with preserved ejection fraction: pathophysiology, diagnosis, and treatment. *Eur Heart J* 32: 670-679, 2011.

67. **Holland DJ, Kumbhani DJ, Ahmed SH, and Marwick TH**. Effects of treatment on exercise tolerance, cardiac function, and mortality in heart failure with preserved ejection fraction. A meta-analysis. *J Am Coll Cardiol* 57: 1676-1686, 2011.

68. **Valero-Muñoz M, Backman W, and Sam F**. Murine Models of Heart Failure with Preserved Ejection Fraction: a "Fishing Expedition". *JACC Basic Transl Sci* 2: 770-789, 2017.

69. **Reddy SS, Agarwal H, and Barthwal MK**. Cilostazol ameliorates heart failure with preserved ejection fraction and diastolic dysfunction in obese and non-obese hypertensive mice. *J Mol Cell Cardiol* 123: 46-57, 2018.

70. **Deng Y, Xie M, Li Q, Xu X, Ou W, Zhang Y, Xiao H, Yu H, Zheng Y, Liang Y, Jiang C, Chen G, Du D, Zheng W, Wang S, Gong M, Chen Y, Tian R, and Li T**. Targeting Mitochondria-Inflammation Circuit by β-Hydroxybutyrate Mitigates HFpEF. *Circ Res* 128: 232-245, 2021.

71. **Anker SD, Butler J, Filippatos G, Ferreira JP, Bocchi E, Böhm M, Brunner-La Rocca HP, Choi DJ, Chopra V, Chuquiure-Valenzuela E, Giannetti N, Gomez-Mesa JE, Janssens S, Januzzi JL, Gonzalez-Juanatey JR, Merkely B, Nicholls SJ, Perrone SV, Piña IL, Ponikowski P, Senni M, Sim D, Spinar J, Squire I, Taddei S, Tsutsui H, Verma S, Vinereanu D, Zhang J, Carson P, Lam CSP, Marx N, Zeller C, Sattar N, Jamal W, Schnaidt S, Schnee JM, Brueckmann M, Pocock SJ, Zannad F, Packer M, and Investigators E-PT**. Empagliflozin in Heart Failure with a Preserved Ejection Fraction. *N Engl J Med* 385: 1451-1461, 2021.

72. **Hsia DS, Grove O, and Cefalu WT**. An update on sodium-glucose co-transporter-2 inhibitors for the treatment of diabetes mellitus. *Curr Opin Endocrinol Diabetes Obes* 24: 73-79, 2017.

73. **Hasan FM, Alsahli M, and Gerich JE**. SGLT2 inhibitors in the treatment of type 2 diabetes. *Diabetes Res Clin Pract* 104: 297-322, 2014.

74. **Davis PN, Ndefo UA, and Oliver A**. Dapagliflozin: A Sodium Glucose Cotransporter 2 Inhibitor for the Treatment of Diabetes Mellitus. *J Pharm Pract* 29: 165-171, 2016.

75. **Heerspink HJ, Perkins BA, Fitchett DH, Husain M, and Cherney DZ**. Sodium Glucose Cotransporter 2 Inhibitors in the Treatment of Diabetes Mellitus: Cardiovascular and Kidney Effects, Potential Mechanisms, and Clinical Applications. *Circulation* 134: 752-772, 2016.

76. **Fonseca-Correa JI, and Correa-Rotter R**. Sodium-Glucose Cotransporter 2 Inhibitors Mechanisms of Action: A Review. *Front Med (Lausanne)* 8: 777861, 2021.

77. **Wagdy K, and Nagy S**. EMPEROR-Preserved: SGLT2 inhibitors breakthrough in the management of heart failure with preserved ejection fraction. *Glob Cardiol Sci Pract* 2021: e202117, 2021.

78. **Nassif ME, Windsor SL, Borlaug BA, Kitzman DW, Shah SJ, Tang F, Khariton Y, Malik AO, Khumri T, Umpierrez G, Lamba S, Sharma K, Khan SS, Chandra L, Gordon RA, Ryan JJ, Chaudhry SP, Joseph SM, Chow CH, Kanwar MK, Pursley M, Siraj ES, Lewis GD, Clemson BS, Fong M, and Kosiborod MN**. The SGLT2 inhibitor dapagliflozin in heart failure with preserved ejection fraction: a multicenter randomized trial. *Nat Med* 27: 1954-1960, 2021.

79. **Joshi SS, Singh T, Newby DE, and Singh J**. Sodium-glucose co-transporter 2 inhibitor therapy: mechanisms of action in heart failure. *Heart* 2021.

80. **Habibi J, Aroor AR, Sowers JR, Jia G, Hayden MR, Garro M, Barron B, Mayoux E, Rector RS, Whaley-Connell A, and DeMarco VG**. Sodium glucose transporter 2 (SGLT2) inhibition with empagliflozin improves cardiac diastolic function in a female rodent model of diabetes. *Cardiovasc Diabetol* 16: 9, 2017.

81. **Arow M, Waldman M, Yadin D, Nudelman V, Shainberg A, Abraham NG, Freimark D, Kornowski R, Aravot D, Hochhauser E, and Arad M**. Sodium-glucose cotransporter 2 inhibitor Dapagliflozin attenuates diabetic cardiomyopathy. *Cardiovasc Diabetol* 19: 7, 2020.

82. **Bayes-Genis A, Iborra-Egea O, Spitaleri G, Domingo M, Revuelta-López E, Codina P, Cediel G, Santiago-Vacas E, Cserkóová A, Pascual-Figal D, Núñez J, and Lupón J**. Decoding empagliflozin's molecular mechanism of action in heart failure with preserved ejection fraction using artificial intelligence. *Sci Rep* 11: 12025, 2021.

83. **Pabel S, Hamdani N, Singh J, and Sossalla S**. Potential Mechanisms of SGLT2 Inhibitors for the Treatment of Heart Failure With Preserved Ejection Fraction. *Front Physiol* 12: 752370, 2021.

84. **Kolijn D, Pabel S, Tian Y, Lódi M, Herwig M, Carrizzo A, Zhazykbayeva S, Kovács Á, Fülöp G, Falcão-Pires I, Reusch PH, Linthout SV, Papp Z, van Heerebeek L, Vecchione C, Maier LS, Ciccarelli M, Tschöpe C, Mügge A, Bagi Z, Sossalla S, and Hamdani N**. Empagliflozin improves endothelial and cardiomyocyte function in human heart failure with preserved ejection fraction via reduced pro-inflammatory-oxidative pathways and protein kinase Gα oxidation. *Cardiovasc Res* 117: 495-507, 2021.

85. **Bayes-Genis A, Bisbal F, Núñez J, Santas E, Lupón J, Rossignol P, and Paulus W**. Transitioning from Preclinical to Clinical Heart Failure with Preserved Ejection Fraction: A Mechanistic Approach. *J Clin Med* 9: 2020.

86. **Bayes-Genis A, Pascual-Figal D, and Núñez J**. The pre-HFpEF stage: a new entity that requires proper phenotyping for better management. *Eur J Prev Cardiol* 2020.

87. **Banerjee P, Motiwala A, Mustafa HM, Gani MA, Fourali S, and Ali D**. Does left ventricular diastolic dysfunction progress through stages? Insights from a community heart failure study. *Int J Cardiol* 221: 850-854, 2016.

88. **Loredo-Mendoza ML, Ramirez-Sanchez I, Bustamante-Pozo MM, Ayala M, Navarrete V, Garate-Carrillo A, Ito BR, Ceballos G, Omens J, and Villarreal F**. The role of inflammation in driving left ventricular remodeling in a pre-HFpEF model. *Exp Biol Med (Maywood)* 245: 748-757, 2020.

89. **Harada T, and Obokata M**. Obesity-Related Heart Failure with Preserved Ejection Fraction: Pathophysiology, Diagnosis, and Potential Therapies. *Heart Fail Clin* 16: 357-368, 2020.

90. **Haass M, Kitzman DW, Anand IS, Miller A, Zile MR, Massie BM, and Carson PE**. Body mass index and adverse cardiovascular outcomes in heart failure patients with preserved ejection fraction: results from the Irbesartan in Heart Failure with Preserved Ejection Fraction (I-PRESERVE) trial. *Circ Heart Fail* 4: 324-331, 2011.

91. **Obokata M, Reddy YNV, Pislaru SV, Melenovsky V, and Borlaug BA**. Evidence Supporting the Existence of a Distinct Obese Phenotype of Heart Failure With Preserved Ejection Fraction. *Circulation* 136: 6-19, 2017.

92. **Kitzman DW, and Shah SJ**. The HFpEF Obesity Phenotype: The Elephant in the Room. *J Am Coll Cardiol* 68: 200-203, 2016.

93. **Packer M, and Kitzman DW**. Obesity-Related Heart Failure With a Preserved Ejection Fraction: The Mechanistic Rationale for Combining Inhibitors of Aldosterone, Neprilysin, and Sodium-Glucose Cotransporter-2. *JACC Heart Fail* 6: 633-639, 2018.

94. **Tsujimoto T, and Kajio H**. Abdominal Obesity Is Associated With an Increased Risk of All-Cause Mortality in Patients With HFpEF. *J Am Coll Cardiol* 70: 2739-2749, 2017.

95. **Peterson LR, Waggoner AD, Schechtman KB, Meyer T, Gropler RJ, Barzilai B, and Dávila-Román VG**. Alterations in left ventricular structure and function in young healthy obese women: assessment by echocardiography and tissue Doppler imaging. *J Am Coll Cardiol* 43: 1399-1404, 2004.

96. **Wong CY, O'Moore-Sullivan T, Leano R, Byrne N, Beller E, and Marwick TH**. Alterations of left ventricular myocardial characteristics associated with obesity. *Circulation* 110: 3081-3087, 2004.

97. **Neeland IJ, Gupta S, Ayers CR, Turer AT, Rame JE, Das SR, Berry JD, Khera A, McGuire DK, Vega GL, Grundy SM, de Lemos JA, and Drazner MH**. Relation of regional fat distribution to left ventricular structure and function. *Circ Cardiovasc Imaging* 6: 800-807, 2013.

98. **Selvaraj S, Martinez EE, Aguilar FG, Kim KY, Peng J, Sha J, Irvin MR, Lewis CE, Hunt SC, Arnett DK, and Shah SJ**. Association of Central Adiposity With Adverse Cardiac Mechanics: Findings From the Hypertension Genetic Epidemiology Network Study. *Circ Cardiovasc Imaging* 9: 2016.

99. **Alvarez GE, Beske SD, Ballard TP, and Davy KP**. Sympathetic neural activation in visceral obesity. *Circulation* 106: 2533-2536, 2002.

100. **Badimon L, Bugiardini R, Cenko E, Cubedo J, Dorobantu M, Duncker DJ, Estruch R, Milicic D, Tousoulis D, Vasiljevic Z, Vilahur G, de Wit C, and Koller A**. Position paper of the European Society of Cardiology-working group of coronary pathophysiology and microcirculation: obesity and heart disease. *Eur Heart J* 38: 1951-1958, 2017.

101. **Reddy YNV, Lewis GD, Shah SJ, Obokata M, Abou-Ezzedine OF, Fudim M, Sun JL, Chakraborty H, McNulty S, LeWinter MM, Mann DL, Stevenson LW, Redfield MM, and Borlaug BA**. Characterization of the Obese Phenotype of Heart Failure With Preserved Ejection Fraction: A RELAX Trial Ancillary Study. *Mayo Clin Proc* 94: 1199-1209, 2019.

102. **Patel VB, Mori J, McLean BA, Basu R, Das SK, Ramprasath T, Parajuli N, Penninger JM, Grant MB, Lopaschuk GD, and Oudit GY**. ACE2 Deficiency Worsens Epicardial Adipose Tissue Inflammation and Cardiac Dysfunction in Response to Diet-Induced Obesity. *Diabetes* 65: 85-95, 2016.

103. **Mazurek T, Zhang L, Zalewski A, Mannion JD, Diehl JT, Arafat H, Sarov-Blat L, O'Brien S, Keiper EA, Johnson AG, Martin J, Goldstein BJ, and Shi Y**. Human epicardial adipose tissue is a source of inflammatory mediators. *Circulation* 108: 2460-2466, 2003.

104. **Packer M**. Epicardial Adipose Tissue May Mediate Deleterious Effects of Obesity and Inflammation on the Myocardium. *J Am Coll Cardiol* 71: 2360-2372, 2018.

105. **Schiattarella GG, Rodolico D, and Hill JA**. Metabolic inflammation in heart failure with preserved ejection fraction. *Cardiovasc Res* 117: 423-434, 2021.

106. **Paulus WJ, and Zile MR**. From Systemic Inflammation to Myocardial Fibrosis: The Heart Failure With Preserved Ejection Fraction Paradigm Revisited. *Circ Res* 128: 1451-1467, 2021.

107. **Magne F, Gotteland M, Gauthier L, Zazueta A, Pesoa S, Navarrete P, and Balamurugan R**. The Firmicutes/Bacteroidetes Ratio: A Relevant Marker of Gut Dysbiosis in Obese Patients? *Nutrients* 12: 2020.

108. **Ley RE, Turnbaugh PJ, Klein S, and Gordon JI**. Microbial ecology: human gut microbes associated with obesity. *Nature* 444: 1022-1023, 2006.

109. **Martinez JE, Kahana DD, Ghuman S, Wilson HP, Wilson J, Kim SCJ, Lagishetty V, Jacobs JP, Sinha-Hikim AP, and Friedman TC**. Unhealthy Lifestyle and Gut Dysbiosis: A Better Understanding of the Effects of Poor Diet and Nicotine on the Intestinal Microbiome. *Front Endocrinol (Lausanne)* 12: 667066, 2021.

110. **Qin J, Li Y, Cai Z, Li S, Zhu J, Zhang F, Liang S, Zhang W, Guan Y, Shen D, Peng Y, Zhang D, Jie Z, Wu W, Qin Y, Xue W, Li J, Han L, Lu D, Wu P, Dai Y, Sun X, Li Z, Tang A, Zhong S, Li X, Chen W, Xu R, Wang M, Feng Q, Gong M, Yu J, Zhang Y, Zhang M, Hansen T, Sanchez G, Raes J, Falony G, Okuda S, Almeida M, LeChatelier E, Renault P, Pons N, Batto JM, Zhang Z, Chen H, Yang R, Zheng W, Yang H, Wang J, Ehrlich SD, Nielsen R, Pedersen O, and Kristiansen K**. A metagenome-wide association study of gut microbiota in type 2 diabetes. *Nature* 490: 55-60, 2012.

111. **Carding S, Verbeke K, Vipond DT, Corfe BM, and Owen LJ**. Dysbiosis of the gut microbiota in disease. *Microb Ecol Health Dis* 26: 26191, 2015.

112. **Hills RD, Pontefract BA, Mishcon HR, Black CA, Sutton SC, and Theberge CR**. Gut Microbiome: Profound Implications for Diet and Disease. *Nutrients* 11: 2019.

113. **Belkaid Y, and Hand TW**. Role of the microbiota in immunity and inflammation. *Cell* 157: 121-141, 2014.

114. **Qin J, Li R, Raes J, Arumugam M, Burgdorf KS, Manichanh C, Nielsen T, Pons N, Levenez F, Yamada T, Mende DR, Li J, Xu J, Li S, Li D, Cao J, Wang B, Liang H, Zheng H, Xie Y, Tap J, Lepage P, Bertalan M, Batto JM, Hansen T, Le Paslier D, Linneberg A, Nielsen HB, Pelletier E, Renault P, Sicheritz-Ponten T, Turner K, Zhu H, Yu C, Jian M, Zhou Y, Li Y, Zhang X, Qin N, Yang H, Wang J, Brunak S, Doré J, Guarner F, Kristiansen K, Pedersen O, Parkhill J, Weissenbach J, Bork P, Ehrlich SD, and Consortium M**. A human gut microbial gene catalogue established by metagenomic sequencing. *Nature* 464: 59-65, 2010.

115. **Turnbaugh PJ, Hamady M, Yatsunenko T, Cantarel BL, Duncan A, Ley RE, Sogin ML, Jones WJ, Roe BA, Affourtit JP, Egholm M, Henrissat B, Heath AC, Knight R, and Gordon JI**. A core gut microbiome in obese and lean twins. *Nature* 457: 480-484, 2009.

116. **Ley RE, Bäckhed F, Turnbaugh P, Lozupone CA, Knight RD, and Gordon JI**. Obesity alters gut microbial ecology. *Proc Natl Acad Sci U S A* 102: 11070-11075, 2005.

117. **Duncan SH, Lobley GE, Holtrop G, Ince J, Johnstone AM, Louis P, and Flint HJ**. Human colonic microbiota associated with diet, obesity and weight loss. *Int J Obes (Lond)* 32: 1720-1724, 2008.

118. **Ravussin Y, Koren O, Spor A, LeDuc C, Gutman R, Stombaugh J, Knight R, Ley RE, and Leibel RL**. Responses of gut microbiota to diet composition and weight loss in lean and obese mice. *Obesity (Silver Spring)* 20: 738-747, 2012.

119. **Turnbaugh PJ, Ley RE, Mahowald MA, Magrini V, Mardis ER, and Gordon JI**. An obesity-associated gut microbiome with increased capacity for energy harvest. *Nature* 444: 1027-1031, 2006.

120. **Young VB**. The role of the microbiome in human health and disease: an introduction for clinicians. *BMJ* 356: j831, 2017.

121. **Kataoka K**. The intestinal microbiota and its role in human health and disease. *J Med Invest* 63: 27-37, 2016.

122. **Lin CS, Chang CJ, Lu CC, Martel J, Ojcius DM, Ko YF, Young JD, and Lai HC**. Impact of the gut microbiota, prebiotics, and probiotics on human health and disease. *Biomed J* 37: 259-268, 2014.

123. **Ahmad AF, Dwivedi G, O'Gara F, Caparros-Martin J, and Ward NC**. The gut microbiome and cardiovascular disease: current knowledge and clinical potential. *Am J Physiol Heart Circ Physiol* 317: H923-H938, 2019.

124. **Tang WH, Kitai T, and Hazen SL**. Gut Microbiota in Cardiovascular Health and Disease. *Circ Res* 120: 1183-1196, 2017.

125. **Tang WHW, Bäckhed F, Landmesser U, and Hazen SL**. Intestinal Microbiota in Cardiovascular Health and Disease: JACC State-of-the-Art Review. *J Am Coll Cardiol* 73: 2089-2105, 2019.

126. **Witkowski M, Weeks TL, and Hazen SL**. Gut Microbiota and Cardiovascular Disease. *Circ Res* 127: 553-570, 2020.

127. **Koh A, De Vadder F, Kovatcheva-Datchary P, and Bäckhed F**. From Dietary Fiber to Host Physiology: Short-Chain Fatty Acids as Key Bacterial Metabolites. *Cell* 165: 1332-1345, 2016.

128. **Hill MJ**. Bacterial fermentation of complex carbohydrate in the human colon. *Eur J Cancer Prev* 4: 353-358, 1995.

129. **Chen XF, Chen X, and Tang X**. Short-chain fatty acid, acylation and cardiovascular diseases. *Clin Sci (Lond)* 134: 657-676, 2020.

130. **Rooks MG, and Garrett WS**. Gut microbiota, metabolites and host immunity. *Nat Rev Immunol* 16: 341-352, 2016.

131. **Bourlioux P, Koletzko B, Guarner F, and Braesco V**. The intestine and its microflora are partners for the protection of the host: report on the Danone Symposium "The Intelligent Intestine," held in Paris, June 14, 2002. *Am J Clin Nutr* 78: 675-683, 2003.

132. **Cummings JH, Pomare EW, Branch WJ, Naylor CP, and Macfarlane GT**. Short chain fatty acids in human large intestine, portal, hepatic and venous blood. *Gut* 28: 1221-1227, 1987.

133. **Kim S, Goel R, Kumar A, Qi Y, Lobaton G, Hosaka K, Mohammed M, Handberg EM, Richards EM, Pepine CJ, and Raizada MK**. Imbalance of gut microbiome and intestinal epithelial barrier dysfunction in patients with high blood pressure. *Clin Sci (Lond)* 132: 701-718, 2018.

134. **Roediger WE**. Role of anaerobic bacteria in the metabolic welfare of the colonic mucosa in man. *Gut* 21: 793-798, 1980.

135. **Ardawi MS, and Newsholme EA**. Fuel utilization in colonocytes of the rat. *Biochem J* 231: 713-719, 1985.

136. **Canfora EE, Jocken JW, and Blaak EE**. Short-chain fatty acids in control of body weight and insulin sensitivity. *Nat Rev Endocrinol* 11: 577-591, 2015.

137. **Ruppin H, Bar-Meir S, Soergel KH, Wood CM, and Schmitt MG**. Absorption of short-chain fatty acids by the colon. *Gastroenterology* 78: 1500-1507, 1980.

138. **Ritzhaupt A, Wood IS, Ellis A, Hosie KB, and Shirazi-Beechey SP**. Identification and characterization of a monocarboxylate transporter (MCT1) in pig and human colon: its potential to transport L-lactate as well as butyrate. *J Physiol* 513 (Pt 3): 719-732, 1998.

139. **Moschen I, Bröer A, Galić S, Lang F, and Bröer S**. Significance of short chain fatty acid transport by members of the monocarboxylate transporter family (MCT). *Neurochem Res* 37: 2562-2568, 2012.

140. **Bloemen JG, Venema K, van de Poll MC, Olde Damink SW, Buurman WA, and Dejong CH**. Short chain fatty acids exchange across the gut and liver in humans measured at surgery. *Clin Nutr* 28: 657-661, 2009.

141. **Wong JM, de Souza R, Kendall CW, Emam A, and Jenkins DJ**. Colonic health: fermentation and short chain fatty acids. *J Clin Gastroenterol* 40: 235-243, 2006.

142. **Cummings JH, and Macfarlane GT**. Colonic microflora: nutrition and health. *Nutrition* 13: 476-478, 1997.

143. **Cummings JH, and Macfarlane GT**. Role of intestinal bacteria in nutrient metabolism. *JPEN J Parenter Enteral Nutr* 21: 357-365, 1997.

144. **Ríos-Covián D, Ruas-Madiedo P, Margolles A, Gueimonde M, de Los Reyes-Gavilán CG, and Salazar N**. Intestinal Short Chain Fatty Acids and their Link with Diet and Human Health. *Front Microbiol* 7: 185, 2016.

145. **Velasquez MT**. Altered Gut Microbiota: A Link Between Diet and the Metabolic Syndrome. *Metab Syndr Relat Disord* 16: 321-328, 2018.

146. **Brown AJ, Goldsworthy SM, Barnes AA, Eilert MM, Tcheang L, Daniels D, Muir AI, Wigglesworth MJ, Kinghorn I, Fraser NJ, Pike NB, Strum JC, Steplewski KM, Murdock PR, Holder JC, Marshall FH, Szekeres PG, Wilson S, Ignar DM, Foord SM, Wise A, and Dowell SJ**. The Orphan G protein-coupled receptors GPR41 and GPR43 are activated by propionate and other short chain carboxylic acids. *J Biol Chem* 278: 11312-11319, 2003.

147. **Le Poul E, Loison C, Struyf S, Springael JY, Lannoy V, Decobecq ME, Brezillon S, Dupriez V, Vassart G, Van Damme J, Parmentier M, and Detheux M**. Functional characterization of human receptors for short chain fatty acids and their role in polymorphonuclear cell activation. *J Biol Chem* 278: 25481-25489, 2003.

148. **Karaki S, Tazoe H, Hayashi H, Kashiwabara H, Tooyama K, Suzuki Y, and Kuwahara A**. Expression of the short-chain fatty acid receptor, GPR43, in the human colon. *J Mol Histol* 39: 135-142, 2008.

149. **Li G, Su H, Zhou Z, and Yao W**. Identification of the porcine G protein-coupled receptor 41 and 43 genes and their expression pattern in different tissues and development stages. *PLoS One* 9: e97342, 2014.

150. **Tazoe H, Otomo Y, Karaki S, Kato I, Fukami Y, Terasaki M, and Kuwahara A**. Expression of short-chain fatty acid receptor GPR41 in the human colon. *Biomed Res* 30: 149-156, 2009.

151. **Thangaraju M, Cresci GA, Liu K, Ananth S, Gnanaprakasam JP, Browning DD, Mellinger JD, Smith SB, Digby GJ, Lambert NA, Prasad PD, and Ganapathy V**. GPR109A is a G-protein-coupled receptor for the bacterial fermentation product butyrate and functions as a tumor suppressor in colon. *Cancer Res* 69: 2826-2832, 2009.

152. **Chen G, Ran X, Li B, Li Y, He D, Huang B, Fu S, Liu J, and Wang W**. Sodium Butyrate Inhibits Inflammation and Maintains Epithelium Barrier Integrity in a TNBS-induced Inflammatory Bowel Disease Mice Model. *EBioMedicine* 30: 317-325, 2018.

153. **Fu SP, Wang JF, Xue WJ, Liu HM, Liu BR, Zeng YL, Li SN, Huang BX, Lv QK, Wang W, and Liu JX**. Anti-inflammatory effects of BHBA in both in vivo and in vitro Parkinson's disease models are mediated by GPR109A-dependent mechanisms. *J Neuroinflammation* 12: 9, 2015.

154. **Liu F, Fu Y, Wei C, Chen Y, Ma S, and Xu W**. The expression of GPR109A, NF-kB and IL-1β in peripheral blood leukocytes from patients with type 2 diabetes. *Ann Clin Lab Sci* 44: 443-448, 2014.

155. **Pluznick JL, Protzko RJ, Gevorgyan H, Peterlin Z, Sipos A, Han J, Brunet I, Wan LX, Rey F, Wang T, Firestein SJ, Yanagisawa M, Gordon JI, Eichmann A, Peti-Peterdi J, and Caplan MJ**. Olfactory receptor responding to gut microbiota-derived signals plays a role in renin secretion and blood pressure regulation. *Proc Natl Acad Sci U S A* 110: 4410-4415, 2013.

156. **Pluznick J**. A novel SCFA receptor, the microbiota, and blood pressure regulation. *Gut Microbes* 5: 202-207, 2014.

157. **Kotlo K, Anbazhagan AN, Priyamvada S, Jayawardena D, Kumar A, Chen Y, Xia Y, Finn PW, Perkins DL, Dudeja PK, and Layden BT**. The olfactory G protein-coupled receptor (Olfr-78/OR51E2) modulates the intestinal response to colitis. *Am J Physiol Cell Physiol* 318: C502-C513, 2020.

158. **Chen JS, Faller DV, and Spanjaard RA**. Short-chain fatty acid inhibitors of histone deacetylases: promising anticancer therapeutics? *Curr Cancer Drug Targets* 3: 219-236, 2003.

159. **Kiefer J, Beyer-Sehlmeyer G, and Pool-Zobel BL**. Mixtures of SCFA, composed according to physiologically available concentrations in the gut lumen, modulate histone acetylation in human HT29 colon cancer cells. *Br J Nutr* 96: 803-810, 2006.

160. **Fellows R, Denizot J, Stellato C, Cuomo A, Jain P, Stoyanova E, Balázsi S, Hajnády Z, Liebert A, Kazakevych J, Blackburn H, Corrêa RO, Fachi JL, Sato FT, Ribeiro WR, Ferreira CM, Perée H, Spagnuolo M, Mattiuz R, Matolcsi C, Guedes J, Clark J, Veldhoen M, Bonaldi T, Vinolo MAR, and Varga-Weisz P**. Microbiota derived short chain fatty acids promote histone crotonylation in the colon through histone deacetylases. *Nat Commun* 9: 105, 2018.

161. **Astbury SM, and Corfe BM**. Uptake and metabolism of the short-chain fatty acid butyrate, a critical review of the literature. *Curr Drug Metab* 13: 815-821, 2012.

162. **Davie JR**. Inhibition of histone deacetylase activity by butyrate. *J Nutr* 133: 2485S-2493S, 2003.

163. **Yuille S, Reichardt N, Panda S, Dunbar H, and Mulder IE**. Human gut bacteria as potent class I histone deacetylase inhibitors in vitro through production of butyric acid and valeric acid. *PLoS One* 13: e0201073, 2018.

164. **Chang PV, Hao L, Offermanns S, and Medzhitov R**. The microbial metabolite butyrate regulates intestinal macrophage function via histone deacetylase inhibition. *Proc Natl Acad Sci U S A* 111: 2247-2252, 2014.

165. **Chriett S, Dąbek A, Wojtala M, Vidal H, Balcerczyk A, and Pirola L**. Prominent action of butyrate over β-hydroxybutyrate as histone deacetylase inhibitor, transcriptional modulator and anti-inflammatory molecule. *Sci Rep* 9: 742, 2019.

166. **Cani PD, Bibiloni R, Knauf C, Waget A, Neyrinck AM, Delzenne NM, and Burcelin R**. Changes in gut microbiota control metabolic endotoxemia-induced inflammation in high-fat diet-induced obesity and diabetes in mice. *Diabetes* 57: 1470-1481, 2008.

167. **Zhang PP, Li LL, Han X, Li QW, Zhang XH, Liu JJ, and Wang Y**. Fecal microbiota transplantation improves metabolism and gut microbiome composition in db/db mice. *Acta Pharmacol Sin* 41: 678-685, 2020.

168. **Vrieze A, Van Nood E, Holleman F, Salojärvi J, Kootte RS, Bartelsman JF, Dallinga-Thie GM, Ackermans MT, Serlie MJ, Oozeer R, Derrien M, Druesne A, Van Hylckama Vlieg JE, Bloks VW, Groen AK, Heilig HG, Zoetendal EG, Stroes ES, de Vos WM, Hoekstra JB, and Nieuwdorp M**. Transfer of intestinal microbiota from lean donors increases insulin sensitivity in individuals with metabolic syndrome. *Gastroenterology* 143: 913-916.e917, 2012.

169. **Coppola S, Avagliano C, Calignano A, and Berni Canani R**. The Protective Role of Butyrate against Obesity and Obesity-Related Diseases. *Molecules* 26: 2021.

170. **Kitai T, Kirsop J, and Tang WH**. Exploring the Microbiome in Heart Failure. *Curr Heart Fail Rep* 13: 103-109, 2016.

171. **Tang WH, and Hazen SL**. The contributory role of gut microbiota in cardiovascular disease. *J Clin Invest* 124: 4204-4211, 2014.

172. **Li J, Zhao F, Wang Y, Chen J, Tao J, Tian G, Wu S, Liu W, Cui Q, Geng B, Zhang W, Weldon R, Auguste K, Yang L, Liu X, Chen L, Yang X, Zhu B, and Cai J**. Gut microbiota dysbiosis contributes to the development of hypertension. *Microbiome* 5: 14, 2017.

173. **Santisteban MM, Qi Y, Zubcevic J, Kim S, Yang T, Shenoy V, Cole-Jeffrey CT, Lobaton GO, Stewart DC, Rubiano A, Simmons CS, Garcia-Pereira F, Johnson RD, Pepine CJ, and Raizada MK**. Hypertension-Linked Pathophysiological Alterations in the Gut. *Circ Res* 120: 312-323, 2017.

174. **Marques FZ, Nelson E, Chu PY, Horlock D, Fiedler A, Ziemann M, Tan JK, Kuruppu S, Rajapakse NW, El-Osta A, Mackay CR, and Kaye DM**. High-Fiber Diet and Acetate Supplementation Change the Gut Microbiota and Prevent the Development of Hypertension and Heart Failure in Hypertensive Mice. *Circulation* 135: 964-977, 2017.

175. **Bartolomaeus H, Balogh A, Yakoub M, Homann S, Markó L, Höges S, Tsvetkov D, Krannich A, Wundersitz S, Avery EG, Haase N, Kräker K, Hering L, Maase M, Kusche-Vihrog K, Grandoch M, Fielitz J, Kempa S, Gollasch M, Zhumadilov Z, Kozhakhmetov S, Kushugulova A, Eckardt KU, Dechend R, Rump LC, Forslund SK, Müller DN, Stegbauer J, and Wilck N**. Short-Chain Fatty Acid Propionate Protects From Hypertensive Cardiovascular Damage. *Circulation* 139: 1407-1421, 2019.

176. **Yang T, Santisteban MM, Rodriguez V, Li E, Ahmari N, Carvajal JM, Zadeh M, Gong M, Qi Y, Zubcevic J, Sahay B, Pepine CJ, Raizada MK, and Mohamadzadeh M**. Gut dysbiosis is linked to hypertension. *Hypertension* 65: 1331-1340, 2015.

177. **Bartolomaeus H, Markó L, Wilck N, Luft FC, Forslund SK, and Muller DN**. Precarious Symbiosis Between Host and Microbiome in Cardiovascular Health. *Hypertension* 73: 926-935, 2019.

178. **Natarajan N, Hori D, Flavahan S, Steppan J, Flavahan NA, Berkowitz DE, and Pluznick JL**. Microbial short chain fatty acid metabolites lower blood pressure via endothelial G protein-coupled receptor 41. *Physiol Genomics* 48: 826-834, 2016.

179. **Battson ML, Lee DM, Li Puma LC, Ecton KE, Thomas KN, Febvre HP, Chicco AJ, Weir TL, and Gentile CL**. Gut microbiota regulates cardiac ischemic tolerance and aortic stiffness in obesity. *Am J Physiol Heart Circ Physiol* 317: H1210-H1220, 2019.

180. **Tang TWH, Chen HC, Chen CY, Yen CYT, Lin CJ, Prajnamitra RP, Chen LL, Ruan SC, Lin JH, Lin PJ, Lu HH, Kuo CW, Chang CM, Hall AD, Vivas EI, Shui JW, Chen P, Hacker TA, Rey FE, Kamp TJ, and Hsieh PCH**. Loss of Gut Microbiota Alters Immune System Composition and Cripples Postinfarction Cardiac Repair. *Circulation* 139: 647-659, 2019.

181. **Moludi J, Maleki V, Jafari-Vayghyan H, Vaghef-Mehrabany E, and Alizadeh M**. Metabolic endotoxemia and cardiovascular disease: A systematic review about potential roles of prebiotics and probiotics. *Clin Exp Pharmacol Physiol* 47: 927-939, 2020.

182. **Wang J, Tang H, Zhang C, Zhao Y, Derrien M, Rocher E, van-Hylckama Vlieg JE, Strissel K, Zhao L, Obin M, and Shen J**. Modulation of gut microbiota during probiotic-mediated attenuation of metabolic syndrome in high fat diet-fed mice. *ISME J* 9: 1-15, 2015.

183. **Ghosh S, Yang X, Wang L, Zhang C, and Zhao L**. Active phase prebiotic feeding alters gut microbiota, induces weight-independent alleviation of hepatic steatosis and serum cholesterol in high-fat diet-fed mice. *Comput Struct Biotechnol J* 19: 448-458, 2021.

184. **Grundy SM, Cleeman JI, Daniels SR, Donato KA, Eckel RH, Franklin BA, Gordon DJ, Krauss RM, Savage PJ, Smith SC, Spertus JA, Costa F, Association AH, and National Heart Ln, and Blood Institue**. Diagnosis and management of the metabolic syndrome. An American Heart Association/National Heart, Lung, and Blood Institute Scientific Statement. Executive summary. *Cardiol Rev* 13: 322-327, 2005.

185. **Cani PD, Amar J, Iglesias MA, Poggi M, Knauf C, Bastelica D, Neyrinck AM, Fava F, Tuohy KM, Chabo C, Waget A, Delmée E, Cousin B, Sulpice T, Chamontin B, Ferrières J, Tanti JF, Gibson GR, Casteilla L, Delzenne NM, Alessi MC, and Burcelin R**. Metabolic endotoxemia initiates obesity and insulin resistance. *Diabetes* 56: 1761-1772, 2007.

186. **Song MJ, Kim KH, Yoon JM, and Kim JB**. Activation of Toll-like receptor 4 is associated with insulin resistance in adipocytes. *Biochem Biophys Res Commun* 346: 739-745, 2006.

187. **Ginsberg HN, Zhang YL, and Hernandez-Ono A**. Metabolic syndrome: focus on dyslipidemia. *Obesity (Silver Spring)* 14 Suppl 1: 41S-49S, 2006.

188. **Byrne CS, Chambers ES, Morrison DJ, and Frost G**. The role of short chain fatty acids in appetite regulation and energy homeostasis. *Int J Obes (Lond)* 39: 1331-1338, 2015.

189. **Cook TM, Gavini CK, Jesse J, Aubert G, Gornick E, Bonomo R, Gautron L, Layden BT, and Mansuy-Aubert V**. Vagal neuron expression of the microbiota-derived metabolite receptor, free fatty acid receptor (FFAR3), is necessary for normal feeding behavior. *Mol Metab* 54: 101350, 2021.

190. **Sukkar AH, Lett AM, Frost G, and Chambers ES**. Regulation of energy expenditure and substrate oxidation by short-chain fatty acids. *J Endocrinol* 242: R1-R8, 2019.

191. **Wang Y, Xu Y, Yang M, Zhang M, Xiao M, and Li X**. Butyrate mitigates TNF-α-induced attachment of monocytes to endothelial cells. *J Bioenerg Biomembr* 52: 247-256, 2020.

192. **Sun X, Luo S, Jiang C, Tang Y, Cao Z, Jia H, Xu Q, Zhao C, Loor JJ, and Xu C**. Sodium butyrate reduces bovine mammary epithelial cell inflammatory responses induced by exogenous lipopolysaccharide, by inactivating NF-κB signaling. *J Dairy Sci* 103: 8388-8397, 2020.

193. **de Lazari MGT, Pereira LX, Orellano LAA, Scheuermann K, Machado CT, Vasconcelos AC, Andrade SP, and Campos PP**. Sodium Butyrate Downregulates Implant-Induced Inflammation in Mice. *Inflammation* 43: 1259-1268, 2020.

194. **Wang F, Jin Z, Shen K, Weng T, Chen Z, Feng J, Zhang Z, Liu J, Zhang X, and Chu M**. Butyrate pretreatment attenuates heart depression in a mice model of endotoxin-induced sepsis via anti-inflammation and anti-oxidation. *Am J Emerg Med* 35: 402-409, 2017.

195. **Aguilar EC, Leonel AJ, Teixeira LG, Silva AR, Silva JF, Pelaez JM, Capettini LS, Lemos VS, Santos RA, and Alvarez-Leite JI**. Butyrate impairs atherogenesis by reducing plaque inflammation and vulnerability and decreasing NFκB activation. *Nutr Metab Cardiovasc Dis* 24: 606-613, 2014.

196. **Gao Z, Yin J, Zhang J, Ward RE, Martin RJ, Lefevre M, Cefalu WT, and Ye J**. Butyrate improves insulin sensitivity and increases energy expenditure in mice. *Diabetes* 58: 1509-1517, 2009.

197. **Badejogbin C, Areola DE, Olaniyi KS, Adeyanju OA, and Adeosun IO**. Sodium butyrate recovers high-fat diet-fed female Wistar rats from glucose dysmetabolism and uric acid-associated cardiac tissue damage. *Naunyn Schmiedebergs Arch Pharmacol* 392: 1411-1419, 2019.

198. **Al-Lahham S, and Rezaee F**. Propionic acid counteracts the inflammation of human subcutaneous adipose tissue: a new avenue for drug development. *Daru* 27: 645-652, 2019.

199. **Lin HV, Frassetto A, Kowalik EJ, Nawrocki AR, Lu MM, Kosinski JR, Hubert JA, Szeto D, Yao X, Forrest G, and Marsh DJ**. Butyrate and propionate protect against diet-induced obesity and regulate gut hormones via free fatty acid receptor 3-independent mechanisms. *PLoS One* 7: e35240, 2012.

200. **Ndisang JF, and Rastogi S**. Cardiometabolic diseases and related complications: current status and future perspective. *Biomed Res Int* 2013: 467682, 2013.

201. **Castro JP, El-Atat FA, McFarlane SI, Aneja A, and Sowers JR**. Cardiometabolic syndrome: pathophysiology and treatment. *Curr Hypertens Rep* 5: 393-401, 2003.

202. **Srivastava AK**. Challenges in the treatment of cardiometabolic syndrome. *Indian J Pharmacol* 44: 155-156, 2012.

203. **Mancia G, and Grassi G**. The autonomic nervous system and hypertension. *Circ Res* 114: 1804-1814, 2014.

204. **Moreira TS, Antunes VR, Falquetto B, and Marina N**. Long-term stimulation of cardiac vagal preganglionic neurons reduces blood pressure in the spontaneously hypertensive rat. *J Hypertens* 36: 2444-2452, 2018.

205. **Annoni EM, Van Helden D, Guo Y, Levac B, Libbus I, KenKnight BH, Osborn JW, and Tolkacheva EG**. Chronic Low-Level Vagus Nerve Stimulation Improves Long-Term Survival in Salt-Sensitive Hypertensive Rats. *Front Physiol* 10: 25, 2019.

206. **Kalla M, Herring N, and Paterson DJ**. Cardiac sympatho-vagal balance and ventricular arrhythmia. *Auton Neurosci* 199: 29-37, 2016.

207. **Grassi G, Mark A, and Esler M**. The sympathetic nervous system alterations in human hypertension. *Circ Res* 116: 976-990, 2015.

208. **DiBona GF**. Sympathetic nervous system and hypertension. *Hypertension* 61: 556-560, 2013.

209. **Cervi AL, Lukewich MK, and Lomax AE**. Neural regulation of gastrointestinal inflammation: role of the sympathetic nervous system. *Auton Neurosci* 182: 83-88, 2014.

210. **Zubcevic J, Richards EM, Yang T, Kim S, Sumners C, Pepine CJ, and Raizada MK**. Impaired Autonomic Nervous System-Microbiome Circuit in Hypertension. *Circ Res* 125: 104-116, 2019.

211. **Duan H, Cai X, Luan Y, Yang S, Yang J, Dong H, Zeng H, and Shao L**. Regulation of the Autonomic Nervous System on Intestine. *Front Physiol* 12: 700129, 2021.

212. **Nagatomo Y, and Tang WH**. Intersections Between Microbiome and Heart Failure: Revisiting the Gut Hypothesis. *J Card Fail* 21: 973-980, 2015.

213. **Luedde M, Winkler T, Heinsen FA, Rühlemann MC, Spehlmann ME, Bajrovic A, Lieb W, Franke A, Ott SJ, and Frey N**. Heart failure is associated with depletion of core intestinal microbiota. *ESC Heart Fail* 4: 282-290, 2017.

214. **Cui X, Ye L, Li J, Jin L, Wang W, Li S, Bao M, Wu S, Li L, Geng B, Zhou X, Zhang J, and Cai J**. Metagenomic and metabolomic analyses unveil dysbiosis of gut microbiota in chronic heart failure patients. *Sci Rep* 8: 635, 2018.

215. **Kummen M, Mayerhofer CCK, Vestad B, Broch K, Awoyemi A, Storm-Larsen C, Ueland T, Yndestad A, Hov JR, and Trøseid M**. Gut Microbiota Signature in Heart Failure Defined From Profiling of 2 Independent Cohorts. *J Am Coll Cardiol* 71: 1184-1186, 2018.

216. **Sandek A, Bauditz J, Swidsinski A, Buhner S, Weber-Eibel J, von Haehling S, Schroedl W, Karhausen T, Doehner W, Rauchhaus M, Poole-Wilson P, Volk HD, Lochs H, and Anker SD**. Altered intestinal function in patients with chronic heart failure. *J Am Coll Cardiol* 50: 1561-1569, 2007.

217. **Niebauer J, Volk HD, Kemp M, Dominguez M, Schumann RR, Rauchhaus M, Poole-Wilson PA, Coats AJ, and Anker SD**. Endotoxin and immune activation in chronic heart failure: a prospective cohort study. *Lancet* 353: 1838-1842, 1999.

218. **Peschel T, Schönauer M, Thiele H, Anker SD, Schuler G, and Niebauer J**. Invasive assessment of bacterial endotoxin and inflammatory cytokines in patients with acute heart failure. *Eur J Heart Fail* 5: 609-614, 2003.

219. **Pastori D, Carnevale R, Nocella C, Novo M, Santulli M, Cammisotto V, Menichelli D, Pignatelli P, and Violi F**. Gut-Derived Serum Lipopolysaccharide is Associated With Enhanced Risk of Major Adverse Cardiovascular Events in Atrial Fibrillation: Effect of Adherence to Mediterranean Diet. *J Am Heart Assoc* 6: 2017.

220. **Silva LG, Ferguson BS, Avila AS, and Faciola AP**. Sodium propionate and sodium butyrate effects on histone deacetylase (HDAC) activity, histone acetylation, and inflammatory gene expression in bovine mammary epithelial cells. *J Anim Sci* 96: 5244-5252, 2018.

221. **Place RF, Noonan EJ, and Giardina C**. HDAC inhibition prevents NF-kappa B activation by suppressing proteasome activity: down-regulation of proteasome subunit expression stabilizes I kappa B alpha. *Biochem Pharmacol* 70: 394-406, 2005.

222. **Xu T, Ma N, Wang Y, Shi X, Chang G, Loor JJ, and Shen X**. Sodium Butyrate Supplementation Alleviates the Adaptive Response to Inflammation and Modulates Fatty Acid Metabolism in Lipopolysaccharide-Stimulated Bovine Hepatocytes. *J Agric Food Chem* 66: 6281-6290, 2018.

223. **Lopaschuk GD, Ussher JR, Folmes CD, Jaswal JS, and Stanley WC**. Myocardial fatty acid metabolism in health and disease. *Physiol Rev* 90: 207-258, 2010
.
224. **Gibb AA, and Hill BG**. Metabolic Coordination of Physiological and Pathological Cardiac Remodeling. *Circ Res* 123: 107-128, 2018.

225. **Taegtmeyer H, Young ME, Lopaschuk GD, Abel ED, Brunengraber H, Darley-Usmar V, Des Rosiers C, Gerszten R, Glatz JF, Griffin JL, Gropler RJ, Holzhuetter HG, Kizer JR, Lewandowski ED, Malloy CR, Neubauer S, Peterson LR, Portman MA, Recchia FA, Van Eyk JE, Wang TJ, and Sciences AHACoBC**. Assessing Cardiac Metabolism: A Scientific Statement From the American Heart Association. *Circ Res* 118: 1659-1701, 2016.

226. **Jeffrey FM, Diczku V, Sherry AD, and Malloy CR**. Substrate selection in the isolated working rat heart: effects of reperfusion, afterload, and concentration. *Basic Res Cardiol* 90: 388-396, 1995.

227. **Kantor PF, Robertson MA, Coe JY, and Lopaschuk GD**. Volume overload hypertrophy of the newborn heart slows the maturation of enzymes involved in the regulation of fatty acid metabolism. *J Am Coll Cardiol* 33: 1724-1734, 1999.

228. **van der Vusse GJ, van Bilsen M, and Glatz JF**. Cardiac fatty acid uptake and transport in health and disease. *Cardiovasc Res* 45: 279-293, 2000.

229. **Sorokina N, O'Donnell JM, McKinney RD, Pound KM, Woldegiorgis G, LaNoue KF, Ballal K, Taegtmeyer H, Buttrick PM, and Lewandowski ED**. Recruitment of compensatory pathways to sustain oxidative flux with reduced carnitine palmitoyltransferase I activity characterizes inefficiency in energy metabolism in hypertrophied hearts. *Circulation* 115: 2033-2041, 2007.

230. **Pound KM, Sorokina N, Ballal K, Berkich DA, Fasano M, Lanoue KF, Taegtmeyer H, O'Donnell JM, and Lewandowski ED**. Substrate-enzyme competition attenuates upregulated anaplerotic flux through malic enzyme in hypertrophied rat heart and restores triacylglyceride content: attenuating upregulated anaplerosis in hypertrophy. *Circ Res* 104: 805-812, 2009.

231. **Lahey R, Carley AN, Wang X, Glass CE, Accola KD, Silvestry S, O'Donnell JM, and Lewandowski ED**. Enhanced Redox State and Efficiency of Glucose Oxidation With miR Based Suppression of Maladaptive NADPH-Dependent Malic Enzyme 1 Expression in Hypertrophied Hearts. *Circ Res* 122: 836-845, 2018.

232. **Kolwicz SC, Olson DP, Marney LC, Garcia-Menendez L, Synovec RE, and Tian R**. Cardiac-specific deletion of acetyl CoA carboxylase 2 prevents metabolic remodeling during pressure-overload hypertrophy. *Circ Res* 111: 728-738, 2012.

233. **Kolwicz SC, and Tian R**. Glucose metabolism and cardiac hypertrophy. *Cardiovasc Res* 90: 194-201, 2011.

234. **Aubert G, Martin OJ, Horton JL, Lai L, Vega RB, Leone TC, Koves T, Gardell SJ, Krüger M, Hoppel CL, Lewandowski ED, Crawford PA, Muoio DM, and Kelly DP**. The Failing Heart Relies on Ketone Bodies as a Fuel. *Circulation* 133: 698-705, 2016.

235. **Horton JL, Davidson MT, Kurishima C, Vega RB, Powers JC, Matsuura TR, Petucci C, Lewandowski ED, Crawford PA, Muoio DM, Recchia FA, and Kelly DP**. The failing heart utilizes 3-hydroxybutyrate as a metabolic stress defense. *JCI Insight* 4: 2019.

236. **Uchihashi M, Hoshino A, Okawa Y, Ariyoshi M, Kaimoto S, Tateishi S, Ono K, Yamanaka R, Hato D, Fushimura Y, Honda S, Fukai K, Higuchi Y, Ogata T, Iwai-Kanai E, and Matoba S**. Cardiac-Specific Bdh1 Overexpression Ameliorates Oxidative Stress and Cardiac Remodeling in Pressure Overload-Induced Heart Failure. *Circ Heart Fail* 10: 2017.

237. **Lewandowski ED, Kudej RK, White LT, O'Donnell JM, and Vatner SF**. Mitochondrial preference for short chain fatty acid oxidation during coronary artery constriction. *Circulation* 105: 367-372, 2002.

238. **Carley AN, Maurya SK, Fasano M, Wang Y, Selzman CH, Drakos SG, and Lewandowski ED**. Short Chain Fatty Acids Outpace Ketone Oxidation in the Failing Heart. *Circulation* 2021.

239. **Beale AL, O'Donnell JA, Nakai ME, Nanayakkara S, Vizi D, Carter K, Dean E, Ribeiro RV, Yiallourou S, Carrington MJ, Marques FZ, and Kaye DM**. The Gut Microbiome of Heart Failure With Preserved Ejection Fraction. *J Am Heart Assoc* 10: e020654, 2021.

240. **Huang Z, Mei X, Jiang Y, Chen T, and Zhou Y**. Gut Microbiota in Heart Failure Patients With Preserved Ejection Fraction (GUMPTION Study). *Front Cardiovasc Med* 8: 803744, 2021.

241. **Carbone S, and Lavie CJ**. Disparate effects of obesity on survival and hospitalizations in heart failure with preserved ejection fraction. *Int J Obes (Lond)* 44: 1543-1545, 2020.

242. **Joseph G, Zaremba T, Johansen MB, Ekeloef S, Heiberg E, Engblom H, Jensen SE, and Sogaard P**. Echocardiographic global longitudinal strain is associated with infarct size assessed by cardiac magnetic resonance in acute myocardial infarction. *Echo Res Pract* 6: 81-89, 2019.

243. **Cimino S, Canali E, Petronilli V, Cicogna F, De Luca L, Francone M, Sardella G, Iacoboni C, and Agati L**. Global and regional longitudinal strain assessed by two-dimensional speckle tracking echocardiography identifies early myocardial dysfunction and transmural extent of myocardial scar in patients with acute ST elevation myocardial infarction and relatively preserved LV function. *Eur Heart J Cardiovasc Imaging* 14: 805-811, 2013.

244. **Shetye A, Nazir SA, Squire IB, and McCann GP**. Global myocardial strain assessment by different imaging modalities to predict outcomes after ST-elevation myocardial infarction: A systematic review. *World J Cardiol* 7: 948-960, 2015.

245. **Edvardsen T, and Haugaa KH**. Strain Echocardiography: From Variability to Predictability. *JACC Cardiovasc Imaging* 11: 35-37, 2018.

246. **Yang H, Wright L, Negishi T, Negishi K, Liu J, and Marwick TH**. Research to Practice: Assessment of Left Ventricular Global Longitudinal Strain for Surveillance of Cancer Chemotherapeutic-Related Cardiac Dysfunction. *JACC Cardiovasc Imaging* 11: 1196-1201, 2018.

247. **Schnelle M, Catibog N, Zhang M, Nabeebaccus AA, Anderson G, Richards DA, Sawyer G, Zhang X, Toischer K, Hasenfuss G, Monaghan MJ, and Shah AM**. Echocardiographic evaluation of diastolic function in mouse models of heart disease. *J Mol Cell Cardiol* 114: 20-28, 2018.

248. **Voigt JU, and Cvijic M**. 2- and 3-Dimensional Myocardial Strain in Cardiac Health and Disease. *JACC Cardiovasc Imaging* 12: 1849-1863, 2019.

249. **McFarland TM, Alam M, Goldstein S, Pickard SD, and Stein PD**. Echocardiographic diagnosis of left ventricular hypertrophy. *Circulation* 57: 1140-1144, 1978.

250. **Vinhas M, Araújo AC, Ribeiro S, Rosário LB, and Belo JA**. Transthoracic echocardiography reference values in juvenile and adult 129/Sv mice. *Cardiovasc Ultrasound* 11: 12, 2013.

251. **Chirinos JA, and Zamani P**. The Nitrate-Nitrite-NO Pathway and Its Implications for Heart Failure and Preserved Ejection Fraction. *Curr Heart Fail Rep* 13: 47-59, 2016.

252. **Westermann D, Kasner M, Steendijk P, Spillmann F, Riad A, Weitmann K, Hoffmann W, Poller W, Pauschinger M, Schultheiss HP, and Tschöpe C**. Role of left ventricular stiffness in heart failure with normal ejection fraction. *Circulation* 117: 2051-2060, 2008.

253. **Bonomo RR, Cook TM, Gavini CK, White CR, Jones JR, Bovo E, Zima AV, Brown IA, Dugas LR, Zakharian E, Aubert G, Alonzo F, Calcutt NA, and Mansuy-Aubert V**. Fecal transplantation and butyrate improve neuropathic pain, modify immune cell profile, and gene expression in the PNS of obese mice. *Proc Natl Acad Sci U S A* 117: 26482-26493, 2020.

254. **Furness JB, Callaghan BP, Rivera LR, and Cho HJ**. The enteric nervous system and gastrointestinal innervation: integrated local and central control. *Adv Exp Med Biol* 817: 39-71, 2014.

255. **McCorry LK**. Physiology of the autonomic nervous system. *Am J Pharm Educ* 71: 78, 2007.

256. **Goldstein AM, Hofstra RM, and Burns AJ**. Building a brain in the gut: development of the enteric nervous system. *Clin Genet* 83: 307-316, 2013.

257. **Bonaz B, Bazin T, and Pellissier S**. The Vagus Nerve at the Interface of the Microbiota-Gut-Brain Axis. *Front Neurosci* 12: 49, 2018.

258. **Fülling C, Dinan TG, and Cryan JF**. Gut Microbe to Brain Signaling: What Happens in Vagus…. *Neuron* 101: 998-1002, 2019.

259. **Breit S, Kupferberg A, Rogler G, and Hasler G**. Vagus Nerve as Modulator of the Brain-Gut Axis in Psychiatric and Inflammatory Disorders. *Front Psychiatry* 9: 44, 2018.

260. **Mayer EA, Savidge T, and Shulman RJ**. Brain-gut microbiome interactions and functional bowel disorders. *Gastroenterology* 146: 1500-1512, 2014.

261. **Cryan JF, and O'Mahony SM**. The microbiome-gut-brain axis: from bowel to behavior. *Neurogastroenterol Motil* 23: 187-192, 2011.

262. **Forsythe P, Sudo N, Dinan T, Taylor VH, and Bienenstock J**. Mood and gut feelings. *Brain Behav Immun* 24: 9-16, 2010.

263. **Bercik P, Verdu EF, Foster JA, Macri J, Potter M, Huang X, Malinowski P, Jackson W, Blennerhassett P, Neufeld KA, Lu J, Khan WI, Corthesy-Theulaz I, Cherbut C, Bergonzelli GE, and Collins SM**. Chronic gastrointestinal inflammation induces anxiety-like behavior and alters central nervous system biochemistry in mice. *Gastroenterology* 139: 2102-2112.e2101, 2010.

264. **Logan AC, and Katzman M**. Major depressive disorder: probiotics may be an adjuvant therapy. *Med Hypotheses* 64: 533-538, 2005.

265. **Rao AV, Bested AC, Beaulne TM, Katzman MA, Iorio C, Berardi JM, and Logan AC**. A randomized, double-blind, placebo-controlled pilot study of a probiotic in emotional symptoms of chronic fatigue syndrome. *Gut Pathog* 1: 6, 2009.

266. **O'Leary OF, Wu X, and Castren E**. Chronic fluoxetine treatment increases expression of synaptic proteins in the hippocampus of the ovariectomized rat: role of BDNF signalling. *Psychoneuroendocrinology* 34: 367-381, 2009.

267. **Bravo JA, Forsythe P, Chew MV, Escaravage E, Savignac HM, Dinan TG, Bienenstock J, and Cryan JF**. Ingestion of Lactobacillus strain regulates emotional behavior and central GABA receptor expression in a mouse via the vagus nerve. *Proc Natl Acad Sci U S A* 108: 16050-16055, 2011.

268. **Berthoud HR**. Vagal and hormonal gut-brain communication: from satiation to satisfaction. *Neurogastroenterol Motil* 20 Suppl 1: 64-72, 2008.

269. **Bai L, Mesgarzadeh S, Ramesh KS, Huey EL, Liu Y, Gray LA, Aitken TJ, Chen Y, Beutler LR, Ahn JS, Madisen L, Zeng H, Krasnow MA, and Knight ZA**. Genetic Identification of Vagal Sensory Neurons That Control Feeding. *Cell* 179: 1129-1143.e1123, 2019.

270. **De Vadder F, Kovatcheva-Datchary P, Goncalves D, Vinera J, Zitoun C, Duchampt A, Bäckhed F, and Mithieux G**. Microbiota-generated metabolites promote metabolic benefits via gut-brain neural circuits. *Cell* 156: 84-96, 2014.

271. **Li Z, Yi CX, Katiraei S, Kooijman S, Zhou E, Chung CK, Gao Y, van den Heuvel JK, Meijer OC, Berbée JFP, Heijink M, Giera M, Willems van Dijk K, Groen AK, Rensen PCN, and Wang Y**. Butyrate reduces appetite and activates brown adipose tissue via the gut-brain neural circuit. *Gut* 67: 1269-1279, 2018.

272. **Kimura I, Inoue D, Maeda T, Hara T, Ichimura A, Miyauchi S, Kobayashi M, Hirasawa A, and Tsujimoto G**. Short-chain fatty acids and ketones directly regulate sympathetic nervous system via G protein-coupled receptor 41 (GPR41). *Proc Natl Acad Sci U S A* 108: 8030-8035, 2011.

273. **Bellahcene M, O'Dowd JF, Wargent ET, Zaibi MS, Hislop DC, Ngala RA, Smith DM, Cawthorne MA, Stocker CJ, and Arch JR**. Male mice that lack the G-protein-coupled receptor GPR41 have low energy expenditure and increased body fat content. *Br J Nutr* 109: 1755-1764, 2013.

274. **Triposkiadis F, Karayannis G, Giamouzis G, Skoularigis J, Louridas G, and Butler J**. The sympathetic nervous system in heart failure physiology, pathophysiology, and clinical implications. *J Am Coll Cardiol* 54: 1747-1762, 2009.

275. **Floras JS**. Sympathetic nervous system activation in human heart failure: clinical implications of an updated model. *J Am Coll Cardiol* 54: 375-385, 2009.

276. **Schwartz PJ**. Vagal stimulation for heart diseases: from animals to men. - An example of translational cardiology.-. *Circ J* 75: 20-27, 2011.

277. **Zhang DY, and Anderson AS**. The sympathetic nervous system and heart failure. *Cardiol Clin* 32: 33-45, vii, 2014.

278. **Olshansky B, Sabbah HN, Hauptman PJ, and Colucci WS**. Parasympathetic nervous system and heart failure: pathophysiology and potential implications for therapy. *Circulation* 118: 863-871, 2008.

279. **Schwartz PJ, and De Ferrari GM**. Sympathetic-parasympathetic interaction in health and disease: abnormalities and relevance in heart failure. *Heart Fail Rev* 16: 101-107, 2011.

280. **Mancia G, and Grassi G**. The central sympathetic nervous system in hypertension. *Handb Clin Neurol* 117: 329-335, 2013.

281. **Mancia G, Grassi G, Giannattasio C, and Seravalle G**. Sympathetic activation in the pathogenesis of hypertension and progression of organ damage. *Hypertension* 34: 724-728, 1999.

282. **Grassi G**. Counteracting the sympathetic nervous system in essential hypertension. *Curr Opin Nephrol Hypertens* 13: 513-519, 2004.

283. **Esler M**. The 2009 Carl Ludwig Lecture: Pathophysiology of the human sympathetic nervous system in cardiovascular diseases: the transition from mechanisms to medical management. *J Appl Physiol (1985)* 108: 227-237, 2010.

284. **Edwards KM, Wilson KL, Sadja J, Ziegler MG, and Mills PJ**. Effects on blood pressure and autonomic nervous system function of a 12-week exercise or exercise plus DASH-diet intervention in individuals with elevated blood pressure. *Acta Physiol (Oxf)* 203: 343-350, 2011.

285. **Polónia J, Amaral C, Bertoquini S, and Martins L**. Attenuation of heart rate recovery after exercise in hypertensive patients with blunting of the nighttime blood pressure fall. *Int J Cardiol* 106: 238-243, 2006.

286. **Colucci WS**. The effects of norepinephrine on myocardial biology: implications for the therapy of heart failure. *Clin Cardiol* 21: I20-24, 1998.

287. **Bristow MR, Ginsburg R, Minobe W, Cubicciotti RS, Sageman WS, Lurie K, Billingham ME, Harrison DC, and Stinson EB**. Decreased catecholamine sensitivity and beta-adrenergic-receptor density in failing human hearts. *N Engl J Med* 307: 205-211, 1982.

288. **Bristow MR, Ginsburg R, Umans V, Fowler M, Minobe W, Rasmussen R, Zera P, Menlove R, Shah P, and Jamieson S**. Beta 1- and beta 2-adrenergic-receptor subpopulations in nonfailing and failing human ventricular myocardium: coupling of both receptor subtypes to muscle contraction and selective beta 1-receptor down-regulation in heart failure. *Circ Res* 59: 297-309, 1986.

289. **Port JD, and Bristow MR**. Altered beta-adrenergic receptor gene regulation and signaling in chronic heart failure. *J Mol Cell Cardiol* 33: 887-905, 2001.

290. **Rengo G, Lymperopoulos A, Leosco D, and Koch WJ**. GRK2 as a novel gene therapy target in heart failure. *J Mol Cell Cardiol* 50: 785-792, 2011.

291. **Ungerer M, Böhm M, Elce JS, Erdmann E, and Lohse MJ**. Altered expression of beta-adrenergic receptor kinase and beta 1-adrenergic receptors in the failing human heart. *Circulation* 87: 454-463, 1993.

292. **Rengo G, Perrone-Filardi P, Femminella GD, Liccardo D, Zincarelli C, de Lucia C, Pagano G, Marsico F, Lymperopoulos A, and Leosco D**. Targeting the β-adrenergic receptor system through G-protein-coupled receptor kinase 2: a new paradigm for therapy and prognostic evaluation in heart failure: from bench to bedside. *Circ Heart Fail* 5: 385-391, 2012.

293. **Hogg K, and McMurray J**. Neurohumoral pathways in heart failure with preserved systolic function. *Prog Cardiovasc Dis* 47: 357-366, 2005.

294. **Somsen GA, Dubois EA, Brandsma K, de Jong J, van der Wouw PA, Batink HD, van Royen EA, Lie KI, and van Zwieten PA**. Cardiac sympathetic neuronal function in left ventricular volume and pressure overload. *Cardiovasc Res* 31: 132-138, 1996.

295. **Piccirillo G, Germanò G, Vitarelli A, Ragazzo M, di Carlo S, De Laurentis T, Torrini A, Matera S, Magnanti M, Marchitto N, Bonanni L, and Magrì D**. Autonomic cardiovascular control and diastolic dysfunction in hypertensive subjects. *Int J Cardiol* 110: 160-166, 2006.

296. **Tepper D**. Frontiers in congestive heart failure: Effect of Metoprolol CR/XL in chronic heart failure: Metoprolol CR/XL Randomised Intervention Trial in Congestive Heart Failure (MERIT-HF). *Congest Heart Fail* 5: 184-185, 1999.

297. **Packer M, Coats AJ, Fowler MB, Katus HA, Krum H, Mohacsi P, Rouleau JL, Tendera M, Castaigne A, Roecker EB, Schultz MK, DeMets DL, and Group CPRCSS**. Effect of carvedilol on survival in severe chronic heart failure. *N Engl J Med* 344: 1651-1658, 2001.

298. **Packer M, Fowler MB, Roecker EB, Coats AJ, Katus HA, Krum H, Mohacsi P, Rouleau JL, Tendera M, Staiger C, Holcslaw TL, Amann-Zalan I, DeMets DL, and Group CPRCSCS**. Effect of carvedilol on the morbidity of patients with severe chronic heart failure: results of the carvedilol prospective randomized cumulative survival (COPERNICUS) study. *Circulation* 106: 2194-2199, 2002.

299. **Ardell JL, Andresen MC, Armour JA, Billman GE, Chen PS, Foreman RD, Herring N, O'Leary DS, Sabbah HN, Schultz HD, Sunagawa K, and Zucker IH**. Translational neurocardiology: preclinical models and cardioneural integrative aspects. *J Physiol* 594: 3877-3909, 2016.

300. **Buckley U, Shivkumar K, and Ardell JL**. Autonomic Regulation Therapy in Heart Failure. *Curr Heart Fail Rep* 12: 284-293, 2015.

301. **Konstam MA, Udelson JE, Butler J, Klein HU, Parker JD, Teerlink JR, Wedge PM, Saville BR, Ardell JL, Libbus I, and DiCarlo LA**. Impact of Autonomic Regulation Therapy in Patients with Heart Failure: ANTHEM-HFrEF Pivotal Study Design. *Circ Heart Fail* 12: e005879, 2019.

302. **DiCarlo LA, Libbus I, Kumar HU, Mittal S, Premchand RK, Amurthur B, KenKnight BH, Ardell JL, and Anand IS**. Autonomic regulation therapy to enhance myocardial function in heart failure patients: the ANTHEM-HFpEF study. *ESC Heart Fail* 5: 95-100, 2018.

303. **Zweerink A, van der Lingen ACJ, Handoko ML, van Rossum AC, and Allaart CP**. Chronotropic Incompetence in Chronic Heart Failure. *Circ Heart Fail* 11: e004969, 2018.

304. **Brubaker PH, and Kitzman DW**. Chronotropic incompetence: causes, consequences, and management. *Circulation* 123: 1010-1020, 2011.

305. **Rivera-Brown AM, and Frontera WR**. Principles of exercise physiology: responses to acute exercise and long-term adaptations to training. *PM R* 4: 797-804, 2012.

306. **Fleg JL, Piña IL, Balady GJ, Chaitman BR, Fletcher B, Lavie C, Limacher MC, Stein RA, Williams M, and Bazzarre T**. Assessment of functional capacity in clinical and research applications: An advisory from the Committee on Exercise, Rehabilitation, and Prevention, Council on Clinical Cardiology, American Heart Association. *Circulation* 102: 1591-1597, 2000.

307. **Witte KK, Cleland JG, and Clark AL**. Chronic heart failure, chronotropic incompetence, and the effects of beta blockade. *Heart* 92: 481-486, 2006.

308. **Houstis NE, Eisman AS, Pappagianopoulos PP, Wooster L, Bailey CS, Wagner PD, and Lewis GD**. Exercise Intolerance in Heart Failure With Preserved Ejection Fraction: Diagnosing and Ranking Its Causes Using Personalized O. *Circulation* 137: 148-161, 2018.

309. **Borlaug BA, Melenovsky V, Russell SD, Kessler K, Pacak K, Becker LC, and Kass DA**. Impaired chronotropic and vasodilator reserves limit exercise capacity in patients with heart failure and a preserved ejection fraction. *Circulation* 114: 2138-2147, 2006.

310. **Sarma S, Stoller D, Hendrix J, Howden E, Lawley J, Livingston S, Adams-Huet B, Holmes C, Goldstein DS, and Levine BD**. Mechanisms of Chronotropic Incompetence in Heart Failure With Preserved Ejection Fraction. *Circ Heart Fail* 13: e006331, 2020.

311. **Fitzgerald SM, Gan L, Wickman A, and Bergström G**. Cardiovascular and renal phenotyping of genetically modified mice: a challenge for traditional physiology. *Clin Exp Pharmacol Physiol* 30: 207-216, 2003.

312. **Chaves AA, Weinstein DM, and Bauer JA**. Non-invasive echocardiographic studies in mice: influence of anesthetic regimen. *Life Sci* 69: 213-222, 2001.

313. **Lujan HL, Janbaih H, Feng HZ, Jin JP, and DiCarlo SE**. Ventricular function during exercise in mice and rats. *Am J Physiol Regul Integr Comp Physiol* 302: R68-74, 2012.

314. **Ho D, Zhao X, Gao S, Hong C, Vatner DE, and Vatner SF**. Heart Rate and Electrocardiography Monitoring in Mice. *Curr Protoc Mouse Biol* 1: 123-139, 2011.

315. **Miller TL, and Wolin MJ**. Pathways of acetate, propionate, and butyrate formation by the human fecal microbial flora. *Appl Environ Microbiol* 62: 1589-1592, 1996.

316. **Silva YP, Bernardi A, and Frozza RL**. The Role of Short-Chain Fatty Acids From Gut Microbiota in Gut-Brain Communication. *Front Endocrinol (Lausanne)* 11: 25, 2020.
317. **Cook SI, and Sellin JH**. Review article: short chain fatty acids in health and disease. *Aliment Pharmacol Ther* 12: 499-507, 1998.

318. **Panagia M, He H, Baka T, Pimentel DR, Croteau D, Bachschmid MM, Balschi JA, Colucci WS, and Luptak I**. Increasing mitochondrial ATP synthesis with butyrate normalizes ADP and contractile function in metabolic heart disease. *NMR Biomed* 33: e4258, 2020.

319. **Patel BM**. Sodium Butyrate Controls Cardiac Hypertrophy in Experimental Models of Rats. *Cardiovasc Toxicol* 18: 1-8, 2018.

320. **Zhang L, Deng M, Lu A, Chen Y, Wu C, Tan Z, Boini KM, Yang T, Zhu Q, and Wang L**. Sodium butyrate attenuates angiotensin II-induced cardiac hypertrophy by inhibiting COX2/PGE2 pathway via a HDAC5/HDAC6-dependent mechanism. *J Cell Mol Med* 23: 8139-8150, 2019.

321. **Chen Y, Du J, Zhao YT, Zhang L, Lv G, Zhuang S, Qin G, and Zhao TC**. Histone deacetylase (HDAC) inhibition improves myocardial function and prevents cardiac remodeling in diabetic mice. *Cardiovasc Diabetol* 14: 99, 2015.

322. **Thomas SP, and Denu JM**. Short-chain fatty acids activate acetyltransferase p300. *Elife* 10: 2021.

323. **Pandey A, Parashar A, Kumbhani D, Agarwal S, Garg J, Kitzman D, Levine B, Drazner M, and Berry J**. Exercise training in patients with heart failure and preserved ejection fraction: meta-analysis of randomized control trials. *Circ Heart Fail* 8: 33-40, 2015.

324. **Kiilavuori K, Toivonen L, Näveri H, and Leinonen H**. Reversal of autonomic derangements by physical training in chronic heart failure assessed by heart rate variability. *Eur Heart J* 16: 490-495, 1995.

325. **Myers J, Hadley D, Oswald U, Bruner K, Kottman W, Hsu L, and Dubach P**. Effects of exercise training on heart rate recovery in patients with chronic heart failure. *Am Heart J* 153: 1056-1063, 2007.

326. **Keteyian SJ, Brawner CA, Schairer JR, Levine TB, Levine AB, Rogers FJ, and Goldstein S**. Effects of exercise training on chronotropic incompetence in patients with heart failure. *Am Heart J* 138: 233-240, 1999.

327. **Zhao X, Zhang Z, Hu B, Huang W, Yuan C, and Zou L**. Response of Gut Microbiota to Metabolite Changes Induced by Endurance Exercise. *Front Microbiol* 9: 765, 2018.

328. **Jost L**. Partitioning diversity into independent alpha and beta components. *Ecology* 88: 2427-2439, 2007.

329. **Estaki M, Pither J, Baumeister P, Little JP, Gill SK, Ghosh S, Ahmadi-Vand Z, Marsden KR, and Gibson DL**. Cardiorespiratory fitness as a predictor of intestinal microbial diversity and distinct metagenomic functions. *Microbiome* 4: 42, 2016.

330. **Cook MD, Martin SA, Williams C, Whitlock K, Wallig MA, Pence BD, and Woods JA**. Forced treadmill exercise training exacerbates inflammation and causes mortality while voluntary wheel training is protective in a mouse model of colitis. *Brain Behav Immun* 33: 46-56, 2013.

331. **Lai ZL, Tseng CH, Ho HJ, Cheung CKY, Lin JY, Chen YJ, Cheng FC, Hsu YC, Lin JT, El-Omar EM, and Wu CY**. Fecal microbiota transplantation confers beneficial metabolic effects of diet and exercise on diet-induced obese mice. *Sci Rep* 8: 15625, 2018.

332. **Nay K, Jollet M, Goustard B, Baati N, Vernus B, Pontones M, Lefeuvre-Orfila L, Bendavid C, Rué O, Mariadassou M, Bonnieu A, Ollendorff V, Lepage P, Derbré F, and Koechlin-Ramonatxo C**. Gut bacteria are critical for optimal muscle function: a potential link with glucose homeostasis. *Am J Physiol Endocrinol Metab* 317: E158-E171, 2019.

333. **Frampton J, Murphy KG, Frost G, and Chambers ES**. Short-chain fatty acids as potential regulators of skeletal muscle metabolism and function. *Nat Metab* 2: 840-848, 2020.

334. **Walsh ME, Bhattacharya A, Sataranatarajan K, Qaisar R, Sloane L, Rahman MM, Kinter M, and Van Remmen H**. The histone deacetylase inhibitor butyrate improves metabolism and reduces muscle atrophy during aging. *Aging Cell* 14: 957-970, 2015.

335. **Hutson SM, Sweatt AJ, and Lanoue KF**. Branched-chain [corrected] amino acid metabolism: implications for establishing safe intakes. *J Nutr* 135: 1557S-1564S, 2005.

336. **Harper AE, Miller RH, and Block KP**. Branched-chain amino acid metabolism. *Annu Rev Nutr* 4: 409-454, 1984.

337. **Blomstrand E, Eliasson J, Karlsson HK, and Köhnke R**. Branched-chain amino acids activate key enzymes in protein synthesis after physical exercise. *J Nutr* 136: 269S-273S, 2006.

338. **Norton LE, and Layman DK**. Leucine regulates translation initiation of protein synthesis in skeletal muscle after exercise. *J Nutr* 136: 533S-537S, 2006.

339. **Lynch CJ, and Adams SH**. Branched-chain amino acids in metabolic signalling and insulin resistance. *Nat Rev Endocrinol* 10: 723-736, 2014.

340. **Schwartz GJ**. Central leucine sensing in the control of energy homeostasis. *Endocrinol Metab Clin North Am* 42: 81-87, 2013.

341. **Potier M, Darcel N, and Tomé D**. Protein, amino acids and the control of food intake. *Curr Opin Clin Nutr Metab Care* 12: 54-58, 2009.

342. **Vilela TC, Scaini G, Furlanetto CB, Pasquali MA, Santos JP, Gelain DP, Moreira JC, Schuck PF, Ferreira GC, and Streck EL**. Apoptotic signaling pathways induced by acute administration of branched-chain amino acids in an animal model of maple syrup urine disease. *Metab Brain Dis* 32: 115-122, 2017.

343. **Skeie B, Kvetan V, Gil KM, Rothkopf MM, Newsholme EA, and Askanazi J**. Branch-chain amino acids: their metabolism and clinical utility. *Crit Care Med* 18: 549-571, 1990.

344. **Kainulainen H, Hulmi JJ, and Kujala UM**. Potential role of branched-chain amino acid catabolism in regulating fat oxidation. *Exerc Sport Sci Rev* 41: 194-200, 2013.

345. **Ye Z, Wang S, Zhang C, and Zhao Y**. Coordinated Modulation of Energy Metabolism and Inflammation by Branched-Chain Amino Acids and Fatty Acids. *Front Endocrinol (Lausanne)* 11: 617, 2020.

346. **Sweatt AJ, Wood M, Suryawan A, Wallin R, Willingham MC, and Hutson SM**. Branched-chain amino acid catabolism: unique segregation of pathway enzymes in organ systems and peripheral nerves. *Am J Physiol Endocrinol Metab* 286: E64-76, 2004.

347. **Suryawan A, Hawes JW, Harris RA, Shimomura Y, Jenkins AE, and Hutson SM**. A molecular model of human branched-chain amino acid metabolism. *Am J Clin Nutr* 68: 72-81, 1998.

348. **Hutson SM, Wallin R, and Hall TR**. Identification of mitochondrial branched chain aminotransferase and its isoforms in rat tissues. *J Biol Chem* 267: 15681-15686, 1992.

349. **Brosnan JT, and Brosnan ME**. Branched-chain amino acids: enzyme and substrate regulation. *J Nutr* 136: 207S-211S, 2006.

350. **Bröer S**. Amino acid transport across mammalian intestinal and renal epithelia. *Physiol Rev* 88: 249-286, 2008.

351. **Verrey F**. System L: heteromeric exchangers of large, neutral amino acids involved in directional transport. *Pflugers Arch* 445: 529-533, 2003.

352. **Zhang ZY, Monleon D, Verhamme P, and Staessen JA**. Branched-Chain Amino Acids as Critical Switches in Health and Disease. *Hypertension* 72: 1012-1022, 2018.

353. **Walejko JM, Christopher BA, Crown SB, Zhang GF, Pickar-Oliver A, Yoneshiro T, Foster MW, Page S, van Vliet S, Ilkayeva O, Muehlbauer MJ, Carson MW, Brozinick JT, Hammond CD, Gimeno RE, Moseley MA, Kajimura S, Gersbach CA, Newgard CB, White PJ, and McGarrah RW**. Branched-chain α-ketoacids are preferentially reaminated and activate protein synthesis in the heart. *Nat Commun* 12: 1680, 2021.

354. **Adeva-Andany MM, López-Maside L, Donapetry-García C, Fernández-Fernández C, and Sixto-Leal C**. Enzymes involved in branched-chain amino acid metabolism in humans. *Amino Acids* 49: 1005-1028, 2017.

355. **Hutson SM**. Regulation of substrate availability for the branched-chain alpha-keto acid dehydrogenase enzyme complex. *Ann N Y Acad Sci* 573: 230-239, 1989.

356. **Schadewaldt P, and Wendel U**. Metabolism of branched-chain amino acids in maple syrup urine disease. *Eur J Pediatr* 156 Suppl 1: S62-66, 1997.

357. **Huang Y, Zhou M, Sun H, and Wang Y**. Branched-chain amino acid metabolism in heart disease: an epiphenomenon or a real culprit? *Cardiovasc Res* 90: 220-223, 2011.

358. **Zhou M, Lu G, Gao C, Wang Y, and Sun H**. Tissue-specific and nutrient regulation of the branched-chain α-keto acid dehydrogenase phosphatase, protein phosphatase 2Cm (PP2Cm). *J Biol Chem* 287: 23397-23406, 2012.

359. **Lu G, Ren S, Korge P, Choi J, Dong Y, Weiss J, Koehler C, Chen JN, and Wang Y**. A novel mitochondrial matrix serine/threonine protein phosphatase regulates the mitochondria permeability transition pore and is essential for cellular survival and development. *Genes Dev* 21: 784-796, 2007.

360. **Lu G, Sun H, She P, Youn JY, Warburton S, Ping P, Vondriska TM, Cai H, Lynch CJ, and Wang Y**. Protein phosphatase 2Cm is a critical regulator of branched-chain amino acid catabolism in mice and cultured cells. *J Clin Invest* 119: 1678-1687, 2009.

361. **Liu R, Hong J, Xu X, Feng Q, Zhang D, Gu Y, Shi J, Zhao S, Liu W, Wang X, Xia H, Liu Z, Cui B, Liang P, Xi L, Jin J, Ying X, Zhao X, Li W, Jia H, Lan Z, Li F, Wang R, Sun Y, Yang M, Shen Y, Jie Z, Li J, Chen X, Zhong H, Xie H, Zhang Y, Gu W, Deng X, Shen B, Yang H, Xu G, Bi Y, Lai S, Wang J, Qi L, Madsen L, Ning G, Kristiansen K, and Wang W**. Gut microbiome and serum metabolome alterations in obesity and after weight-loss intervention. *Nat Med* 23: 859-868, 2017.

362. **Pedersen HK, Gudmundsdottir V, Nielsen HB, Hyotylainen T, Nielsen T, Jensen BA, Forslund K, Hildebrand F, Prifti E, Falony G, Le Chatelier E, Levenez F, Doré J, Mattila I, Plichta DR, Pöhö P, Hellgren LI, Arumugam M, Sunagawa S, Vieira-Silva S, Jørgensen T, Holm JB, Trošt K, Kristiansen K, Brix S, Raes J, Wang J, Hansen T, Bork P, Brunak S, Oresic M, Ehrlich SD, Pedersen O, and Consortium M**. Human gut microbes impact host serum metabolome and insulin sensitivity. *Nature* 535: 376-381, 2016.

363. **Zhang L, Yue Y, Shi M, Tian M, Ji J, Liao X, Hu X, and Chen F**. Dietary Luffa cylindrica (L.) Roem promotes branched-chain amino acid catabolism in the circulation system via gut microbiota in diet-induced obese mice. *Food Chem* 320: 126648, 2020.

364. **Chen H, Nie Q, Hu J, Huang X, Yin J, and Nie S**. Multiomics Approach to Explore the Amelioration Mechanisms of Glucomannans on the Metabolic Disorder of Type 2 Diabetic Rats. *J Agric Food Chem* 69: 2632-2645, 2021.

365. **Zeng SL, Li SZ, Xiao PT, Cai YY, Chu C, Chen BZ, Li P, Li J, and Liu EH**. Citrus polymethoxyflavones attenuate metabolic syndrome by regulating gut microbiome and amino acid metabolism. *Sci Adv* 6: eaax6208, 2020.

366. **Sun H, Olson KC, Gao C, Prosdocimo DA, Zhou M, Wang Z, Jeyaraj D, Youn JY, Ren S, Liu Y, Rau CD, Shah S, Ilkayeva O, Gui WJ, William NS, Wynn RM, Newgard CB, Cai H, Xiao X, Chuang DT, Schulze PC, Lynch C, Jain MK, and Wang Y**. Catabolic Defect of Branched-Chain Amino Acids Promotes Heart Failure. *Circulation* 133: 2038-2049, 2016.

367. **Uddin GM, Zhang L, Shah S, Fukushima A, Wagg CS, Gopal K, Al Batran R, Pherwani S, Ho KL, Boisvenue J, Karwi QG, Altamimi T, Wishart DS, Dyck JRB, Ussher JR, Oudit GY, and Lopaschuk GD**. Impaired branched chain amino acid oxidation contributes to cardiac insulin resistance in heart failure. *Cardiovasc Diabetol* 18: 86, 2019.

368. **Wang W, Zhang F, Xia Y, Zhao S, Yan W, Wang H, Lee Y, Li C, Zhang L, Lian K, Gao E, Cheng H, and Tao L**. Defective branched chain amino acid catabolism contributes to cardiac dysfunction and remodeling following myocardial infarction. *Am J Physiol Heart Circ Physiol* 311: H1160-H1169, 2016.

369. **Lian K, Guo X, Wang Q, Liu Y, Wang RT, Gao C, Li CY, Li CX, and Tao L**. PP2Cm overexpression alleviates MI/R injury mediated by a BCAA catabolism defect and oxidative stress in diabetic mice. *Eur J Pharmacol* 866: 172796, 2020.

370. **Zhenyukh O, Civantos E, Ruiz-Ortega M, Sánchez MS, Vázquez C, Peiró C, Egido J, and Mas S**. High concentration of branched-chain amino acids promotes oxidative stress, inflammation and migration of human peripheral blood mononuclear cells via mTORC1 activation. *Free Radic Biol Med* 104: 165-177, 2017.

371. **Sun H, Lu G, Ren S, Chen J, and Wang Y**. Catabolism of branched-chain amino acids in heart failure: insights from genetic models. *Pediatr Cardiol* 32: 305-310, 2011.

372. **Yang J, Savvatis K, Kang JS, Fan P, Zhong H, Schwartz K, Barry V, Mikels-Vigdal A, Karpinski S, Kornyeyev D, Adamkewicz J, Feng X, Zhou Q, Shang C, Kumar P, Phan D, Kasner M, López B, Diez J, Wright KC, Kovacs RL, Chen PS, Quertermous T, Smith V, Yao L, Tschöpe C, and Chang CP**. Targeting LOXL2 for cardiac interstitial fibrosis and heart failure treatment. *Nat Commun* 7: 13710, 2016.

373. **Barry-Hamilton V, Spangler R, Marshall D, McCauley S, Rodriguez HM, Oyasu M, Mikels A, Vaysberg M, Ghermazien H, Wai C, Garcia CA, Velayo AC, Jorgensen B, Biermann D, Tsai D, Green J, Zaffryar-Eilot S, Holzer A, Ogg S, Thai D, Neufeld G, Van Vlasselaer P, and Smith V**. Allosteric inhibition of lysyl oxidase-like-2 impedes the development of a pathologic microenvironment. *Nat Med* 16: 1009-1017, 2010.

374. **Ikenaga N, Peng ZW, Vaid KA, Liu SB, Yoshida S, Sverdlov DY, Mikels-Vigdal A, Smith V, Schuppan D, and Popov YV**. Selective targeting of lysyl oxidase-like 2 (LOXL2) suppresses hepatic fibrosis progression and accelerates its reversal. *Gut* 66: 1697-1708, 2017.

375. **Pan TC, Zhang RZ, Mattei MG, Timpl R, and Chu ML**. Cloning and chromosomal location of human alpha 1(XVI) collagen. *Proc Natl Acad Sci U S A* 89: 6565-6569, 1992.

376. **Gutierrez LS, and Gutierrez J**. Thrombospondin 1 in Metabolic Diseases. *Front Endocrinol (Lausanne)* 12: 638536, 2021.

377. **Daubon T, Léon C, Clarke K, Andrique L, Salabert L, Darbo E, Pineau R, Guérit S, Maitre M, Dedieu S, Jeanne A, Bailly S, Feige JJ, Miletic H, Rossi M, Bello L, Falciani F, Bjerkvig R, and Bikfalvi A**. Deciphering the complex role of thrombospondin-1 in glioblastoma development. *Nat Commun* 10: 1146, 2019.

378. **Leshchyns'ka I, and Sytnyk V**. Reciprocal Interactions between Cell Adhesion Molecules of the Immunoglobulin Superfamily and the Cytoskeleton in Neurons. *Front Cell Dev Biol* 4: 9, 2016.

379. **Gao Y, Kong L, Liu S, Liu K, and Zhu J**. Impact of Neurofascin on Chronic Inflammatory Demyelinating Polyneuropathy. *Front Mol Neurosci* 14: 779385, 2021.

380. **Siritantikorn A, Johansson K, Ahlen K, Rinaldi R, Suthiphongchai T, Wilairat P, and Morgenstern R**. Protection of cells from oxidative stress by microsomal glutathione transferase 1. *Biochem Biophys Res Commun* 355: 592-596, 2007.

381. **Verkerk AO, Lodder EM, and Wilders R**. Aquaporin Channels in the Heart-Physiology and Pathophysiology. *Int J Mol Sci* 20: 2019.

382. **Rutkovskiy A, Stensløkken KO, Mariero LH, Skrbic B, Amiry-Moghaddam M, Hillestad V, Valen G, Perreault MC, Ottersen OP, Gullestad L, Dahl CP, and Vaage J**. Aquaporin-4 in the heart: expression, regulation and functional role in ischemia. *Basic Res Cardiol* 107: 280, 2012.

383. **Periasamy M, and Janssen PM**. Molecular basis of diastolic dysfunction. *Heart Fail Clin* 4: 13-21, 2008.

384. **Bers DM**. Cardiac excitation-contraction coupling. *Nature* 415: 198-205, 2002.

385. **Cheng YS, Tang YQ, Dai DZ, and Dai Y**. AQP4 knockout mice manifest abnormal expressions of calcium handling proteins possibly due to exacerbating pro-inflammatory factors in the heart. *Biochem Pharmacol* 83: 97-105, 2012.

386. **Yang L, Katchman A, Morrow JP, Doshi D, and Marx SO**. Cardiac L-type calcium channel (Cav1.2) associates with gamma subunits. *FASEB J* 25: 928-936, 2011.

387. **Taylor GA, Collazo CM, Yap GS, Nguyen K, Gregorio TA, Taylor LS, Eagleson B, Secrest L, Southon EA, Reid SW, Tessarollo L, Bray M, McVicar DW, Komschlies KL, Young HA, Biron CA, Sher A, and Vande Woude GF**. Pathogen-specific loss of host resistance in mice lacking the IFN-gamma-inducible gene IGTP. *Proc Natl Acad Sci U S A* 97: 751-755, 2000.

388. **Fu J, Menzies K, Freeman RS, and Taubman MB**. EGLN3 prolyl hydroxylase regulates skeletal muscle differentiation and myogenin protein stability. *J Biol Chem* 282: 12410-12418, 2007.

389. **Liao H, Winkfein RJ, Mack G, Rattner JB, and Yen TJ**. CENP-F is a protein of the nuclear matrix that assembles onto kinetochores at late G2 and is rapidly degraded after mitosis. *J Cell Biol* 130: 507-518, 1995.

390. **Zhu X, Mancini MA, Chang KH, Liu CY, Chen CF, Shan B, Jones D, Yang-Feng TL, and Lee WH**. Characterization of a novel 350-kilodalton nuclear phosphoprotein that is specifically involved in mitotic-phase progression. *Mol Cell Biol* 15: 5017-5029, 1995.

391. **Hare JM**. Oxidative stress and apoptosis in heart failure progression. *Circ Res* 89: 198-200, 2001.

392. **Del Campo A, Perez G, Castro PF, Parra V, and Verdejo HE**. Mitochondrial function, dynamics and quality control in the pathophysiology of HFpEF. *Biochim Biophys Acta Mol Basis Dis* 1867: 166208, 2021.

393. **Xiao M, Zhong H, Xia L, Tao Y, and Yin H**. Pathophysiology of mitochondrial lipid oxidation: Role of 4-hydroxynonenal (4-HNE) and other bioactive lipids in mitochondria. *Free Radic Biol Med* 111: 316-327, 2017.

394. **Mitchell NS, Catenacci VA, Wyatt HR, and Hill JO**. Obesity: overview of an epidemic. *Psychiatr Clin North Am* 34: 717-732, 2011.

395. **Chambers ES, Preston T, Frost G, and Morrison DJ**. Role of Gut Microbiota-Generated Short-Chain Fatty Acids in Metabolic and Cardiovascular Health. *Curr Nutr Rep* 7: 198-206, 2018.

396. **Spyropoulos F, Sorrentino A, van der Reest J, Yang P, Waldeck-Weiermair M, Steinhorn B, Eroglu E, Saeedi Saravi SS, Yu P, Haigis M, Christou H, and Michel T**. Metabolomic and Transcriptomic Signatures of Chemogenetic Heart Failure. *Am J Physiol Heart Circ Physiol* 2022.

397. **Scantlebury DC, and Borlaug BA**. Why are women more likely than men to develop heart failure with preserved ejection fraction? *Curr Opin Cardiol* 26: 562-568, 2011.

398. **Sotomi Y, Hikoso S, Nakatani D, Mizuno H, Okada K, Dohi T, Kitamura T, Sunaga A, Kida H, Oeun B, Sato T, Komukai S, Tamaki S, Yano M, Hayashi T, Nakagawa A, Nakagawa Y, Yasumura Y, Yamada T, Sakata Y, and Investigators PH**. Sex Differences in Heart Failure With Preserved Ejection Fraction. *J Am Heart Assoc* 10: e018574, 2021.

399. **Garawi F, Devries K, Thorogood N, and Uauy R**. Global differences between women and men in the prevalence of obesity: is there an association with gender inequality? *Eur J Clin Nutr* 68: 1101-1106, 2014.

400. **Hales CM, Carroll MD, Fryar CD, and Ogden CL**. Prevalence of Obesity and Severe Obesity Among Adults: United States, 2017-2018. *NCHS Data Brief* 1-8, 2020.

401. **Hong J, Stubbins RE, Smith RR, Harvey AE, and Núñez NP**. Differential susceptibility to obesity between male, female and ovariectomized female mice. *Nutr J* 8: 11, 2009.

402. **Maric I, Krieger JP, van der Velden P, Börchers S, Asker M, Vujicic M, Wernstedt Asterholm I, and Skibicka KP**. Sex and Species Differences in the Development of Diet-Induced Obesity and Metabolic Disturbances in Rodents. *Front Nutr* 9: 828522, 2022.

403. **Pearce MM, Hilt EE, Rosenfeld AB, Zilliox MJ, Thomas-White K, Fok C, Kliethermes S, Schreckenberger PC, Brubaker L, Gai X, and Wolfe AJ**. The female urinary microbiome: a comparison of women with and without urgency urinary incontinence. *mBio* 5: e01283-01214, 2014.

404. **Chong J, Liu P, Zhou G, and Xia J**. Using MicrobiomeAnalyst for comprehensive statistical, functional, and meta-analysis of microbiome data. *Nat Protoc* 15: 799-821, 2020.

VITA

The author, Jomana Hatahet, was born in Damascus, Syria to Dr.Abed Hatahet and Dr.Hala Harbol. She attended Illinois Institute of Technology in Chicago, IL where she earned a Bachelor of Science in Chemistry in May 2017. During her undergraduate studies, Jomana worked in the lab of Dr.Jean-Luc Ayitou, studying the synthesis, photo-physics, and application of pyrene amides as fluorescence sensors. Jomana matriculated into the Loyola University Chicago Interdisciplinary Program in Biomedical Sciences in 2018 and began her graduate education in the Cellular and Molecular Physiology under the mentorship of Dr.Gregory Aubert.

Jomana's dissertation work focuses on investigating the role of gut microbiome in the progression of obesity associated HFpEF. After completion of her graduate studies, Jomana will pursue a postdoctoral fellowship at AbbVie.